Alma Mater Studiorum · Università di Bologna

School of Science
Department of Physics and Astronomy
Master Degree in Physics

Implementing the Neutrino Option with the Inverse Seesaw Model

Supervisor:
Prof. Ilaria Brivio

Defended by:
Katja Brunelli

Academic Year 2024/2025

"Fare il fisico è una faticaccia,
ma è sempre meglio che lavorare"
— Aurelio Grillo

Abstract

The Neutrino Option is a scenario that, adopting the EFT approach, addresses two important issues of the Standard Model: the absence of a neutrino mass term in the SM Lagrangian and the lack of a dynamical origin for the Higgs potential. In this minimal scenario the neutrino masses and the Higgs potential are simultaneously generated through the matching contributions given by the Type 1 Seesaw model. This implementation of the Neutrino Option predicts a mass for the heavy neutrino of $10^6 - 10^7$ GeV, which is far out of the energy range of current experiments, making this model untestable (at least for now). The aim of this project is to conduct a similar analysis by implementing the Neutrino Option with the Inverse Seesaw (ISS) mechanism. Using the additional freedom in the parameter space of the ISS, we show that it is possible to lower the prediction of the heavy mass down to $10^3 - 10^6$ GeV, reaching experimentally testable energy scales. We first perform the analysis in the case of one flavour generation in order to get some order-of-magnitude predictions and we later introduce a more realistic flavour structure, which however is consistent with the results of the first case.

Contents

Chapter 1

Introduction

The Standard Model (SM) [1–3] is certainly one of the greatest achievements of modern theoretical physics and using it we are able to describe a very wide range of phenomena at an astounding precision level. However, despite its enormous success, it is a well established fact that the SM comes with several problems and open questions. Some of them are: neutrino masses, Dark Matter, baryogenesis, hierarchy problems, unification of matter and interactions, the strong CP problem and the flavour puzzle.

Throughout the years, several solutions have been proposed that address one or more of the above mentioned issues. In this work we investigate an alternative realization of the Neutrino Option [4, 5], a scenario that simultaneously attempts to solve the problem of neutrino masses and the Higgs hierarchy problem through an Effective Field Theory approach.

Effective Field Theories are one of the most powerful and elegant tools we have to search for beyond the Standard Model physics. It is not unusual to hear, especially since the discoveries of the last century, that the great goal of theoretical physics is to find the so called "theory of everything". Such fundamental theory should be able to consistently describe every physical phenomenon, at any arbitrarily big or small energy scale. However, until we find such a theory we must rely on what we have discovered so far in order to make predictions. We could ask ourselves whether these predictions are reliable or not, since they are made with theories that are not fundamental (in the above sense). The answer in most cases is yes, and the reason is that Nature decouples [6]. This means that some effects that are relevant at a certain energy scale, may be totally negligible at another. A practical example is that engineers are able to build totally stable bridges without knowing General Relativity and chemists can study any reaction without the need of accounting for the strong interactions that take place inside of nucleons. This is exactly the intuitive idea behind Effective Field Theories: we do not need to know the exact theory to make good predictions. This concept may sound almost trivial, but translating it into a consistent mathematical formulation is far from obvious.

The problem of neutrino masses constitutes one of the main experimental evidence that some BSM physics is required. Ever since Pauli first suggested their existence in 1930 [7], neutrinos have always been an intriguing puzzle, and despite the many discoveries that followed, after almost a century they remain one of the most elusive and mysterious particles we know of. In 1956, the same year neutrinos were discovered [8], Madame Wu proved that weak interactions violate parity [9] and just two years later Goldhaber, Grodzins and Sunyar [10] showed that neutrinos are left-handed particles. This lead Landau [11], Lee and Yang [12] and Salam [13] to propose that they can be described by a left-handed Weyl spinor. However, this implied that neutrinos could not have a mass term in the SM Lagrangian, or at least not one like the other fermions. In 1957 Pontecorvo put forward the idea of neutrino oscillations [14, 15], and the work was later expanded and completed also thanks to Maki, Nakagawa, Sakata and Gribov [16–22]. If neutrino oscillations proved to be true, it would necessarily indicate that neutrinos (at least two of them) must be massive. This turned out to be exactly the case, as proved by experiments on solar neutrino detection. The first observation came from Kamiokande [23] and later in 2001 the SNO experiment [24] definitely confirmed it. After this discovery, it was clear that the SM needs to be expanded in order to account for a neutrino mass term. Among all the models that were proposed ever since to generate the neutrino masses, the Seesaw mechanisms are certainly the most promising ones.

Unlike the problem of neutrino masses, the Higgs hierarchy problem (HP) [25, 26] is not something that requires the existence of BSM physics from some experimental evidence, but it is rather a consequence of the presence of some new physics at higher energy scales, which we are now convinced must exist (due to gravitational interaction if nothing else). In the presence of some heavy BSM physics that couples to the Higgs its mass receives corrections, in addition to the ones from the SM particles, that are proportional to the heavy mass itself. If the new mass is much higher than the Higgs mass, then we would have to perform some heavy fine tuning in order to have a cancellation that leads to the much smaller measured value of the Higgs mass. However, if this were not the case and the threshold for new physics were close in energy to the Higgs mass, we would not have a HP because the cancellations (if needed) would be small with respect to the starting point, making them more natural. So, another way to phrase the HP is: why is the Higgs mass so much smaller than the threshold for new physics? Many solutions have been proposed throughout the years, some of the most popular rely on Supersymmetry [27, 28] or composite Higgs models [29, 30].

The Neutrino Option attempts to solve the problem of neutrino masses and the HP by generating the Higgs potential and neutrino masses through the matching contributions of the Type 1 Seesaw model starting from an almost conformal UV embedding, where the only dimensional scale is the heavy mass. In particular, the neutrino masses

are generated at tree-level at dimension 5 and the Higgs potential (that we recall is set to zero in the UV) in generated through 1-loop diagrams. The matching procedure fixes the generated quantities at some high energy scale, that can be taken equal to the heavy mass. By requesting that they are generated simultaneously and imposing some consistency with neutrino physics constraints, it is possible to get a prediction of the mass of the heavy neutrino and the Yukawa coupling. The original implementation of the Neutrino Option produces a prediction of 10^6 GeV $\lesssim M \lesssim 10^7$ GeV, which is far above the energy range of current experiments.

In this work, we propose an alternative implementation of the Neutrino Option that aims at lowering the prediction of the heavy mass. The idea is to generate the matching contributions in the Inverse Seesaw model, which offers more freedom with respect to the Type 1 Seesaw thanks to the introduction of an additional parameter in the Lagrangian. Our goal is to identify a region in the ISS parameter space compatible with experimental constraints on the Higgs and neutrino masses and to verify that this implementation of the Neutrino Option produces a scenario compatible with a well-behaved theory, i.e. a theory which is weakly interacting and does not require fine tuning. We first perform the numerical analysis in the limit of one flavour generation to get some order-of-magnitude predictions. Afterwards we repeat the analysis by considering a more realistic flavour structure, but the results confirm the main conclusions of the one flavour case.

Chapter 2

Effective Field Theories

Effective Field Theories can be seen as the low-energy limit of some more fundamental theory, and they are an incredibly powerful and elegant tool that we can use to search for BSM physics. Formally, an EFT is an expansion in a small quantity δ called the power counting parameter, which is usually a ratio between masses or energy scales. We can use this parameter to organize the terms appearing in the Lagrangian given their order in δ. It is important to underline the fact that an EFT is a perfectly self-consistent theory within its finite range of validity and it can be used to make predictions. In this chapter, we show how to properly construct an EFT and how we can use it to perform calculations.

2.1 Handbook of Effective Field Theories

Let us start the discussion about EFTs by pointing out some of the reasons why it is convenient (or even mandatory) to use them [31]:

- Sometimes we have no other choice, because we may not have any knowledge of the physics at higher energies.
- Every theory is an EFT. For example, QED is approximation of the Standard Model and it is obtained by integrating out every particle except the photon and the electron.
- Performing calculations in the EFT can be much simpler than using the full theory.
- It provides methods to sum large logarithms, using the renormalization-group improved perturbation theory. This approach can be used just for UV logs, but this is not an issue since it is possible to convert IR logs of the full theory into UV logs in the EFT, which can then be summed.

There are many ways to write a generic EFT Lagrangian, depending in which quantity we choose to expand. In particular, we are interested in the case where the power counting is the mass dimension of the operators. The general form of an EFT Lagrangian of this kind is:

$$\mathcal{L}_{EFT} = \sum_{D\geq 0,\, i} \frac{c_i^{(D)} \mathcal{O}_i^{(D)}}{\Lambda^{D-d}} = \sum_{D\geq 0} \frac{\mathcal{L}_D}{\Lambda^{D-d}}, \tag{2.1}$$

where D is the mass dimension and d is the number of spacetime dimensions. $\mathcal{O}_i^{(D)}$ are the allowed operators of dimension D and Λ is a mass scale that is introduced in order to make the Wilson coefficients $c_i^{(D)}$ dimensionless. Λ is considered the cut-off, i.e. the energy scale at which the UV physics starts to arise and the EFT expansion breaks down. For $d = 4$ we have:

$$\mathcal{L}_{EFT} = \mathcal{L}_{D\leq 4} + \frac{\mathcal{L}_5}{\Lambda} + \frac{\mathcal{L}_6}{\Lambda^2} + ... \tag{2.2}$$

and $\mathcal{L}_{EFT}$ must be treated as a series expanded in $1/\Lambda$. If we consider a scattering amplitude, the insertion of a set of operators with $d > 4$ leads to:

$$\mathcal{A} \sim p^{4-N} \left(\frac{p}{\Lambda}\right)^n, \quad \text{with} \quad n = \sum_i (D_i - 4), \tag{2.3}$$

where i runs on all the inserted operators, p is the external momentum and N the number of external legs. A more detailed derivation can be fond in Appendix A. The expression for n in eq.(2.3) is known as the power counting formula and indicates the (p/Λ) suppression of a graph. One remarkable fact about EFTs, is that this formula is valid not only for tree-level graphs, but also for loop diagrams in which we perform an integration over loop momenta in the range $-\infty < k < \infty$, which includes also the region where the EFT expansion in k/Λ breaks down.

Thanks to the power counting formula we can understand the difference between an EFT and a renormalizable theory. If we start from only the operators in the renormalizable Lagrangian $\mathcal{L}_{D\leq 4}$, we do not generate any new operator of higher dimension and the counterterms needed for the renormalization all have $D \leq 4$. This is however not true for non-renormalizable operators. For example, two insertions of a dimension 5 operator generate a dimension 6 operator, in fact:

$$n = (5-4) + (5-4) = 2 \quad \rightarrow \quad \mathcal{A} \sim \left(\frac{p}{\Lambda}\right)^2. \tag{2.4}$$

So, to renormalize the theory we must include a $\mathcal{L}_6$ counterterm. More in general, by multiple insertions of a higher dimension operator we can generate other operators up to arbitrarily high dimension, so we end up with an infinite series. However, if we are interested in evaluating corrections up to a finite value of n, then an EFT is just as good as a renormalizable theory, since the series is truncated and therefore has a finite number

of terms.

Now we want to start building an EFT and to do it we must perform two steps. The first step is the so called the bottom-up approach, which consists in computing the observables we are interested in as functions of the Wilson coefficients (WCs) of the EFT. Since we are not specifying any UV theory, this first part is model-independent. In particular, to build an EFT we must specify: its field content, the symmetries that must be respected and the power counting parameter δ. Finally, to write the Lagrangian we perform the following steps:

1. Write down all possible independent interaction terms allowed by the symmetries. This point is discussed in more detail at the end of the chapter.

2. Sort the terms by orders in the power counting.

3. Truncate the series at a desired order in δ.

The second step consists in the top-down approach, in which we compute the WCs in terms of the masses and couplings of a specific UV theory. This procedure is called matching and it is performed by integrating out the heavy particles of the UV theory. This can be done using either a diagrammatic approach or through the functional method. Later in this work we show an explicit example of the latter method, but for now we focus on the diagrammatic approach.
It is important to notice that different UV theories can have the same EFT as their low-energy limit; but the opposite is never true, different EFTs have necessarily different UV completions.

Before moving on to an explicit example, it is important to dedicate some time to understand why we choose dimensional regularization as a regulator and to summarize its key aspects.

2.2 Dimensional Regularizations

It is important to choose a good regulator for performing EFT calculations, because otherwise we end up with incorrect results. For example, this is the case when we use a cut-off. Let us consider the Lagrangian:

$$\mathcal{L} = \mathcal{L}_{D\leq 4} + \frac{c_6}{\Lambda^2}\frac{1}{6!}\phi^6. \tag{2.5}$$

The dimension 6 operator gives a contribution to the scattering $\phi\phi \to \phi\phi$ of the form:

$$\mathcal{A} = -\frac{c_6}{2\Lambda^2}\int \frac{d^4k}{(2\pi)^4}\,\frac{1}{k^2 - m_\phi^2} \tag{2.6}$$

We recall that the EFT is valid only for $k < \Lambda$, so we can choose the cut-off such that $\Lambda_c < \Lambda$. In the limit $m_\phi \ll \Lambda_c$ we have:

$$\mathcal{A} \approx -\frac{c_6}{2\Lambda^2}\frac{\Lambda_c^2}{16\pi^2}. \tag{2.7}$$

This result presents many issues:

- Since Λ_c is of the same order as Λ, it breaks down the expansion in $1/\Lambda$, leading to a violation of the power counting formula in eq.(2.3).
- Cut-offs do not allow to sum large logarithms, which is one of the main reasons we use EFTs in the first place.
- It violates a set of axioms for good regulators [32,33], in particular it breaks chiral and gauge symmetries.

For these reasons, we use dimensional regularization to perform EFT calculations. An example of an integral computed in dim-reg is [34]:

$$\begin{aligned} I &= \mu^{2\varepsilon}\int \frac{d^dk}{(2\pi)^d}\frac{1}{(k^2-M^2)^2} = \frac{i\mu^{2\varepsilon}}{(4\pi)^{2-\varepsilon}}\frac{\Gamma(\varepsilon)}{\Gamma(2)}(M^2)^{-\varepsilon} \\ &= \frac{i}{16\pi^2}\left(\frac{1}{\varepsilon}-\gamma+\log\frac{4\pi\mu^2}{M^2}+\mathcal{O}(\varepsilon)\right), \end{aligned} \tag{2.8}$$

where $d = 4-2\varepsilon$. In the $\overline{MS}$ renormalization scheme we have:

$$\mu^2 = \bar{\mu}^2\frac{e^\gamma}{4\pi} \tag{2.9}$$

and we can cancel the divergence $1/\varepsilon$ using a counterterm, so that we are left with the renormalized integral:

$$I + \text{c.t.} = \frac{i}{16\pi^2}\log\frac{\bar{\mu}^2}{M^2}. \tag{2.10}$$

Dim-reg has many important features that are desirable when performing EFT calculations:

- $\bar{\mu}^2$ does not appear in any power, just in logarithms.
- A property that we heavily rely on in the following sections is that scaleless integral vanish:

$$\mu^{2\varepsilon}\int\frac{d^dk}{(2\pi)^d}\frac{(k^2)^a}{(k^2)^b} = 0. \tag{2.11}$$

- There are no power divergences, since there is no dependence on any UV scale such as a cut-off, but only IR scales appear. For example:

$$\int \frac{d^d k}{(2\pi)^d} \frac{k^2}{(k^2-m^2)^2} = \frac{i\, m^2}{16\pi^2} \left(\frac{1}{\varepsilon} + \log \frac{\bar{\mu}^2}{m^2} + 1 + \mathcal{O}(\varepsilon) \right). \tag{2.12}$$

Evaluating integrals in dim-reg is similar to evaluating them by using the method of residues. Under the assumptions that the integrand vanishes sufficiently fast as $k \to \infty$, it can be written as the sum of the residues at the pole. The poles are determined solely by IR physical scales appearing in the denominators, so the results have no dependence on any unphysical UV scale (like when we used the cut-off Λ_c).

2.3 Matching a UV theory to an EFT

In this section we show an example of a matching procedure. We compute a two-scale loop integral using both the full theory and the EFT and then see how we can match the two results. Consider the integral in the full theory:

$$I_F = g^2 \mu^{2\varepsilon} \int \frac{d^d k}{(2\pi)^d} \frac{1}{(k^2-m^2)(k^2-M^2)}, \tag{2.13}$$

where we have set all external momenta to zero for simplicity. We also have $m \ll M$, so that m is the IR scale and M the UV scale. Computing the integral in dim-reg we get:

$$I_F = \frac{ig^2}{16\pi^2} \left(\frac{1}{\varepsilon} - \log \frac{M^2}{\bar{\mu}^2} + \frac{m^2}{M^2-m^2} \log \frac{m^2}{M^2} + 1 \right). \tag{2.14}$$

In order to evaluate the integral using the EFT we must integrate out the heavy particle, i.e. we must expand the heavy propagator in the limit $k/M \ll 1$:

$$\frac{1}{k^2-M^2} = -\frac{1}{M^2} \left(1 + \frac{k^2}{M^2} + \frac{k^4}{M^4} + ... \right). \tag{2.15}$$

Inserting this expansion in the integral we get:

$$\begin{aligned} I_{EFT} =& g^2 \mu^{2\varepsilon} \int \frac{d^d k}{(2\pi)^d} \frac{1}{(k^2-m^2)} \left(-\frac{1}{M^2} - \frac{k^2}{M^4} - \frac{k^4}{M^6} - ... \right) \\ =& \frac{ig^2 m^2}{16\pi^2 M^2} \left(-\frac{1}{\varepsilon} + \log \frac{m^2}{\bar{\mu}^2} - 1 \right) + \frac{ig^2 m^4}{16\pi^2 M^4} \left(-\frac{1}{\varepsilon} + \log \frac{m^2}{\bar{\mu}^2} - 1 \right) \\ &+ \frac{ig^2 m^6}{16\pi^2 M^6} \left(-\frac{1}{\varepsilon} + \log \frac{m^2}{\bar{\mu}^2} - 1 \right) + ... \\ =& \frac{ig^2}{16\pi^2} \left(-\frac{1}{\varepsilon} \frac{m^2}{M^2-m^2} + \frac{m^2}{M^2-m^2} \log \frac{m^2}{\bar{\mu}^2} - \frac{m^2}{M^2-m^2} \right). \end{aligned} \tag{2.16}$$

Looking at the two results we can make some important observations:

- The first thing we can notice is that $I_F \neq I_{EFT}$. Their difference $I_F - I_{EFT} = I_M$ comes from the UV part of the integral and it is local (i.e. analytic) in the IR parameter m. I_M is called matching contribution to the Lagrangian and it is included in the EFT result by absorbing it into shifts of the EFT Lagrangian coefficients.

- The $\log m^2$ terms, which are non-analytical in the IR scale, agree in both theories. This is correct because the purpose of EFTs is precisely to describe the physics at low energies, so the dependence of I_F on the IR scale must be reproduced.

- The $\log M^2$ terms, which are non-analytical in the UV scale, are present just in I_F. In fact, we obtained I_{EFT} by performing an expansion in $1/M$, eliminating all non-analyticities in M.

- I_F has a $\log(M^2/m^2)$ term, which contains a ratio between the UV and IR scales. This types of logs can be summed using the RGE in the EFT.

Let us now focus on the matching contribution. Taking the expressions in eq.(2.14) and eq.(2.16) and adding the counterterms to renormalize them, we have::

$$\begin{aligned} I_M &= (I_F + I_{F,c.t.}) - (I_{EFT} + I_{EFT,c.t.}) \\ &= \frac{ig^2}{16\pi^2}\left[\left(\log\frac{\bar{\mu}^2}{M^2}+1\right) + \frac{m^2}{M^2}\left(\log\frac{\bar{\mu}^2}{M^2}+1\right) + ...\right]. \end{aligned} \tag{2.17}$$

We now illustrate the "method of regions", which is a simpler way to evaluate I_M that does not require us to compute both I_F and I_{EFT} and then take the difference.

Method of Regions

Looking at eq.(2.13) we see that I_F is divergent in two different regions:

$$\begin{aligned} k \sim m \ll M \quad &\rightarrow \quad \text{soft region} \\ m \ll k \sim M \quad &\rightarrow \quad \text{hard region} \end{aligned}$$

The method of regions [35] tells us that we can compute the integral in eq.(2.13) by expanding it in both the soft and the hard region and then summing the two results. First of all, we can rewrite eq.(2.13) as:

$$I_F = \frac{g^2\mu^{2\varepsilon}}{M^2-m^2}\int\frac{d^dk}{(2\pi)^d}\left(\frac{1}{k^2-M^2}-\frac{1}{k^2-m^2}\right). \tag{2.18}$$

Now we can start by expanding I_F in the soft region $k \ll M$, which we point out is also the EFT expansion:

$$\begin{aligned} I_F^{\text{soft}} = I_{EFT} &= \frac{g^2\mu^{2\varepsilon}}{M^2-m^2}\int \frac{d^dk}{(2\pi)^d}\left[-\frac{1}{M^2}\left(1+\frac{k^2}{M^2}+\frac{k^4}{M^4}+...\right)-\frac{1}{k^2-m^2}\right] \\ &= -\frac{ig^2}{16\pi^2}\frac{m^2}{M^2-m^2}\left(\frac{1}{\varepsilon}+1+\log\frac{\bar{\mu}^2}{m^2}\right). \end{aligned} \tag{2.19}$$

The next step is to expand I_F in the hard region $k \ll m$:

$$\begin{aligned} I_F^{\text{hard}} &= \frac{g^2\mu^{2\varepsilon}}{M^2-m^2}\int \frac{d^dk}{(2\pi)^d}\left[\frac{1}{k^2-M^2}+\frac{1}{k^2}\left(1+\frac{m^2}{k^2}+\frac{m^4}{k^4}+...\right)\right] \\ &= \frac{ig^2}{16\pi^2}\frac{M^2}{M^2-m^2}\left(\frac{1}{\varepsilon}+1+\log\frac{\bar{\mu}^2}{M^2}\right). \end{aligned} \tag{2.20}$$

Computing $I_F^{\text{soft}} + I_F^{\text{hard}}$ and confronting the result with eq.(2.14) we can see that:

$$I_F^{\text{soft}} + I_F^{\text{hard}} = I_F. \tag{2.21}$$

As previously mentioned, we also have that $I_F^{\text{soft}} = I_{EFT}$. It is interesting to see what happens when we apply the method of regions to I_{EFT}. Since I_{EFT} is already expanded in the soft region, i.e. it is non-analytical only in the IR scale, let us consider the expansion in the hard region:

$$\begin{aligned} I_{EFT}^{\text{hard}} &= \frac{g^2\mu^{2\varepsilon}}{M^2-m^2}\int \frac{d^dk}{(2\pi)^d}\left[\left(-\frac{1}{M^2}-\frac{k^2}{M^4}-\frac{k^4}{M^6}-...\right)+\left(\frac{1}{k^2}+\frac{m^2}{k^4}+\frac{m^4}{k^6}+...\right)\right] \\ &= 0. \end{aligned} \tag{2.22}$$

The reason why I_{EFT}^{hard} vanishes is because every term in eq.(2.22) is a scaleless integral, that when computed in dim-reg gives precisely zero, so we can write:

$$I_F = I_F^{\text{soft}} + I_F^{\text{hard}} = (I_{EFT}^{\text{hard}} + I_{EFT}^{\text{soft}}) + I_F^{\text{hard}} = I_{EFT}^{\text{soft}} + I_F^{\text{hard}}. \tag{2.23}$$

This is a very non-trivial result, because I_{EFT}^{soft} and I_F^{hard} are different expansions of the same quantity I_F, so we could think that their sum would give $2I_F$, but from eq.(2.23) we see that this is not the case. We recall that we got I_{EFT}^{soft} by expanding in $k \ll M$ and I_F^{hard} by expanding in $m \ll k$, so it might seem like we have double-counted the region $m \ll k \ll M$. However, the contribution in this region from I_{EFT} is precisely I_{EFT}^{hard}, which we have seen vanishes in dim-reg.

Finally, let us consider the matching contribution. Using the first line in eq.(2.17) and eq.(2.23) we have (up to counter terms):

$$I_M = I_F - I_{EFT} = I_F^{\text{soft}} + I_F^{\text{hard}} - I_F^{\text{soft}} = I_F^{\text{hard}}. \tag{2.24}$$

We can conclude that in order to get the matching contribution it is sufficient to expand I_F in the IR scale, without having to compute I_{EFT}. Moreover, we notice that even if I_F and I_{EFT} are non-analytic in m, their difference is analytical (i.e. local) in m, so it can be matched to the local EFT Lagrangian.

At the beginning of this chapter we have mentioned that EFTs allow us to turn IR poles of the full theory in UV poles in the EFT, and now we show how. Before renormalization, we can write a general EFT amplitude as:

$$I^E = \left(\frac{A^E}{\varepsilon_{UV}} + \frac{B}{\varepsilon_{IR}} + C^E\right) + \left(\frac{A^E}{\varepsilon_{UV}} - \frac{A^E}{\varepsilon_{IR}}\right), \tag{2.25}$$

where the terms in the first bracket are the soft region contribution, while the ones in the second bracket correspond to the hard region. As we previously showed, the EFT contribution in the hard region vanishes, in fact it has no finite part C^E, but just the divergences, for which we have $\varepsilon_{UV} = \varepsilon_{IR}$. Similarly, we can write a general amplitude for the full theory as:

$$I^F = \left(\frac{D^F}{\varepsilon_{UV}} + \frac{B}{\varepsilon_{IR}} + C_s^F\right) + \left(\frac{A^F}{\varepsilon_{UV}} - \frac{D^F}{\varepsilon_{IR}} + C_h^F\right). \tag{2.26}$$

We notice that in general the UV poles of the two theories A^E and A^F are different, so they have to be renormalized independently. Using the fact that soft regions must agree in both theories, we find that:

$$A^E = D^F, \quad C^E = C_s^F. \tag{2.27}$$

This way, we have turned the IR pole of the full theory D^F into the UV pole of the EFT A^E. By doing this we can turn IR logs into UV logs that can be summed using the renormalization group equations of the EFT, that we present in the next section.

2.4 RG Improved Perturbation Theory

At the beginning of the previous section we computed I_F in the full theory and we got eq.(2.14). In the result we see a term like $\log(m^2/M^2)$, which contains the ratio between the IR and the UV scale. At higher order, we get corrections like:

$$\left(\frac{g^2}{16\pi^2}\log\frac{m^2}{M^2}\right)^n. \tag{2.28}$$

If $M \gg m$, perturbation theory is spoiled when $(g^2/16\pi^2)\log(M^2/m^2) \sim 1$. However, after performing the matching procedure, we see that the log is split in two pieces:

$$\log\frac{m^2}{M^2} = \log\frac{m^2}{\bar{\mu}^2} - \log\frac{M^2}{\bar{\mu}^2}. \tag{2.29}$$

The first term is contained in the EFT result eq.(2.16) and second one is in the matching contribution eq.(2.17). In this way, instead of having to compute a two-scale calculation we are left with two one-scale calculations, which are much easier to deal with. In particular, we evaluate I_M at $\bar{\mu} \sim M$ and I_{EFT} at $\bar{\mu} \sim m$, and the change in $\bar{\mu}$ is taken care by the renormalization group equations in the EFT.

There are two types of RGs [36]. One is the "Wilsonian RG" [37], which is based on an intuitive approach that however breaks gauge invariance, since it introduces a hard cut-off. The RG that we use instead is the so called "continuum RG", which is a version of the RG compatible with dim-reg.

Let us start by deriving the renormalization group equations [38]. A bare Wilson coefficient C^0 is renormalized by introducing a counterterm such that:

$$C^0 = Z\mu^{n\varepsilon} C^r. \tag{2.30}$$

For a perturbative model we have:

$$Z = 1 + \mathcal{O}(C^r, \alpha^r). \tag{2.31}$$

The Callan-Symanzik equation [39–41] tells us that the bare Lagrangian cannot have any dependence on the unphysical RG parameter $\bar{\mu}$:

$$\bar{\mu}\frac{d}{d\bar{\mu}} C^0 = \bar{\mu}\frac{d}{d\bar{\mu}} \left(Z\mu^{n\varepsilon} C^r\right) = 0. \tag{2.32}$$

Working out the calculations we find that the RGE can be written as:

$$\frac{d}{d\log\bar{\mu}^2} C_n^r = \gamma_{nm} C_m^r, \tag{2.33}$$

where γ_{nm} is the anomalous dimension that accounts also for quantum effects and operator mixing. Its role is to account for the small change in the mass dimension of a WC as it is evolved from a high scale $\bar{\mu}_H$ to a low scale $\bar{\mu}_L$. From eq.(2.33) we see that in order to sum large logs of the form $\log(M^2/m^2)$, it is necessary to split them in pieces with an explicit dependence on $\bar{\mu}$, just like we did in the matching procedure.

Now we proceed by considering a toy model to give an explicit example of how we can sum large logs. In particular, we use a single particle EFT with the interaction Lagrangian:

$$\mathcal{L}_{int}^{EFT} = -\frac{1}{4!} C_4 \phi^4, \tag{2.34}$$

then we compute the amplitude of the process $\phi\phi \to \phi\phi$ at the scale $\bar{\mu}_H$ up to 1-loop precision. From the 1-loop contributions we generate the logs that we then sum by

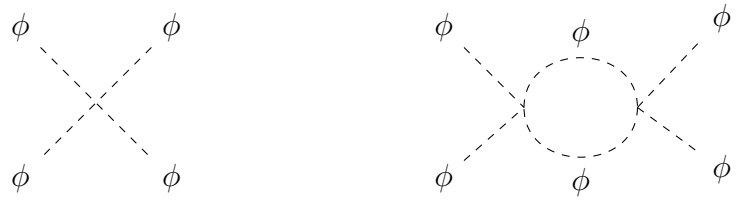

Figure 2.1: Tree-level and 1-loop diagrams contributing to $\phi\phi \to \phi\phi$.

running from $\bar{\mu}_H^2$ to $\bar{\mu}_L^2$. In Fig.2.1 we can see the two diagrams that contribute to the process we are interested in. The total renormalized amplitude is:

$$i\mathcal{A}^{EFT} = i\mathcal{A}^{EFT}_{tree-lev.} + i\mathcal{A}^{EFT}_{1-loop} = -iC_4^r \left[1 - \frac{3}{32\pi^2} C_4^r \left(\log \frac{\bar{\mu}_H^2}{m^2} - \frac{2}{3}\right)\right]. \tag{2.35}$$

We see that if $\bar{\mu}_H \gg m$ the perturbative expansion breaks down, but we later show that using the summing technique we presented above it is possible to have a well behaved expansion across a wider range of scales. The anomalous dimension of C_4 turns out to be [38]:

$$\gamma_{44} = \frac{3}{32\pi^2} C_4^r. \tag{2.36}$$

Inserting this expression in eq.(2.33) we get the RGE that runs C_4^r:

$$\frac{d}{d\log\bar{\mu}^2} C_4^r = \frac{3}{32\pi^2} (C_4^r)^2. \tag{2.37}$$

This RGE can be solved by performing the integration:

$$\int_{C_4^r(\bar{\mu}_L)}^{C_4^r(\bar{\mu}_H)} \frac{dC_4^r}{(C_4^r)^2} = \frac{3}{32\pi^2} \int_{\bar{\mu}_L^2}^{\bar{\mu}_H^2} d\log\bar{\mu}^2 \quad \to \quad C_4^r(\bar{\mu}_L) = \frac{C_4^r(\bar{\mu}_H)}{1 + C_4^r(\bar{\mu}_H)\frac{3}{32\pi^2}\log\frac{\bar{\mu}_H^2}{\bar{\mu}_L^2}}. \tag{2.38}$$

This calculation gives us a running coupling, and using it to perform EFT calculations is called "RG improved" perturbation theory. Now we have a well behaved theory for any choice of the low scale $\bar{\mu}_L$. However, it is still possible to break the perturbative regime. Inverting the last expression in eq.(2.38) we get:

$$\bar{\mu}_H^2 = \bar{\mu}_L^2 \exp\left(\frac{1 - \frac{C_4^r(\bar{\mu}_L)}{C_4^r(\bar{\mu}_H)}}{\frac{3}{32\pi^2} C_4^r(\bar{\mu}_L)}\right). \tag{2.39}$$

We enter the non-perturbative regime at the scale $\bar{\mu}_H = \Lambda_{pole}$ such that $C_4^r(\Lambda_{pole}) \to \infty$. This condition automatically defines Λ_{pole}, known as the Landau pole, as:

$$\Lambda_{pole}^2 = \bar{\mu}_L^2 \exp\left(\frac{1}{\frac{3}{32\pi^2} C_4^r(\bar{\mu}_L)}\right). \tag{2.40}$$

In conclusion, we can say that even if cannot make predictions at arbitrarily high energy as shown by eq.(2.40), RG improvement still gives us a very large range of validity for our EFT. This method can be generalized to more complicated situations, but from this toy model we were able to get the key points and understand the power of RG improved perturbation theory.

2.5 The SMEFT

Even though we are (almost) certain of the existence of some heavy Beyond the Standard Model physics, we can still use the SM to make good predictions without any knowledge of what happens at higher energies. This is because of the decoupling theorem [42], which is the reason why EFTs are valid theories: if we work at a certain scale, we are not sensitive to the physics at much higher energies.

There are two ways to formulate the Standard Model as an EFT. If the SM Higgs doublet is present in the EFT construction we have the Standard Model EFT (SMEFT), otherwise we have the Higgs EFT (HEFT). In this work we use the SMEFT as framework and we now illustrate its main features. See Refs. [43,44] for recent SMEFT reviews.

The SMEFT is an EFT constructed with the SM fields, the SM gauge symmetries and canonical dimension as the power counting parameter. It is built using the bottom-up approach: we know that the SM is the low energy limit, but we do not know what the UV physics is. This way, we get a general description, in terms of higher-dimensional operators, of the effects generated by integrating out heavy degrees of freedom that are a priori unknown. The general SMEFT Lagrangian can be written as:

$$\mathcal{L}_{SMEFT} = \mathcal{L}_{SM} + \frac{\mathcal{L}_5}{\Lambda} + \frac{\mathcal{L}_6}{\Lambda^2} + \frac{\mathcal{L}_7}{\Lambda^3} + \frac{\mathcal{L}_8}{\Lambda^4} + \dots , \tag{2.41}$$

where the terms $\mathcal{L}_{D\geq 5}$ are the ones that capture potential BSM effects. This formulation of the SMEFT is valid only if up to $\sim$ 100 GeV the only particles are the ones of the SM and if the BSM physics is nearly decoupled. if we discovered some particle below the GeV scale, then we would have to modify the SMEFT accordingly.

It is important to notice that if the SM were the ultimate theory of nature, then we would not have any $D \geq 5$ operator. Instead, if some BSM physics exists, then we necessarily have some $\mathcal{L}_{D\geq 5} \neq 0$. On the other hand, from a top-down perspective, every BSM theory must have the SMEFT as its low-energy limit, no other operators are allowed. This is why EFT techniques are such a good tool to investigate potential BSM phenomena.

2.5.1 Constructing Operator Bases

If for every dimension $D \geq 5$ we write down all the allowed interaction terms made of SM fields, we would get hundreds of them. However, a lot of them are redundant, meaning that they bring the same physical effect of a linear combination of other operators. We must remove such redundancies and we can do it in several ways:

(a) *Integration by parts.* The action $S = \int \mathrm{d}^4x\, \mathcal{L}$ is always invariant under integration by parts (IBP). In QFT we generally assume that the field configurations that describe physical states vanish sufficiently fast at infinity (except for some non-perturbative configurations like instantons). Under this assumption, we can neglect total derivatives when performing IBP, since their contribution to the action vanishes. For example, we can write the kinetic therm of the Higgs in two equivalent ways:

$$(D_\mu H)^\dagger (D^\mu H) = -H^\dagger D^2 H. \tag{2.42}$$

We can do the same for higher-dimensional operators.

(b) *Field redefinitions.* The LSZ reduction formula [45] allows us to perform field redefinitions, as long as they still create correctly all the relevant states from the vacuum. Doing this has no effect on the physical observables, which remain unchanged [46–48]. In many cases, including the SMEFT, using the equations of motion is equivalent (at leading order) as performing a field redefinition. In particular, we can redefine a field as:

$$\phi \to \tilde{\phi} = \phi + \varepsilon\, \delta\phi \quad \text{with} \quad \varepsilon \ll 1. \tag{2.43}$$

Expanding the shifted action around ϕ we get:

$$\begin{aligned} S[\phi] \to S[\tilde{\phi}] &= S[\tilde{\phi}]\,\big|_{\tilde{\phi}=\phi} + \varepsilon \frac{\delta S[\tilde{\phi}]}{\delta \tilde{\phi}}\bigg|_{\tilde{\phi}=\phi} \delta\phi + \mathcal{O}(\varepsilon^2) \\ &= S[\phi] + \varepsilon \int \mathrm{d}^4x\, E[\phi]\, \delta\phi + \mathcal{O}(\varepsilon^2), \end{aligned} \tag{2.44}$$

where $E[\phi]$ are the equations of motion of the field ϕ. The two generating functionals $Z[J]$ and $\tilde{Z}[J]$ yield the same S-matrix element. We recall that the generating functional is defined as:

$$Z[J] = \int \mathcal{D}\phi\, \exp\left(iS[\phi] + \int \mathrm{d}^4x\, J\phi \right). \tag{2.45}$$

(c) *Fierz identities.* We can use Fierz identities of the Lorentz group [49] to rearrange the order of the spinors appearing in four-fermion operators. Consider the chiral

basis for the Dirac algebra in four spacetime dimensions:

$$\{\Gamma^n\} = \{P_L, P_R, \gamma^\mu P_L, \gamma^\mu P_R, \sigma^{\mu\nu}\} \tag{2.46}$$

$$\{\widetilde{\Gamma}_n\} = \{P_L, P_R, \gamma_\mu P_L, \gamma_\mu P_R, \sigma_{\mu\nu}\}. \tag{2.47}$$

The chiral Fierz identities can than be written as [50]:

$$(\Gamma^A)[\Gamma^B] = \frac{1}{4}\,\mathrm{Tr}\{\Gamma^A\widetilde{\Gamma}_C\Gamma^B\widetilde{\Gamma}_D\}(\Gamma^D)[\Gamma^C), \tag{2.48}$$

where the parentheses ( ) and brackets [ ] indicate matrix indices, such that each parenthesis/bracket represents a different index in an unambiguous way. One example of application of a Fierz identity is:

$$(\bar{\ell}^i\gamma^\mu q_i)(\bar{d}\gamma_\mu e) = -2\,(\bar{\ell}^i e)(\bar{d}q_i). \tag{2.49}$$

Using these techniques, we can construct for each $\mathcal{L}_{D\geq 5}$ a basis of operators, i.e. a set of operators which is complete and non-redundant. At $D = 5$ we have that the only allowed term is the Weinberg operator:

$$\mathcal{L}_5 = \frac{C_5}{\Lambda}(\bar{\ell_L^c}\widetilde{H}^*)(\widetilde{H}^\dagger\ell_L) + h.c.\,. \tag{2.50}$$

We notice that this operator violates the lepton number symmetry by two units. In general, it can be proven that any odd-dimension SMEFT operator violates baryon (B) and/or lepton (L) number [51]. We know that B and L are accidental symmetries in the SM, however if the are not respected in the UV, we expect them to be violated by the higher-dimensional SMEFT operators.

The first attempt at constructing a basis for $\mathcal{L}_{D\geq 6}$ was done by Buchmüller and Wyler [52], however their result was overcomplete. The actual basis was found in 2010 by Grzadkowski, Iskrzyński, Misiak, and Rosiek [53]. Today it is referred to as the "Warsaw basis" and it is the most used one. To construct this specific basis, we use IBP and equations of motion to remove operators with more derivatives in favour of operators with fewer derivatives. Then we use the Fierz identities such that: leptons and quarks do not appear in the same fermion currents, the gauge indices of the largest gauge group are contracted within each bilinear, each current is a Hypercharge singlet. So far, we have constructed the bases for $\mathcal{L}_5$, $\mathcal{L}_6$, $\mathcal{L}_7$, $\mathcal{L}_8$, $\mathcal{L}_9$, $\mathcal{L}_{10}$, $\mathcal{L}_{11}$, $\mathcal{L}_{12}$ [52–61].

Chapter 3

The Problem of Neutrino Masses

The Standard Model Lagrangian $\mathcal{L}_{SM}$ does not contain a mass term of any kind for neutrinos and the reason is that in the SM we work under the assumption that the right-handed component of the neutrino does not exist. However, from experimental measurements of solar neutrino flux and neutrino oscillation, we strongly believe that at least 2 of the light neutrinos must be massive, so we must include a mass term in $\mathcal{L}_{SM}$. All the other SM fermions (quarks and charged leptons) have a Dirac mass term in $\mathcal{L}_{SM}$, but this is not the only possibility. In this chapter we present all possible mass terms for fermion fields and we introduce the Seesaw mechanisms, which are the most popular solution for generating neutrino masses. See Ref. [62, 63] for comprehensive reviews of neutrino physics.

3.1 Possible Fermion Mass Terms

As we said, there are different ways to write a mass term for fermion field. In particular, we can have a Dirac mass, a Majorana mass or even both terms, depending on the nature of the spinor.

3.1.1 Dirac Mass

As mentioned above, quarks and charged leptons are Dirac spinors, which means that they can be generically written as:

$$\psi = \psi_L + \psi_R, \tag{3.1}$$

where ψ_L and ψ_R are the left-handed (LH) and right-handed (RH) Weyl components respectively and together they form the 4-dimensional Dirac spinor ψ. We can write the Weyl components as:

$$\psi_L = P_L\psi, \quad \psi_R = P_R\psi, \tag{3.2}$$

where P_L and P_R are projection operators that can be written as:

$$P_L = \frac{1}{2}(1-\gamma_5), \quad P_R = \frac{1}{2}(1+\gamma_5). \tag{3.3}$$

In Appendix B we show the algebra of the gamma matrices and we present some useful relations that are used to derive the following results. Using these properties, we can write the free fermion Lagrangian in terms of Weyl components. For simplicity, let us start with the case of just one flavour:

$$\mathcal{L}_{kin} = \bar{\psi} i\gamma^\mu \partial_\mu \psi = \bar{\psi} i\gamma^\mu \partial_\mu (P_L\psi + P_R\psi) = \bar{\psi_L} i\gamma^\mu \partial_\mu \psi_L + \bar{\psi_R} i\gamma^\mu \partial_\mu \psi_R, \tag{3.4}$$

$$\mathcal{L}_{mass} = -m\,\bar{\psi}\psi = -m\,\psi^\dagger \gamma^0 (P_L\psi + P_R\psi) = -m\,(\bar{\psi_R}\psi_L + \bar{\psi_L}\psi_R). \tag{3.5}$$

From the expression in $\mathcal{L}_{mass}$ it is clear that if ν_R does not exist (as we assume in the SM), neutrinos cannot have a Dirac mass term. Now, considering the case with N flavours we have:

$$\mathcal{L}_{free} = \bar{\psi_L} i\mathbb{1}\partial\!\!\!/ \psi_L + \bar{\psi_R} i\mathbb{1}\partial\!\!\!/ \psi_R - (\bar{\psi_L} M \psi_R + h.c.), \tag{3.6}$$

where $\mathbb{1}$ is the $N \times N$ identity matrix and M is the mass matrix, which is in general a complex and non diagonal $N \times N$ matrix. M can always be diagonalized and made real via the rotation:

$$M_{diag} = U_L^\dagger M U_R \quad \text{with} \quad U_{L,R} \in SU(N). \tag{3.7}$$

Rotating also the Weyl spinors as:

$$\begin{cases} \psi_L = U_L \psi'_L \\ \psi_R = U_R \psi'_R \end{cases}, \tag{3.8}$$

we get the diagonal free Lagrangian (where we omitted the prime):

$$\mathcal{L}_{free} = \bar{\psi_L} i\mathbb{1}\partial\!\!\!/ \psi_L + \bar{\psi_R} i\mathbb{1}\partial\!\!\!/ \psi_R - (\bar{\psi_L} M_{diag} \psi_R + h.c.). \tag{3.9}$$

There are two important things to notice:

- $\mathcal{L}_{free}$ can always be made diagonal simultaneously. However, if we consider also the interaction Lagrangian, we can have some mixing left. For example, consider the charged current Lagrangian:

  $$\mathcal{L}_{cc} \supset -\frac{g}{\sqrt{2}} W_\mu^+ \bar{u}_L \gamma^\mu d_L + h.c.. \tag{3.10}$$

  Rotating the the fields of the up and down quark as described above, we get:

  $$\mathcal{L}_{cc} \supset -\frac{g}{\sqrt{2}} W_\mu^+ \bar{u}_L (U_u^\dagger U_d) \gamma^\mu d_L + h.c., \tag{3.11}$$

  where $U_u^\dagger U_d = V_{CKM} \in SU(3)$ is a unitary 3×3 matrix which can be parametrized as a complex rotation by three real angles $\theta_{1,2,3}$ and a complex phase δ. V_{CKM} is not diagonal, so we have some mixing left.

- $\mathcal{L}_{free}$ conserves any charge. ψ_L and ψ_R carry the same charge as ψ, so the term $\bar{\psi}_L\psi_R$ is indeed neutral. One important example of a charge which is conserved by a Dirac mass term is lepton number, which as we shall see can be broken by a different mass term.

3.1.2 Majorana Mass

As we previously mentioned, a Dirac mass term is not the only possibility. Since neutrinos are the only SM fermions that are eligible to be Majorana particles, we now show how to write a Majorana mass term. Majorana particles, are defined by the Majorana condition:

$$\chi = \chi^c, \tag{3.12}$$

where c denotes the charge conjugation; in Appendix B we show some useful relations. In terms of Weyl components, the Majorana spinor becomes:

$$\chi = \chi_L + \chi_L^c. \tag{3.13}$$

Opposed to a Dirac spinor, the Weyl components of a Majorana spinor are not independent, so it it has just 2 instead of 4 independent components. It easy to see that a spinor defined as in eq.(3.13) satisfies the Majorana condition in eq.(3.12). The free Lagrangian for a Majorana fermion with N flavours is:

$$\mathcal{L}_{free} = \frac{1}{2}\bar{\chi} i\mathbb{1}\partial\!\!\!/\chi - \frac{1}{2}\bar{\chi}M\chi, \tag{3.14}$$

which in Weyl components reads:

$$\mathcal{L}_{free} = \frac{1}{2}\bar{\chi_L} i\mathbb{1}\partial\!\!\!/\chi_L + \frac{1}{2}\bar{\chi_L^c} i\mathbb{1}\partial\!\!\!/\chi_L^c - \frac{1}{2}(\bar{\chi_L^c}M\chi_L + h.c.). \tag{3.15}$$

Notice that in this case we have some extra $1/2$ factors, that were not present in the Lagrangian of a Dirac spinor. The relation between Dirac and Majorana fermions is similar to the one between complex and real scalars. The mass matrix of a Majorana field is a complex symmetric $N \times N$ matrix which can be made diagonal and real via:

$$M_{diag} = U^T M U \quad \text{with} \quad U \in SU(N). \tag{3.16}$$

Unlike for the Dirac case, now M is diagonalized with a single unitary matrix U instead of two. This is due to the fact that the Weyl components are not independent from one another, (so they cannot be rotated separately) and to the fact that we have $M = M^T$. In particular, performing the field rotation:

$$\chi_L = U\chi_L' \quad \rightarrow \quad \bar{\chi_L^c} = \bar{\chi_L^c}' U^T, \tag{3.17}$$

We get the diagonal Lagrangian (where again we omit the prime):

$$\mathcal{L}_{free} = \frac{1}{2}\bar{\chi_L} i\not{\partial} \chi_L + \frac{1}{2}\bar{\chi_L^c} i\not{\partial} \chi_L^c - \frac{1}{2}(\bar{\chi_L^c} M_{diag} \chi_L + h.c.). \tag{3.18}$$

Also in this case there are some important comments to be made:

- If neutrinos had a mass term (of any kind), this would lead to a mixing in the charged currents and we would have the same exact situation as we had in the quark sector:

$$\mathcal{L}_{cc} \supset -\frac{g}{\sqrt{2}} W_\mu^- \bar{e}_L (U_e^\dagger U_\nu) \gamma^\mu \nu_L + h.c., \tag{3.19}$$

  where $(U_e^\dagger U_\nu) = U_{PMNS} \in SU(3)$ is the equivalent of V_{CKM} and can be parametrized in the same way. If neutrinos are Majorana fermions (so that their RH component would be ν_L^c), the total mixing matrix has two additional independent Majorana phases $\alpha_{1,2}$:

$$U_{tot} = U_{PMNS}\, \mathrm{diag}(1, e^{i\alpha_1}, e^{i\alpha_2}). \tag{3.20}$$

- A very important property of a Majorana spinor is that it is not a charge eigenstate (unlike a Dirac fermion), because it is a superposition of oppositely charged states.Its components however can carry a charge and if they do, it is always violated by two units by the Majorana mass term. For this reason, if they carry a charge which is associated to an exact symmetry of the theory, then the Majorana mass term is forbidden. In order to write a mass term of this kind, the filed must be neutral under all the exact symmetries. The only SM field that satisfies this requirement is the neutrino.

3.1.3 Dirac + Majorana Mass

The most general mass term we can write is by including both Dirac and Majorana masses in the Lagrangian:

$$\mathcal{L}_{mass} = -\frac{1}{2}\bar{\psi_L^c} M_L \psi_L - \frac{1}{2}\bar{\psi_R} M_R \psi_R^c - \bar{\psi_R} m_D \psi_L + h.c., \tag{3.21}$$

however from this expression it is not clear whether the mass eigenstate in a Dirac or Majorana fermion. Diagonalizing the mass matrix we get:

$$\mathcal{L}_{mass} = -\frac{1}{2}\bar{n_L^c} M n_L + h.c., \tag{3.22}$$

with

$$n_L = \begin{pmatrix} \psi_L \\ \psi_R^c \end{pmatrix}, \quad n_R = n_L^c = \begin{pmatrix} \psi_L^c \\ \psi_R \end{pmatrix} \quad \text{and} \quad M = \begin{pmatrix} M_L & m_D^T \\ m_D & M_R \end{pmatrix}. \tag{3.23}$$

Since $M = M^T$ and $n = n_L + n_L^c = n^c$, we see that the mass term corresponds to the one of a Majorana field. To get the mass eigenstates, we can diagonalize M as we previously did for the Majorana mass using a rotation matrix $U \in SU(N_R + N_L)$, where N_R and N_L are the numbers of RH and LH fields respectively.

3.2 Possible Scenarios for Neutrinos

The SM does not contain a mass term for neutrinos because of the absence of the RH counterpart of ν_L. As we showed in previous section, we can write the RH Weyl component of light neutrinos either as ν_R or ν_L^c, depending on how we want to build the mass term. In particular, the two choices we must make is whether we want to allow for the presence of ν_R and whether we want the lepton number symmetry to be conserved. In Tab.3.1 we show all possible scenarios.

	Forbid light ν_R	**Admit light** ν_R
Conserve L	*Scenario A*	*Scenario B*
Violate L	*Scenario C*	*Scenario D*

Table 3.1: Possible options for building neutrino masses.

(a) *Scenario A*. This scenario corresponds to the Standard Model as it is, without any mass term for neutrinos. This possibility however is ruled out by experiments.

(b) *Scenario B*. In this scenario we are adding ν_R to the SM particle content as a gauge singlet under the SM gauge group. Since we want L to be conserved we cannot have a Majorana mass, but just a Dirac mass. This would make the neutrino a Dirac fermion, just like charged leptons and quarks, with a mass term like:

$$\mathcal{L}_{mass} = -\bar{\nu_R} Y_\nu \widetilde{H}^\dagger \ell_L + h.c. \overset{\text{EWSB}}{=} -\bar{\nu_R} m_\nu \nu_L + h.c. \quad \text{with} \quad m_\nu = \frac{Y_\nu v}{\sqrt{2}}. \tag{3.24}$$

The upsides of this scenario are that the mass term is renormalizable and that there are no Majorana phases. However, if this were the case, the Yukawa coupling should be much smaller that the ones for all other SM fermions, and there is no way to justify such hierarchy.

(c) *Scenario C*. In this scenario we forbid the presence of ν_R, so the only possibility is to have a Majorana mass term for the neutrino. It is possible to write such mass

term at dim-5 in the SMEFT through the Weinberg operator:

$$\mathcal{L}_{mass} = \frac{C_5}{\Lambda}(\bar{\ell_L^c}\widetilde{H}^*)(\widetilde{H}^\dagger \ell_L) + h.c. \overset{\text{EWSB}}{=} \frac{v^2}{2\Lambda}\bar{\nu_L^c} C_5 \nu_L + h.c. \tag{3.25}$$

This is the minimal and most natural explanation for the smallness of m_ν, that is suppressed by the mass scale Λ, which is also the scale of lepton number violation.

(d) *Scenario D.* In this scenario, since we admit both ν_R and L violation, we write all possible Dirac and Majorana mass terms:

$$\begin{aligned}\mathcal{L}_{mass} &= -\bar{\nu_R} Y_\nu \widetilde{H}^\dagger \ell_L + \frac{C_5}{\Lambda}(\bar{\ell_L^c}\widetilde{H}^*)(\widetilde{H}^\dagger \ell_L) - \frac{1}{2}\bar{\nu_R} m_R \nu_R^c + h.c. \\ &\overset{\text{EWSB}}{=} -\bar{\nu_R}\frac{Y_\nu v}{\sqrt{2}}\nu_L + \frac{v^2}{2\Lambda}\bar{\nu_L^c} C_5 \nu_L - \frac{1}{2}\bar{\nu_R} m_R \nu_R^c + h.c.\,,\end{aligned} \tag{3.26}$$

where $m_R = m_R^T$, $C_5 = C_5^T$ and Y_ν are complex 3×3 matrices. $\mathcal{L}_{mass}$ can be written as in eq.(3.22), with:

$$n_L = \begin{pmatrix}\nu_L \\ \nu_R^c\end{pmatrix} \quad \text{and} \quad M = \begin{pmatrix} m_L & m_D^T \\ m_D & m_R \end{pmatrix}, \tag{3.27}$$

where $m_D = Y_\nu v/\sqrt{2}$ and $m_L = v^2 C_5/\Lambda$. The issue with this scenario is that for $m_R \sim$ eV, it predicts the existence of light sterile neutrino, which do not contribute to EW interactions. This scenario has been vastly studied because of the discovery of some possible signals, that however have never been confirmed. If instead m_R is a heavier mass scale, we get the Seesaw models, that are discussed in the following section.

3.3 Seesaw Models

The Seesaw mechanisms are to this day the most popular UV completions of the Weinberg operator in the *Scenario C* that we previously presented. The idea behind this models is similar to one used for the Fermi theory, where a 4-fermion interaction at low energies is mediated by a new particle at tree-level at higher energies. The Seesaw models differ form one another by the type of new mediator they introduce, but they are all based on the same logic. At tree-level, the Weinberg operator gives the interaction shown in Fig.3.1. All possible tree-level UV completion [64] are represented by the three "vanilla" options:

- Type 1 Seesaw [65–68] $\rightarrow$ introduces a heavy fermion singlet N.
- Type 2 Seesaw [69–72] $\rightarrow$ introduces a heavy scalar $SU(2)$ triplet Δ.

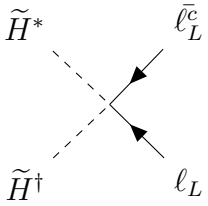

Figure 3.1: Weinberg operator at tree-level.

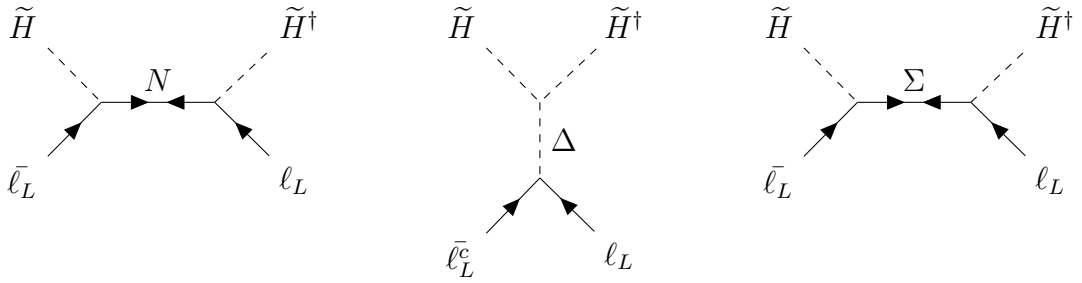

Figure 3.2: Tree-level diagram of Type 1,2,3 Seesaw models, from left to right.

- Type 3 Seesaw [73, 74] → introduces a heavy fermion $SU(2)$ triplet Σ.

In Fig.3.2 we show the tree-level diagrams corresponding to each of these models. These models are called "Seesaw" because the smallness of m_ν is achieved through the suppression of a heavy scale, generally the mass of the new mediator. The Type 2 Seesaw gives us even more freedom, since the suppression of m_ν is given by the ratio of a small mass scale over a heavy mass scale. Another reason that gives popularity to the Seesaw models is that they can be embedded in GUT theories [75]. For instance, the Type 1 Seesaw naturally emerges in $SO(10)$ models.

In this work we focus on the Type 1 Seesaw and one of its extension, called the Inverse Seesaw. In the next sections we present these models.

3.3.1 Type 1 Seesaw Model

In the Type 1 Seesaw model, the particle content of the Standard Model is extended by adding a heavy Majorana neutrino (also called heavy neutral lepton) that can be written as:

$$N = N_R + N_R^c, \tag{3.28}$$

where N_R is a singlet under the SM gauge group. In order to give mass to at least 2 of the light SM neutrino, we need to introduce 2 generations of heavy neutrinos. However for now we do not make any assumption on the number of flavours and we write the

most general Lagrangian, which is:

$$\mathcal{L} = \frac{1}{2}\bar{N}(i\partial\!\!\!/ - M)N - (\bar{N}Y\widetilde{H}^{\dagger}\ell_L + \bar{\ell_L}\widetilde{H}Y^{\dagger}N), \tag{3.29}$$

where Y is a complex matrix and M is complex symmetric matrix. This Lagrangian corresponds to the Dirac+Majorana case and the mass term can be written as:

$$\mathcal{L}_{mass} = -\frac{1}{2}\bar{n_L^c}\mathcal{M}n_L + h.c., \tag{3.30}$$

with

$$\mathcal{M} = \begin{pmatrix} 0 & m_D^T \\ m_D & M_R \end{pmatrix} \quad \text{and} \quad n_L = \begin{pmatrix} \ell_L \\ N_R^c \end{pmatrix}, \tag{3.31}$$

where M_R is a symmetric matrix and $m_D = Y\widetilde{H}^{\dagger}$.

Now we discuss the matching with the Weinberg operator and the light neutrino masses that arise from this model. There are several ways to it, for example in the next chapter we show how to do it using the functional method. However, we now present another way which can be very useful and it consists in the diagonalization of the mass matrix. To diagonalize $\mathcal{M}$ we follow the procedure presented in [76], which consists in two steps.The first one is to perform a block diagonalization. In particular, we want to find the rotation matrix R_1 such that:

$$R_1^T\mathcal{M}R_1 = \mathcal{M}_{block-diag.} = \begin{pmatrix} M_\nu & 0 \\ 0 & M_N \end{pmatrix}. \tag{3.32}$$

We recall that at this point M_ν and M_N are still not diagonal. To find R_1, we use the ansatz proposed in [77] and parametrize it as:

$$R_1 = \begin{pmatrix} \sqrt{1 - BB^{\dagger}} & B \\ -B^{\dagger} & \sqrt{1 - BB^{\dagger}} \end{pmatrix}. \tag{3.33}$$

Inserting R_1 in eq.(3.32) and imposing that the off-diagonal elements vanish, we get the following constraint:

$$\sqrt{1 - B^T B^*}\, m_D \sqrt{1 - BB^{\dagger}} - B^T m_D^T B^{\dagger} - \sqrt{1 - B^T B^*}\, M_R B^{\dagger} = 0. \tag{3.34}$$

In the limit $m_D \ll M_R$, this equation is solved by the power series:

$$B = B_1 + B_2 + B_3 + \dots, \tag{3.35}$$

where $B_i \sim (m_D/M_R)^i$. The explicit expression of each B_i is found by solving recursively, order by order, eq.(3.34). Finally, we can use the solution of B to find R_1, which turns out to be:

$$R_1 \simeq \begin{pmatrix} 1 - \frac{1}{2}\, m_D^{\dagger}(M_R M_R^{\dagger})^{-1} m_D & m_D^{\dagger}(M_R^{\dagger})^{-1} \\ -M_R^{-1} m_D & 1 - \frac{1}{2}\, M_R^{-1} m_D\, m_D^{\dagger}(M_R^{\dagger})^{-1} \end{pmatrix}. \tag{3.36}$$

Performing this rotation on $\mathcal{M}$ we get (at leading order):

$$\mathcal{M}_{block-diag.} \simeq \begin{pmatrix} -m_D^T M_R^{-1} m_D & 0 \\ 0 & M_R \end{pmatrix}. \tag{3.37}$$

Substituting the explicit expression for m_D and comparing with the Weinberg operator, we get the prediction of the light neutrinos mass matrix from the type 1 Seesaw:

$$\frac{C_5}{\Lambda} = \frac{1}{2} Y^T M_R^{-1} Y \overset{\text{EWSB}}{=} -\frac{M_\nu}{v^2} \qquad \rightarrow \qquad M_\nu = -\frac{v^2}{2} Y^T M_R^{-1} Y. \tag{3.38}$$

It is important to notice that this result is an approximation and it is valid only if $m_D \ll M_R$. The last step that we need to do, is to diagonalize the light and the heavy block in eq.(3.32) by performing a second rotation R_2 so that:

$$R_2^T (R_1^T \mathcal{M} R_1) R_2 = \mathcal{M}_{diag.} = \begin{pmatrix} \text{diag}(m_i) & 0 \\ 0 & \text{diag}(M_i) \end{pmatrix}. \tag{3.39}$$

The second rotation has the form:

$$R_2 = \begin{pmatrix} U_{PMNS} & 0 \\ 0 & W \end{pmatrix}, \tag{3.40}$$

where U_{PMNS} is the known Pontecorvo-Maki-Nakagawa-Sakata matrix (the equivalent of the CKM for the lepton sector), while W is the matrix that diagonalizes the heavy block and depends on the explicit structure of M_R. Now that we have both R_1 and R_2 we can write the total rotation:

$$R = R_1 R_2 \simeq \begin{pmatrix} \left[1 - \frac{1}{2} m_D^\dagger (M_R M_R^\dagger)^{-1} m_D\right] U_{PMNS} & m_D^\dagger (M_R^\dagger)^{-1} W \\ -M_R^{-1} m_D \, U_{PMNS} & \left[1 - \frac{1}{2} M_R^{-1} m_D \, m_D^\dagger (M_R^\dagger)^{-1}\right] W \end{pmatrix}, \tag{3.41}$$

so that $R^T \mathcal{M} R = \mathcal{M}_{diag.}$.

3.3.2 Inverse Seesaw Model

A common feature of the three "vanilla" Seesaw models, is that they point to heavy BSM particles with a mass far out of the experimental range, making them untestable. One way to resolve this issue and lower the mass of the heavy particle, is to introduce some new parameters in the model in order to have more freedom, similarly to what happens in the Type 2 Seesaw. One of the minimal extensions of the Type 1 Seesaw model that provides such a solution is the Inverse Seesaw [78, 79], where we introduce 2 heavy Majorana singlets, each with its flavours, instead of just one:

$$N = N_R + N_R^c \quad \text{and} \quad S = S_R + S_R^c. \tag{3.42}$$

One important feature of this model is the lepton number charge assignment:

$$L = \begin{cases} +1 & \text{for} \quad N_R \\ -1 & \text{for} \quad S_R \end{cases} . \tag{3.43}$$

The Lagrangian of this model is:

$$\mathcal{L} = -\frac{1}{2}\, \bar{n^c}\, \mathcal{M}\, n + h.c.\,, \tag{3.44}$$

where n is the vector containing all left-handed neutrinos and $\mathcal{M}$ is the mass matrix:

$$n = \begin{pmatrix} \ell_L \\ N_R^c \\ S_R^c \end{pmatrix} ; \qquad \mathcal{M} = \begin{pmatrix} 0 & Y^T \widetilde{H}^* & 0 \\ Y \widetilde{H}^\dagger & 0 & \Lambda \\ 0 & \Lambda^T & \mu \end{pmatrix} . \tag{3.45}$$

From the charge assignments in eq.(3.43) we see that the terms on the diagonal of $\mathcal{M}$ are lepton number violating, since they are the ones giving rise to Majorana mass terms. In our case, the only parameter of this kind is μ. Since setting $\mu = 0$ would increase the symmetry of the Lagrangian (we would recover lepton number conservation), μ is said to be naturally small in 't Hooft sense.

As we did before, now we diagonalize the mass matrix to get the prediction for the light neutrino masses. To do it, we can actually use the result that we got from the Type 1 Seesaw. Following the procedure in [80], let us start by rewriting the mass matrix in as:

$$\mathcal{M} = \begin{pmatrix} 0 & m_D^T & 0 \\ m_D & 0 & \Lambda \\ 0 & \Lambda^T & \mu \end{pmatrix} \equiv \begin{pmatrix} 0 & M_D^T \\ M_D & M_R \end{pmatrix} . \tag{3.46}$$

where we have defined:

$$M_D = \begin{pmatrix} m_D \\ 0 \end{pmatrix} , \quad M_R = \begin{pmatrix} 0 & \Lambda \\ \Lambda^T & \mu \end{pmatrix} . \tag{3.47}$$

From eq.(3.46) we see that the mass matrix has the same form as the one of the type 1 Seesaw. In the limit $\Lambda \gg m_D$, so when the eigenvalues of the heavy block M_R are grater than m_D, we can apply the same exact procedure that we used in the previous case and get the block diagonal matrix:

$$\mathcal{M}_{block-diag.} \simeq \begin{pmatrix} -M_D^T M_R^{-1} M_D & 0 \\ 0 & M_R \end{pmatrix} . \tag{3.48}$$

The explicit expression of M_R^{-1} is:

$$M_R^{-1} = \begin{pmatrix} -\Lambda^{T^{-1}} \mu\, \Lambda^{-1} & \Lambda^{T^{-1}} \\ \Lambda^{-1} & 0 \end{pmatrix} , \tag{3.49}$$

and substituting it in eq.(3.48), along with the expression of M_D, we get:

$$\mathcal{M}_{block-diag.} \simeq \begin{pmatrix} m_D^T \Lambda^{T^{-1}} \mu \, \Lambda^{-1} m_D & 0 \\ 0 & M_R \end{pmatrix}. \tag{3.50}$$

We notice that the expression of M_R^{-1} is exact and that we have made no assumption on μ. From eq.(3.50), we get the mass matrix of the light neutrinos predicted by the Inverse Seesaw:

$$\frac{C_5}{\Lambda_{EFT}} = -\frac{1}{2} Y^T \Lambda^{T^{-1}} \mu \, \Lambda^{-1} Y \overset{\text{EWSB}}{=} -\frac{M_\nu}{v^2} \quad \rightarrow \quad M_\nu = \frac{v^2}{2} Y^T \Lambda^{T^{-1}} \mu \, \Lambda^{-1} Y. \tag{3.51}$$

The diagonalization of the light and heavy blocks can be done in same way as in the previous case and the total rotation matrix can be written in the same way. So in order to diagonalize eq.(3.44) we perform the rotations:

$$\mathcal{M} = R \mathcal{M}_{diag} R^T \quad \text{and} \quad \begin{pmatrix} \nu_{L,i} \\ N^c_{R,j} \\ S^c_{R,k} \end{pmatrix} = R \begin{pmatrix} \psi_{1,i} \\ \psi^c_{2,j} \\ \psi^c_{3,k} \end{pmatrix}, \tag{3.52}$$

where ψ_n are the mass eigenstates and i, j, k are the number of flavour generations of the light and heavy neutrinos. Notice that we have substituted the doublet ℓ_L in n with just the light neutrinos ν_L.

One way that we have to test the Inverse Seesaw, is to look at how some physical SM processes are modified. We are interested in the interactions between the mass eigenstates and the SM particles at tree level, and such interactions come mainly from the charged currents. To see how they are modified, we substitute the field ν_L in the SM Lagrangian with the corresponding superposition of mass eigenstates. First of all, let us rewrite the rotation matrix R in eq.(3.41) as [81]:

$$R = \begin{pmatrix} U & V \\ X & W \end{pmatrix}. \tag{3.53}$$

The flavour structure that we eventually consider is 3 generations of light neutrinos and 2 generations for each of the heavy neutrinos. In this case, U is a 3×3 matrix and V can be split in two 3×2 blocks V_1 and V_2 such that $V = (V_1 \quad V_2)$, and each block parametrizes the mixing with one of the heavy eigenstates $\psi_{2,j}$ and $\psi_{3,k}$. Using this notation we have:

$$\nu_{L,\ell} = \sum_{i=1}^{3} U_{\ell i} \, \psi_{1,i} + \sum_{j=1}^{2} V_{1,\ell j} \, \psi^c_{2,j} + \sum_{k=1}^{2} V_{2,\ell k} \, \psi^c_{3,k}, \tag{3.54}$$

where $\ell = e, \mu, \tau$. Now we can substitute this expression in the SM Lagrangian to get:

$$\begin{aligned}
\mathcal{L} \supset & -\frac{g}{\sqrt{2}} W_\mu^+ \sum_{\ell=e}^{\tau} \sum_{i=1}^{3} \overline{\psi_{1,i}} U_{\ell i}^* \gamma^\mu \ell_L^- - \frac{g}{\sqrt{2}} W_\mu^+ \sum_{\ell=e}^{\tau} \sum_{j=1}^{2} \overline{\psi_{2,j}^c} V_{1,\ell j}^* \gamma^\mu \ell_L^- \\
& - \frac{g}{\sqrt{2}} W_\mu^+ \sum_{\ell=e}^{\tau} \sum_{k=1}^{2} \overline{\psi_{3,k}^c} V_{2,\ell k}^* \gamma^\mu \ell_L^- \\
& - \frac{g}{2\cos\theta_W} Z_\mu \sum_{\ell=e}^{\tau} \sum_{i=1}^{3} \overline{\psi_{1,i}} U_{\ell i}^* \gamma^\mu \nu_L - \frac{g}{2\cos\theta_W} Z_\mu \sum_{\ell=e}^{\tau} \sum_{j=1}^{2} \overline{\psi_{2,j}^c} V_{1,\ell j}^* \gamma^\mu \nu_L \\
& - \frac{g}{2\cos\theta_W} Z_\mu \sum_{\ell=e}^{\tau} \sum_{k=1}^{2} \overline{\psi_{3,k}^c} V_{2,\ell k}^* \gamma^\mu \nu_L \\
& - \frac{g}{2M_W} h \sum_{\ell=e}^{\tau} \sum_{j=1}^{2} m_{\psi_{2,j}} \overline{\psi_{2,j}^c} V_{1,\ell j}^* \nu_L - \frac{g}{2M_W} h \sum_{\ell=e}^{\tau} \sum_{k=1}^{2} m_{\psi_{3,k}} \overline{\psi_{3,k}^c} V_{2,\ell k}^* \nu_L + h.c. \quad (3.55)
\end{aligned}$$

We see that the matrix V parametrizes the mixing between active and heavy neutrinos and its explicit expression is model dependent. We are interested in evaluating V in the limits of one and two flavours per each heavy neutrino.

1 Flavour

In the limit of just one flavour generation, the mass matrix of the Inverse Seesaw in eq.(3.46) is a 3×3 symmetric matrix where Y, Λ and μ are just real numbers. In order to write the total rotation matrix R in eq.(3.53), we need to find the matrix W that diagonalizes the heavy block M_R. In this limit, the heavy block is a 2×2 matrix that can be written as:

$$M_R = \begin{pmatrix} 0 & \Lambda \\ \Lambda & \mu \end{pmatrix}, \quad (3.56)$$

and it can be diagonalized via the 2×2 rotation:

$$W = \begin{pmatrix} i\cos\theta & \sin\theta \\ -i\sin\theta & \cos\theta \end{pmatrix} \quad \text{with} \quad \tan(2\theta) = \frac{2\Lambda}{\mu}. \quad (3.57)$$

Applying this rotation we have:

$$M_R^{diag.} = W^T M_R W = \begin{pmatrix} m_1 & 0 \\ 0 & m_2 \end{pmatrix} \quad \text{with} \quad \begin{cases} m_1 = \frac{1}{2}(-\mu + \sqrt{4\Lambda^2 + \mu^2}) \\ m_2 = \frac{1}{2}(\mu + \sqrt{4\Lambda^2 + \mu^2}) \end{cases} . \quad (3.58)$$

Notice that we inserted the i factors in W such that in the limit $\mu \ll \Lambda$, both masses m_1 and m_2 are positive at leading order in Λ, while μ is a tiny splitting that lifts the

degeneracy. Now that we have everything we need (in this limit $U_{PMNS} = 1$), we can use eq.(3.41) to write the explicit expression of the total rotation matrix in eq.(3.53) as:

$$R \simeq \begin{pmatrix} 1 & -\frac{iYv}{\Lambda^2\sqrt{2}}(\mu\cos\theta + \Lambda\sin\theta) & \frac{Yv}{\Lambda^2\sqrt{2}}(\Lambda\cos\theta - \mu\sin\theta) \\ \frac{Yv\mu}{\Lambda^2\sqrt{2}} & i\cos\theta & \sin\theta \\ -\frac{Yv}{\Lambda\sqrt{2}} & -i\sin\theta & \cos\theta \end{pmatrix}, \tag{3.59}$$

which gives us the following expression for the diagonal form of the mass matrix of the Inverse Seesaw:

$$\mathcal{M}_{diag.} = \begin{pmatrix} \frac{Y^2v^2\mu}{2\Lambda^2} & 0 & 0 \\ 0 & \frac{1}{2}(-\mu + \sqrt{4\Lambda^2 + \mu^2}) & 0 \\ 0 & 0 & \frac{1}{2}(\mu + \sqrt{4\Lambda^2 + \mu^2}) \end{pmatrix}, \tag{3.60}$$

where the entries correspond to the mass eigenvalues of the 3 mass eigenstates. In particular, the relation between the flavour and mass eigenstates is:

$$\begin{pmatrix} \nu_L \\ N_R^c \\ S_R^c \end{pmatrix} = \begin{pmatrix} \psi_1 + \psi_2^c(-\frac{iYv\mu}{\sqrt{2}\Lambda^2}\cos\theta - \frac{iYv}{\sqrt{2}\Lambda}\sin\theta) + \psi_3^c(\frac{Yv\mu}{\sqrt{2}\Lambda}\cos\theta - \frac{Yv\mu}{\sqrt{2}\Lambda^2}\sin\theta) \\ \psi_1\frac{Yv\mu}{\sqrt{2}\Lambda^2} + \psi_2^c\, i\cos\theta + \psi_3^c\sin\theta \\ -\psi_1\frac{Yv}{\sqrt{2}\Lambda} + \psi_3^c\cos\theta - \psi_2^c\, i\sin\theta \end{pmatrix}. \tag{3.61}$$

It is easy to see that inverting this expression we find that the mass eigenstate ψ_1 is mainly composed of the left-handed SM neutrino, while the eigenstates $\psi_{1,2}^c$ are mainly composed of the heavy neutrinos N_R^c,S_R^c. This is due to the $1/\Lambda$ suppression. From eq.(3.59) we can get the elements of the mixing matrix V and in particular we have:

$$\begin{cases} V_{e\,\psi_2} = -\frac{iYv}{\sqrt{2}\Lambda^2}(\mu\cos\theta + \Lambda\sin\theta) \\ V_{e\,\psi_3} = \frac{Yv}{\sqrt{2}\Lambda^2}(\Lambda\cos\theta - \mu\sin\theta) \end{cases}. \tag{3.62}$$

2 Flavours

In the one flavour limit we are able to generate a mass term for just one of the light neutrinos. However, as we previously mentioned, we want at least two of them to be massive, so now we perform the diagonalization of the mass matrix by considering 3 generations of light neutrinos and 2 generations for each heavy neutrino. In this case the mass matrix in eq.(3.45) is a 7×7 matrix, and we define:

$$Y = \begin{pmatrix} Y_{11} & Y_{12} & Y_{13} \\ Y_{21} & Y_{22} & Y_{23} \end{pmatrix}, \quad \Lambda = \begin{pmatrix} \Lambda_1 & 0 \\ 0 & \Lambda_2 \end{pmatrix} \quad \mu = \begin{pmatrix} \mu_1 & 0 \\ 0 & \mu_2 \end{pmatrix}. \tag{3.63}$$

We can always assume that one among Λ and μ is diagonal without loss of generality, but to simplify calculations we take them both to be diagonal. Now the heavy block M_R

is diagonalized by the rotation matrix:

$$W = \begin{pmatrix} i\cos\phi_1 & \sin\phi_1 & 0 & 0 \\ 0 & 0 & i\cos\phi_2 & \sin\phi_2 \\ -i\sin\phi_1 & \cos\phi_1 & 0 & 0 \\ 0 & 0 & -i\sin\phi_2 & \cos\phi_2 \end{pmatrix}, \tag{3.64}$$

where the rotation angles $\phi_{1,2}$ are defined by:

$$\tan(2\phi_1) = \frac{2\Lambda_1}{\mu_1} \quad \text{and} \quad \tan(2\phi_2) = \frac{2\Lambda_2}{\mu_2}. \tag{3.65}$$

Applying this rotation we get the diagonal heavy block:

$$M_R^{diag.} = W^T M_R W = \begin{pmatrix} m_{1a} & 0 & 0 & 0 \\ 0 & m_{1b} & 0 & 0 \\ 0 & 0 & m_{2a} & 0 \\ 0 & 0 & 0 & m_{2b} \end{pmatrix}, \tag{3.66}$$

with:

$$\begin{cases} m_{1a} = \frac{1}{2}(-\mu_1 + \sqrt{4\Lambda_1^2 + \mu_1^2}) \\ m_{1b} = \frac{1}{2}(\mu_1 + \sqrt{4\Lambda_1^2 + \mu_1^2}) \end{cases} \quad \text{and} \quad \begin{cases} m_{2a} = \frac{1}{2}(-\mu_2 + \sqrt{4\Lambda_2^2 + \mu_2^2}) \\ m_{2b} = \frac{1}{2}(\mu_2 + \sqrt{4\Lambda_2^2 + \mu_2^2}) \end{cases}, \tag{3.67}$$

where m_i are the masses of the eigenstates $\psi_{2a}, \psi_{2b}, \psi_{3a}, \psi_{3b}$. Now that we have the rotation matrix W, we can get the mixing matrix V as defined in the top-right element of eq.(3.41). It turns out to be a 3×4 matrix, each column containing the mixings of one of the of the 4 heavy eigenstates with each of the 3 light eigenstates. In particular we have:

$$V = \begin{pmatrix} V_{e\,\psi_{2a}} & V_{e\,\psi_{2b}} & V_{e\,\psi_{3a}} & V_{e\,\psi_{3b}} \\ V_{\mu\,\psi_{2a}} & V_{\mu\,\psi_{2b}} & V_{\mu\,\psi_{3a}} & V_{\mu\,\psi_{3b}} \\ V_{\tau\,\psi_{2a}} & V_{\tau\,\psi_{2b}} & V_{\tau\,\psi_{3a}} & V_{\tau\,\psi_{3b}} \end{pmatrix}, \tag{3.68}$$

where the elements are given by:

$$\begin{cases} V_{e\,\psi_{2a}} = -\frac{ivY_{11}^\dagger}{\sqrt{2}\Lambda_1^2}(\mu_1\cos\phi_1 + \Lambda_1\sin\phi_1) \\ V_{\mu\,\psi_{2a}} = -\frac{ivY_{12}^\dagger}{\sqrt{2}\Lambda_1^2}(\mu_1\cos\phi_1 + \Lambda_1\sin\phi_1) \\ V_{\tau\,\psi_{2a}} = -\frac{ivY_{13}^\dagger}{\sqrt{2}\Lambda_1^2}(\mu_1\cos\phi_1 + \Lambda_1\sin\phi_1) \end{cases}, \quad \begin{cases} V_{e\,\psi_{2b}} = \frac{vY_{11}^\dagger}{\sqrt{2}\Lambda_1^2}(\Lambda_1\cos\phi_1 - \mu_1\sin\phi_1) \\ V_{\mu\,\psi_{2b}} = \frac{vY_{12}^\dagger}{\sqrt{2}\Lambda_1^2}(\Lambda_1\cos\phi_1 - \mu_1\sin\phi_1) \\ V_{\tau\,\psi_{2b}} = \frac{vY_{13}^\dagger}{\sqrt{2}\Lambda_1^2}(\Lambda_1\cos\phi_1 - \mu_1\sin\phi_1) \end{cases}$$

$$\begin{cases} V_{e\,\psi_{3a}} = -\frac{ivY_{21}^\dagger}{\sqrt{2}\Lambda_2^2}(\mu_2\cos\phi_2 + \Lambda_2\sin\phi_2) \\ V_{\mu\,\psi_{3a}} = -\frac{ivY_{22}^\dagger}{\sqrt{2}\Lambda_2^2}(\mu_2\cos\phi_2 + \Lambda_2\sin\phi_2) \\ V_{\tau\,\psi_{3a}} = -\frac{ivY_{23}^\dagger}{\sqrt{2}\Lambda_2^2}(\mu_2\cos\phi_2 + \Lambda_2\sin\phi_2) \end{cases}, \quad \begin{cases} V_{e\,\psi_{3b}} = \frac{vY_{21}^\dagger}{\sqrt{2}\Lambda_2^2}(\Lambda_2\cos\phi_2 - \mu_2\sin\phi_2) \\ V_{\mu\,\psi_{3b}} = \frac{vY_{22}^\dagger}{\sqrt{2}\Lambda_2^2}(\Lambda_2\cos\phi_2 - \mu_2\sin\phi_2) \\ V_{\tau\,\psi_{3b}} = \frac{vY_{23}^\dagger}{\sqrt{2}\Lambda_2^2}(\Lambda_2\cos\phi_2 - \mu_2\sin\phi_2) \end{cases}. \tag{3.69}$$

3.3.3 Casas-Ibarra Parametrization

The Casas-Ibarra parametrization [82] is a very useful way to write the Yukawa matrix in terms of all the other quantities of the model, and it can be applied to both the Type 1 and the Inverse Seesaw. This parametrization depends on the ordering of the light neutrino masses. Normal ordering (NH) corresponds to the choice of ν_1 being the lightest (or potentially massless) neutrino, while in inverted ordering (IO) it would be ν_3. In this work we choose to adopt the NH:

$$\begin{cases} m_{\nu 1} = 0 \\ m_{\nu 2} = \sqrt{\Delta m^2_{21}} \\ m_{\nu 3} = \sqrt{\Delta m^2_{31}} \end{cases} , \tag{3.70}$$

where Δm^2_{21} and Δm^2_{31} are the measured mass squared differences. For the Type 1 Seesaw, the Casas-Ibarra parametrization of the Yukawa is:

$$Y = \frac{i\sqrt{2}}{v} \operatorname{diag}(\sqrt{M_1}, \sqrt{M_2}) \cdot R \cdot \operatorname{diag}(0, \sqrt{m_{\nu 2}}, \sqrt{m_{\nu 3}}), \tag{3.71}$$

where R is an arbitrary orthogonal matrix such that $R^T R = \mathbb{1}$.

We now derive the same result for the Inverse Seesaw [83,84]. Let us start by writing the mass matrix of the light neutrino masses that we previously found:

$$M_\nu = \frac{v^2}{2} Y^T \Lambda^{T^{-1}} \mu \, \Lambda^{-1} Y. \tag{3.72}$$

We are working in the assumption that the mass matrix of the charged leptons is diagonal to begin with, so that M_ν is diagonalized exactly by the measured $U = U_{PMNS}$ matrix, so we can write:

$$\operatorname{diag}(0, m_{\nu 2}, m_{\nu 3}) \equiv m_\nu^D = U^T M_\nu U = \frac{v^2}{2} U^T Y^T \Lambda^{T^{-1}} \mu \, \Lambda^{-1} Y U. \tag{3.73}$$

Let us now define the square root of a matrix D such that $\sqrt{D}\sqrt{D} = D$. If the matrix is diagonal, we have:

$$\sqrt{D} \equiv \operatorname{diag}(\sqrt{d_1}, ..., \sqrt{d_n}). \tag{3.74}$$

Using this definition and assuming that μ is diagonal, we can write:

$$m_\nu^D = \frac{v^2}{2} U^T Y^T \Lambda^{T^{-1}} \sqrt{\mu}\sqrt{\mu} \, \Lambda^{-1} Y U. \tag{3.75}$$

Now we impose the following relation:

$$\begin{aligned}\mathbb{1} &= \frac{v^2}{2}\sqrt{(m_\nu^D)^{-1}}m_\nu^D\sqrt{(m_\nu^D)^{-1}} \\ &= \frac{v^2}{2}\left(\sqrt{(m_\nu^D)^{-1}}U^T Y^T \Lambda^{T^{-1}}\sqrt{\mu}\right)\left(\sqrt{\mu}\,\Lambda^{-1}YU\sqrt{(m_\nu^D)^{-1}}\right) \\ &= \frac{v}{\sqrt{2}}\left(\sqrt{\mu}\,\Lambda^{-1}YU\sqrt{(m_\nu^D)^{-1}}\right)^T\frac{v}{\sqrt{2}}\left(\sqrt{\mu}\,\Lambda^{-1}YU\sqrt{(m_\nu^D)^{-1}}\right).\end{aligned}$$

From this equation we can identify the orthogonal matrix:

$$R \equiv \frac{v}{\sqrt{2}}\sqrt{\mu}\,\Lambda^{-1}YU\sqrt{(m_\nu^D)^{-1}}, \tag{3.76}$$

and inverting this expression we get:

$$Y = \frac{\sqrt{2}}{v}\,\Lambda\,\sqrt{\mu^{-1}}\,R\,\sqrt{m_\nu^D}\,U^\dagger. \tag{3.77}$$

Since in this work we assume that only 2 of the light neutrinos are massive, we choose to parametrize R as in [4]:

$$R = \begin{pmatrix} 0 & \sqrt{1-r^2} & r \\ 0 & -r & \sqrt{1-r^2}\end{pmatrix}. \tag{3.78}$$

We notice that this procedure depends on the convention used to define the mass matrix of the Inverse Seesaw. Frequently it is defined from the term that in our case is the hermitian conjugate. In such convention the corresponding result of the Casas-Ibarra parametrization can be found in Ref. [85, 86].

3.4 State of the Art

The problem of neutrino masses is just one of the many open questions presented by neutrino physics, namely:

1. What is the mass hierarchy?
2. What is the absolute value of neutrino masses?
3. Is CP violated in the lepton sector? If so, by how much?
4. Are neutrinos Dirac or Majorana particles?
5. Do light sterile neutrinos exist? If so, how many of them are there?

Even if we do not have definitive answers to these questions yet, there a lot of active experiments and future ones that are improving our predictions.

There are a lot of data coming from neutrino oscillation experiments, such as Super-Kamiokande, SNO+, T2K, NOvA, IceCube/DeepCore and many others. From these experiments we can extract predictions for the following quantities:

$$\begin{aligned} &\Delta m^2_{ij} \equiv m^2_i - m^2_j \\ &\theta_1, \theta_2, \theta_3 \\ &\delta_{CP} \end{aligned} \tag{3.79}$$

Some predictions are more accurate than others, for example there is still a lot of uncertainty on the δ_{CP} phase. The most recent values are shown in Tab.3.2, that contains the results of NuFIT-6.0 [87, 88].

Regarding the neutrino masses, there are several quantities that can be measured from experiments other than Δm^2_{ij}. In particular, from neutrino-less double β-decays we can test the Majorana nature of neutrinos and get an upper limit on the effective Majorana mass of the electron neutrino $m_{\beta\beta}$ [89]:

$$m_{\beta\beta} = |\sum_i U^2_{ei} m_i| < 0.16\,\text{eV at } 90\%\text{ CL.} \tag{3.80}$$

The KATRIN experiment [90] gives us the upper limit on the effective electron antineutrino mass m_ν:

$$m_\nu = \sum_i |U_{ei}| m_i < 0.45\,\text{eV at } 90\%\text{ CL.} \tag{3.81}$$

From cosmology we get the upper limits on the sum of the masses of the three light active neutrinos [91]:

$$\sum_i m_i < 0.07 - 0.12\,\text{eV at } 95\%\text{ CL depending on the choice of data,}$$

and on the absolute mass of the lightest neutrino [92]:

$$m_{light} < 0.037\,\text{eV at } 95\%\text{ CL for normal ordering} \tag{3.82}$$

$$m_{light} < 0.042\,\text{eV at } 95\%\text{ CL for inverted ordering.} \tag{3.83}$$

In Fig.3.3 we show the plot from [93] that shows the link between the mass of the lightest neutrino m_{light} and the effective Majorana mass $m_{\beta\beta}$.

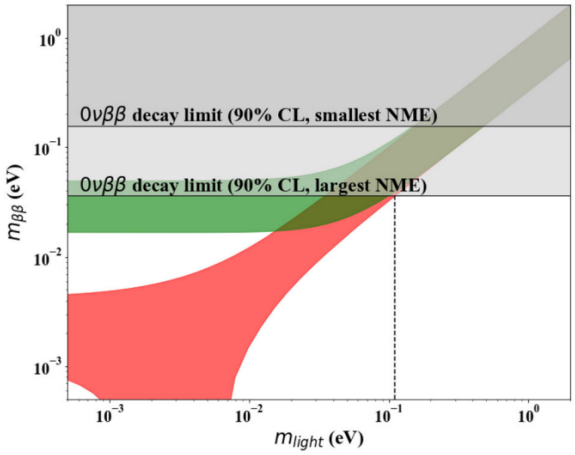

Figure 3.3: The red (green) band corresponds to the normal (inverted) ordering, respectively, in which case m_{light} is equal to $m_1(m_3)$. The bands are drawn by varying the masses and mixing parameters in the range permitted by oscillation experiments. The horizontally excluded region comes from $\beta\beta0\nu$ constraints.

	Normal Ordering ($\Delta\chi^2 = 0.6$)		Inverted Ordering (best fit)	
	bfp $\pm1\sigma$	3σ range	bfp $\pm1\sigma$	3σ range
$\sin^2\theta_{12}$	$0.307^{+0.012}_{-0.011}$	$0.275 \to 0.345$	$0.308^{+0.012}_{-0.011}$	$0.275 \to 0.345$
$\theta_{12}/^\circ$	$33.68^{+0.73}_{-0.70}$	$31.63 \to 35.95$	$33.68^{+0.73}_{-0.70}$	$31.63 \to 35.95$
$\sin^2\theta_{23}$	$0.561^{+0.012}_{-0.015}$	$0.430 \to 0.596$	$0.562^{+0.012}_{-0.015}$	$0.437 \to 0.597$
$\theta_{23}/^\circ$	$48.5^{+0.7}_{-0.9}$	$41.0 \to 50.5$	$48.6^{+0.7}_{-0.9}$	$41.4 \to 50.6$
$\sin^2\theta_{13}$	$0.02195^{+0.00054}_{-0.00058}$	$0.02023 \to 0.02376$	$0.02224^{+0.00056}_{-0.00057}$	$0.02053 \to 0.02397$
$\theta_{13}/^\circ$	$8.52^{+0.11}_{-0.11}$	$8.18 \to 8.87$	$8.58^{+0.11}_{-0.11}$	$8.24 \to 8.91$
$\delta_{\rm CP}/^\circ$	177^{+19}_{-20}	$96 \to 422$	285^{+25}_{-28}	$201 \to 348$
$\frac{\Delta m^2_{21}}{10^{-5}\ \text{eV}^2}$	$7.49^{+0.19}_{-0.19}$	$6.92 \to 8.05$	$7.49^{+0.19}_{-0.19}$	$6.92 \to 8.05$
$\frac{\Delta m^2_{3\ell}}{10^{-3}\ \text{eV}^2}$	$+2.534^{+0.025}_{-0.023}$	$+2.463 \to +2.606$	$-2.510^{+0.024}_{-0.025}$	$-2.584 \to -2.438$

Table 3.2: Three-flavor oscillation parameters from the fit to global data. The numbers in the 1st (2nd) column are obtained assuming NO (IO), *i.e.*, relative to the respective local minimum. Note that $\Delta m^2_{3\ell} \equiv \Delta m^2_{31} > 0$ for NO and $\Delta m^2_{3\ell} \equiv \Delta m^2_{32} < 0$ for IO.

Chapter 4

Seesaw Matching

In this chapter we perform the matching of the Seesaw models to the SMEFT. The way we do it is by deriving the results for the Type 1 Seesaw and then use them to get the ones for the Inverse Seesaw, similarly to what we did diagonalizing the mass matrix.

4.1 Tree level matching

In this section we show how to use the functional method to perform the tree-level matching. The operators that are generated up to order $\mathcal{O}(\Lambda^{-2})$ in the SMEFT, for both the Seesaws we are considering, are:

$$\mathcal{L}^{tree-lev}_{SMEFT} \supset \left[\frac{C_5}{\Lambda_{EFT}}\,(\bar{\ell^c_L}\widetilde{H}^*)(\widetilde{H}^\dagger\ell_L) + h.c.\right] + \frac{C_6}{\Lambda^2_{EFT}}\,(\bar{\ell_L}\widetilde{H})\,i\partial\!\!\!/\,(\widetilde{H}^\dagger\ell_L). \tag{4.1}$$

The first one is the Weinberg operator that we already discussed, and second one is the dim-6 operator. To perform the matching, it is useful to rewrite the Type 1 Seesaw Lagrangian in as:

$$\mathcal{L} = \frac{1}{2}\bar{N}(i\partial\!\!\!/ - M)N - \frac{1}{2}\left(\bar{N}Y\widetilde{H}^\dagger\ell_L + \bar{\ell^c_L}\widetilde{H}^*Y^TN^c + \bar{\ell_L}\widetilde{H}Y^\dagger N + \bar{N}Y^*\widetilde{H}^T\ell^c_L\right), \tag{4.2}$$

where we have split the Yukawa terms in eq.(3.29) using eq.(B.26). To apply the functional method we start by finding the classical equations of motion of the heavy fields we want to integrate out. Using:

$$\frac{\partial\mathcal{L}}{\partial N} - \partial_\mu\frac{\partial\mathcal{L}}{\partial(\partial_\mu N)} = 0, \tag{4.3}$$

we get:

$$\begin{cases}(-i\partial\!\!\!/ + M)\,N = -\,(Y\widetilde{H}^\dagger\ell_L + \widetilde{H}^TY^*\ell^c_L)\\ (i\partial\!\!\!/ + M)\,\bar{N} = -\,(\bar{\ell^c_L}Y^TH^* + \bar{\ell_L}\widetilde{H}Y^\dagger)\end{cases}. \tag{4.4}$$

4.1.1 Weinberg operator

Let us start by performing the matching to the Weinberg operator. Since it is the lower-dimensional operator in the SMEFT, we keep only the solutions of eq.(4.4) at $\mathcal{O}(M^{-1})$:

$$\begin{cases} N \approx -M^{-1}(Y\widetilde{H}^{\dagger}\ell_L + \widetilde{H}^T Y^* \ell_L^c) \\ \bar{N} \approx -M^{-1}(\bar{\ell_L^c} Y^T H^* + \bar{\ell_L}\widetilde{H} Y^{\dagger}) \end{cases} . \tag{4.5}$$

By substituting these solutions in eq.(4.2) and keeping only the solutions of order $\mathcal{O}(M^{-1})$ we get:

$$\mathcal{L} = \frac{1}{2}\,\bar{\ell_L^c}\widetilde{H}^*\,(Y^T M^{-1} Y)\,\widetilde{H}^{\dagger}\ell_L + h.c.\,. \tag{4.6}$$

Comparing with eq.(4.1) we have:

$$\frac{C_5}{\Lambda_{EFT}} = \frac{1}{2}\,Y^T M^{-1} Y, \tag{4.7}$$

which gives us the tree-level matching of the Type 1 Seesaw to the Weinberg operator. To extend this result to the Inverse Seesaw, we just need to make the substitutions:

$$Y \to \begin{pmatrix} Y \\ 0 \end{pmatrix} \quad and \quad M \to M_R = \begin{pmatrix} 0 & \Lambda \\ \Lambda^T & \mu \end{pmatrix}, \tag{4.8}$$

where M_R is the heavy block of the mass matrix. Performing these substitutions and using eq.(3.49) we get:

$$\frac{C_5}{\Lambda_{EFT}} = -\frac{1}{2}\,Y^T \Lambda^{T^{-1}} \mu\, \Lambda^{-1} Y, \tag{4.9}$$

which is exactly the result that we got in eq.(3.51).

4.1.2 Dimension 6 operator

Let us now proceed by performing the matching of the dim-6 operator and let us start as usual from the Type 1 Seesaw. To get the contributions to the dim-6 operator we need to keep the terms up to $\mathcal{O}(M^{-2})$ in the solution of eq.(4.4):

$$\begin{cases} N \approx -M^{-1}\left(1 + M^{-1}\, i\partial\!\!\!/\right)(Y\widetilde{H}^{\dagger}\ell_L + \widetilde{H}^T Y^* \ell_L^c) \\ \bar{N} \approx -M^{-1}\left(1 - M^{-1}\, i\partial\!\!\!/\right)(\bar{\ell_L^c} Y^T H^* + \bar{\ell_L}\widetilde{H} Y^{\dagger}) \end{cases} . \tag{4.10}$$

Substituting these expressions in eq.(4.2) and keeping only the terms of $\mathcal{O}(M^{-2})$ we get:

$$\mathcal{L} = \bar{\ell_L}\widetilde{H}\,(Y^{\dagger} M^{-2} Y)\, i\partial\!\!\!/(\widetilde{H}^{\dagger}\ell_L), \tag{4.11}$$

which leads to the result:

$$\frac{C_6}{\Lambda^2_{EFT}} = Y^\dagger M^{-2} Y, \tag{4.12}$$

in agreement with [94]. The contribution in eq.(4.11) actually comes just from the kinetic term in eq.(4.2), since the ones in the mass and Yukawa terms cancel each other out. We notice that the dim-6 operator is hermitian, in fact we do not write the *h.c.* in the Lagrangian. More details are shown in Appendix B. Now, to extend this result to the Inverse Seesaw we again perform the substitutions in eq.(4.8). The expression for M_R^{-2} is:

$$M_R^{-2} = \begin{pmatrix} (\Lambda^{T^{-1}} \mu \, \Lambda^{-1})^2 + \Lambda^{T^{-1}} \Lambda^{-1} & -\Lambda^{T^{-1}} \mu \, \Lambda^{-1} \Lambda^{T^{-1}} \\ -\Lambda^{-1} \Lambda^{T^{-1}} \mu \, \Lambda^{-1} & \Lambda^{-1} \Lambda^{T^{-1}} \end{pmatrix}, \tag{4.13}$$

and substituting it in eq.(4.11) we get:

$$\frac{C_6}{\Lambda^2_{EFT}} = Y^\dagger \left((\Lambda^{T^{-1}} \mu \, \Lambda^{-1})^2 + \Lambda^{T^{-1}} \Lambda^{-1} \right) Y. \tag{4.14}$$

As a last step of the tree level matching, we write the dim-6 operator as a linear combination of two different operators in Warsaw basis:

$$(\bar{\ell_L} \widetilde{H}) \, i \not{\partial} \, (\widetilde{H}^\dagger \ell_L) = \frac{1}{4} \left[\left(\bar{\ell_L} \gamma^\mu \ell_L \right) \left(H^\dagger i \overleftrightarrow{D}_\mu H \right) - \left(\bar{\ell_L} \gamma^\mu \tau^I \ell_L \right) \left(H^\dagger i \overleftrightarrow{D}^I_\mu H \right) \right], \tag{4.15}$$

where $\overleftrightarrow{D}_\mu \equiv D_\mu - \overleftarrow{D}_\mu$ and $\overleftrightarrow{D}^I_\mu \equiv \tau^I D_\mu - \overleftarrow{D}_\mu \tau^I$ with τ^I (for $I = 1, 2, 3$) being the Pauli matrices and $\overleftarrow{D}_\mu$ acting on the left.

Both operators in eq.(4.15) lead to a modification in the neutral current and charged current interactions. Since there are very strong bounds on the neutral current interactions with the charged leptons, we could think of using them to impose some physical constraints when performing the phenomenological analysis. However, these interactions appear with opposite signs in eq.(4.15) and cancel out, so we cannot use the corresponding bounds in our analysis. The interactions that we can use are the neutral currents with the neutrinos, even though the corresponding bounds are not as strong as the ones coming from the $Z\ell^+\ell^-$ interactions. Moreover, the lack of a precise knowledge of the neutrino flavour structure makes it difficult account for flavours.

4.2 1-loop matching

In this section we to perform the 1-loop matching of the Seesaw models. Among all the operators we can generate at 1-loop, we are interested just in the Higgs potential, because the other would all be of dimension ≥ 5 and would thus be even more suppressed. We can write the SMEFT Lagrangian as:

$$\mathcal{L}^{1-loop}_{SMEFT} = \frac{1}{2} m^2 (H^\dagger H) - \lambda (H^\dagger H)^2. \tag{4.16}$$

We now proceed with evaluating the 1-loop corrections to these operators, that we call δm^2 and $\delta\lambda$.

4.2.1 1-loop Matching of the Type 1 Seesaw Model

As usual, we start from the Type 1 Seesaw, so we take eq.(3.29) as the UV theory.

Let us start with the correction to the Higgs mass. In Fig.4.1 we show the loop diagram that gives δm^2. Since we expect divergences to arise from this loop, we must

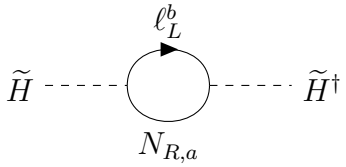

Figure 4.1: Loop diagram contributing to δm^2.

go in dimensional regularization before writing down the amplitude. It is easy to show that the Yukawa vertex in $d = 4 - 2\varepsilon$ dimensions has the form:

$$\mathcal{L}^{(d)} \supset -\mu^{\varepsilon}\bar{N}Y\widetilde{H}^\dagger\ell_L + h.c. \tag{4.17}$$

Using the Feynman rules in [95], we can write the amplitude as:

$$i\mathcal{M} = (-1)(YY^\dagger)^a{}_a\,\mu^{2\varepsilon}\int\frac{d^dk}{(2\pi)^d}\frac{\mathrm{Tr}\left[(\not{k}+M_a)P_L(\not{p}+\not{k})P_R\right]}{(k^2-M_a^2)(p+k)^2}, \tag{4.18}$$

where p is the external momentum and k the loop momentum. Since the mass of the heavy neutrinos is much higher than all the other energy scales involved, we can consider the limit in which all external momenta go to zero $p \to 0$. In this limit, the amplitude becomes:

$$i\mathcal{M} = (-1)\,2\,(YY^\dagger)^a{}_a\,\mu^{2\varepsilon}\int\frac{d^dk}{(2\pi)^d}\frac{1}{(k^2-M_a^2)}. \tag{4.19}$$

We notice that the integral in the last expression is a Tadpole integral that can be evaluated using the formula [34]:

$$\int\frac{d^dk}{(2\pi)^d}\frac{1}{(k^2-\Delta)^n} = \frac{(-1)^n i}{(4\pi)^{d/2}}\frac{\Gamma\left(n-\frac{d}{2}\right)}{\Gamma(n)}\left(\frac{1}{\Delta}\right)^{n-\frac{d}{2}}, \tag{4.20}$$

that for $n = 1$ and $\Delta = M_a^2$ reads:

$$\int\frac{d^dk}{(2\pi)^d}\frac{1}{(k^2-M_a^2)} = \frac{(-i)}{(4\pi)^{d/2}}\Gamma\left(1-\frac{d}{2}\right)(M_a^2)^{\frac{d}{2}-1}. \tag{4.21}$$

Inserting this result in the amplitude we get:

$$i\mathcal{M} = (-1)\, 2\, (YY^\dagger)^a{}_a\, \mu^{2\varepsilon} \frac{(-i)}{(4\pi)^{d/2}} \Gamma\left(1 - \frac{d}{2}\right) (M_a^2)^{\frac{d}{2}-1}. \tag{4.22}$$

The last thing we have to do is to make the substitution $d = 4 - 2\varepsilon$ and expand in the limit $\varepsilon \to 0$:

$$\begin{aligned}
&\mu^{2\varepsilon} = e^{\varepsilon \log \mu^2} = 1 + \varepsilon \log \mu^2 + O(\varepsilon^2), \\
&(4\pi)^{-\frac{d}{2}} = (4\pi)^{-2+\varepsilon} = \frac{1}{(4\pi)^2}(1 + \varepsilon \log 4\pi) + O(\varepsilon^2), \\
&\Gamma\left(1 - \frac{d}{2}\right) = \Gamma(\varepsilon - 1) = -\frac{1}{\varepsilon} + \gamma_E - 1 + O(\varepsilon), \\
&M_a^{d-2} = M_a^2 e^{-\varepsilon \log M_a^2} = M_a^2(1 - \varepsilon \log M_a^2) + O(\varepsilon^2).
\end{aligned} \tag{4.23}$$

Working out the calculations and keeping only the terms up to order $O(\varepsilon^0)$, we can write the final result as:

$$i\mathcal{M} = i\,(-1)\, \frac{(YY^\dagger)^a{}_a}{8\pi^2} M_a^2 \left(1 + \log \frac{\mu^2}{M_a^2} - \gamma_E + \frac{1}{\varepsilon} + \log 4\pi\right). \tag{4.24}$$

If we use the $\overline{MS}$ renormalization scheme, we can reabsorb the constant terms γ_E and $\log 4\pi$ in the definition of μ as in eq.(2.9) and the divergence is eliminated by a counterterm, so the renormalized amplitude is:

$$i\mathcal{M} = i\,(-1)\, \frac{(YY^\dagger)^a{}_a}{8\pi^2} M_a^2 \left(1 + \log \frac{\mu^2}{M_a^2}\right). \tag{4.25}$$

Using this result we can now perform the matching to the Higgs mass term in eq.(4.16). The 1-loop correction that we get is:

$$\delta m^2 = (-1) \frac{(YY^\dagger)^a{}_a}{4\pi^2} M_a^2 \left(1 + \log \frac{\mu^2}{M_a^2}\right). \tag{4.26}$$

We must make an important comment on the notation that we are using. In eq.(4.26) there is no sum over the index a, instead we are just taking the (a, a) element of $YY^\dagger$.

From dimensional analysis we expect δm^2 to scale as a mass squared, in fact we have $\delta m^2 \sim M_a^2$. This is also a manifestation of the hierarchy problem, in fact whenever we have some BSM physics that couples to the Higgs, it produces corrections to m^2 that scale as M^2.

Now we can proceed to evaluate the correction $\delta\lambda$ to the self-interaction of the Higgs and to do so, we follow the same procedure as we did for the previous calculation.

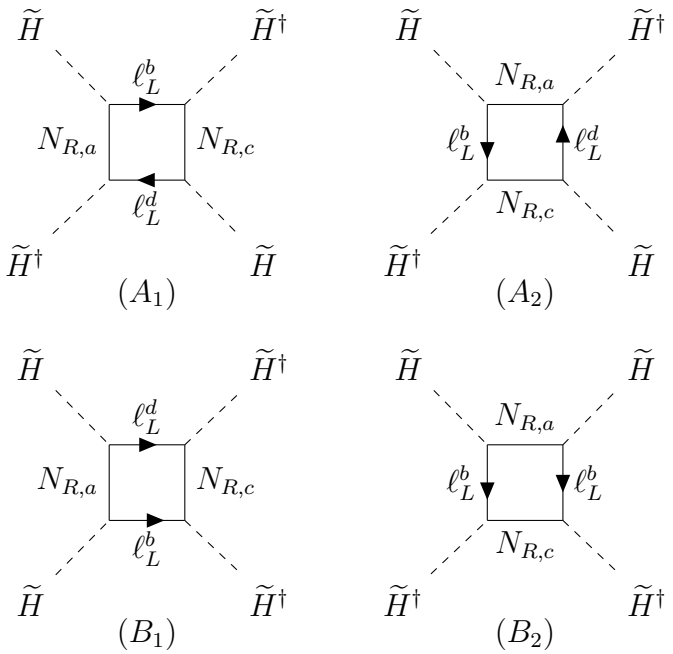

Figure 4.2: Box-loop diagrams contributing to $\delta\lambda$.

However, as we shall see, in this case there are some additional technicalities that must be taken into consideration.

In Fig.4.2 we can see the four diagrams that contribute to the amplitude. Let us start by considering diagrams (A_1) and (A_2), which are two independent diagrams that contribute to the amplitude. They are identical up to a swap of the two $\widetilde{H}^\dagger$, so we can evaluate just one of them and multiply the result by 2. The same can be said for diagrams (B_1) and (B_2). In addition, it is important to notice that diagrams (B) violate lepton number, because the arrows of the Dirac fermion lines point in opposite directions.

Now we can proceed by writing down the contribution of the diagrams (A). Using the Feynman rules in [95, 96] we have[1]:

$$i\mathcal{M}_A = (-1)\,4\,(YY^\dagger)^a{}_c (YY^\dagger)^c{}_a\,\mu^{4\varepsilon}\int \frac{d^dk}{(2\pi)^d}\frac{1}{(k^2-M_a^2)(k^2-M_c^2)}. \tag{4.27}$$

In order to solve the integral we must write it in the form of a Tadpole, and to do so we can use the Feynman parametrization. The general formula is [34]:

$$\frac{1}{D_1^{\alpha_1}...D_N^{\alpha_N}} = \frac{\Gamma(\alpha)}{\Gamma(\alpha_1)...\Gamma(\alpha_1)}\int_0^1 dx_1...dx_N \frac{x_1^{\alpha_1-1}...x_N^{\alpha_N-1}\delta(1-\Sigma_i x_i)}{(x_1D_1+...x_ND_N)^\alpha}, \tag{4.28}$$

[1] We write it directly in dimensional regularization and considering the limit $p_i \to 0$.

where $\alpha = \Sigma_i \alpha_i$ and D_i are the denominators that we get from the propagators and they have the form $D_i = (p^2 - M^2)$. In our case, we can write:

$$\begin{aligned}\frac{1}{D_1 D_2} &= \frac{1}{(k^2 - M_a^2)(k^2 - M_c^2)} \\ &= \int_0^1 \frac{dx}{[x(k^2 - M_a^2) + (1-x)(k^2 - M_c^2)]^2} \\ &= \int_0^1 \frac{dx}{(k^2 - \Delta)^2},\end{aligned} \tag{4.29}$$

where $\Delta = xM_a^2 + M_c^2(1-x)$. Inserting this expression in the amplitude, we see that we have again a Tadpole integral that we can solve using eq.(4.20):

$$i\mathcal{M}_A = (-1)\, 4\, (YY^\dagger)^a{}_c (YY^\dagger)^c{}_a\, \mu^{4\varepsilon} \int_0^1 dx \int \frac{d^d k}{(2\pi)^d} \frac{1}{(k^2 - \Delta)^2}. \tag{4.30}$$

After solving the Tadpole, we must take the limit $\epsilon \to 0$, substitute the expression for Δ and perform the integral over x. This leads to the result (already expressed in the $\overline{MS}$ scheme):

$$i\mathcal{M}_A = \, i\mu^{2\varepsilon} (-1) (YY^\dagger)^a{}_c (YY^\dagger)^c{}_a \, \frac{1}{4\pi^2} \left(1 - \frac{M_c^2 \log \frac{\mu^2}{M_c^2} - M_a^2 \log \frac{\mu^2}{M_a^2}}{M_a^2 - M_c^2} \right), \tag{4.31}$$

where we have factored out the term $\mu^{2\varepsilon}$, which we is needed later to perform the matching procedure.

Now let us consider the diagrams (B). We can write their contribution to the amplitude as:

$$i\mathcal{M}_B = (-1)\, 4\, (Y^\dagger Y)^a{}_c (YY^\dagger)^c{}_a\, \mu^{4\varepsilon} \int \frac{d^d k}{(2\pi)^d} \frac{M_a M_c}{k^2 (k^2 - M_c^2)(k^2 - M_a^2)}. \tag{4.32}$$

Using the Feynman parametrization, we get:

$$i\mathcal{M}_B = (-1)\, 4\, (Y^\dagger Y)^a{}_c (YY^\dagger)^c{}_a\, M_a M_c\, \mu^{4\varepsilon} \int_0^1 dx \int_0^{1-x} dy \int \frac{d^d k}{(2\pi)^d} \frac{\Gamma(3)}{(k^2 - \Delta)^3}, \tag{4.33}$$

with $\Delta = M_a^2(1 - x - y) + M_c^2 y$. We must notice that in this case we can directly set $\epsilon = 0$, because the result of the Tadpole integral gives the term:

$$\Gamma\left(3 - \frac{d}{2}\right) = \Gamma\left(3 - \frac{4 - 2\epsilon}{2}\right) = \Gamma(1 - \epsilon)\,. \tag{4.34}$$

Since the poles of $\Gamma(\epsilon)$ are at $\epsilon = 0, -1, -2, ...$, setting $\epsilon = 0$ doesn't give rise to any divergence. As before, the only term in ε than we keep is $\mu^{2\varepsilon}$. Performing the same steps as we did before, we get the result:

$$i\mathcal{M}_B = i\mu^{2\varepsilon}(-1)\,(Y^\dagger Y)^a{}_c (YY^\dagger)^c{}_a \,\frac{1}{4\pi^2}\left(-M_a M_c \frac{\log\frac{M_a^2}{M_c^2}}{M_a^2 - M_c^2}\right). \tag{4.35}$$

Putting together results (4.31) and (4.35) we get the total amplitude:

$$\begin{aligned} i\mathcal{M} =& i\mu^{2\varepsilon}(-1)(YY^\dagger)^a{}_c (YY^\dagger)^c{}_a \,\frac{1}{4\pi^2}\left(1 - \frac{M_c^2 \log\frac{\mu^2}{M_c^2} - M_a^2 \log\frac{\mu^2}{M_a^2}}{M_a^2 - M_c^2}\right) \\ &+ i\mu^{2\varepsilon}(-1)\,(Y^\dagger Y)^a{}_c (YY^\dagger)^c{}_a \,\frac{1}{4\pi^2}\left(-M_a M_c \frac{\log\frac{M_a^2}{M_c^2}}{M_a^2 - M_c^2}\right). \end{aligned} \tag{4.36}$$

Now we need to perform the matching. To do it, we must impose that the amplitudes in the UV are equal to the amplitudes in the SMEFT. Eq.(4.36) is the UV amplitude, which we rewrite in the following way:

$$i\mathcal{M} = \mu^{2\varepsilon}\, i\mathcal{M}'. \tag{4.37}$$

From the Lagrangian in eq.(4.16) we can get the SMEFT (tree-level) amplitude that contributes to the Higgs self-coupling, which in dim-reg is:

$$i\mathcal{M}_{SMEFT} = -4i\mu^{2\varepsilon}\lambda. \tag{4.38}$$

Imposing $i\mathcal{M} = i\mathcal{M}_{SMEFT}$ we get:

$$\lambda = -\frac{1}{4}\mathcal{M}' \equiv \delta\lambda, \tag{4.39}$$

where the explicit expression of $\delta\lambda$ is:

$$\begin{aligned} \delta\lambda =& \frac{(YY^\dagger)^a{}_c (YY^\dagger)^c{}_a}{16\pi^2}\left(1 - \frac{M_c^2 \log\frac{\mu^2}{M_c^2} - M_a^2 \log\frac{\mu^2}{M_a^2}}{M_a^2 - M_c^2}\right) \\ &+ \frac{(Y^\dagger Y)^a{}_c (YY^\dagger)^c{}_a}{16\pi^2}\left(-M_a M_c \frac{\log\frac{M_a^2}{M_c^2}}{M_a^2 - M_c^2}\right). \end{aligned} \tag{4.40}$$

There are a few non trivial steps in determining the overall factor of the result we just got, that come from the symmetry factors of the box-loops and the matching with the SMEFT. A more detailed derivation of this overall factor can be found in Appendix C.

Again, we must comment the notation we are using. Similarly to what we had before, there is no sum on the indexes a, c.

As a last step, we show also the results in the limit where we have just one flavour, i.e. when $M_a \to M_c = M$:

$$\delta m^2 = (-1)\frac{|Y|^2}{4\pi^2} M^2 \left(1 + \log\frac{\mu^2}{M^2}\right), \tag{4.41}$$

$$\delta\lambda = \frac{|Y|^4}{16\pi^2}\left(\log\frac{\mu^2}{M^2} - 1\right). \tag{4.42}$$

Let us now briefly discuss the decoupling limit. One could naively expect that $\mathcal{L}_{SM}$ is recovered in the limit of $M \to \infty$ and that in such limit the matching contributions that we just evaluated would vanish. However, the issue is more subtle than this and requires further consideration. Let us consider the correction to the self-coupling. Since it is dimensionless, the box loops that contribute to $\delta\lambda$ should scale as:

$$\frac{1}{M^2} \times (\text{some mass scale})^2. \tag{4.43}$$

The issue arises since in our case the only mass scale in the UV theory is M, so we end up with an expression proportional to M^2/M^2. It is obviously impossible to make it vanish by sending the denominator to infinity by keeping the numerator finite, since they are literally the same quantity. We can than conclude that the real decoupling limit is for $Y \to 0$ and it easy to see that in such limit the matching contributions actually vanish. Let us now look at δm^2. Just as $\delta\lambda$, it does not vanish for $M \to \infty$, however in this case it is a manifestation of the Higgs hierarchy problem.

4.2.2 1-loop Matching of the Inverse Seesaw Model

Now we show see how to use the results we just derived to get the matching contributions from the Inverse Seesaw. One substantial difference is that in the previous case N was both a flavour and mass eigenstate. This however in nor true for N and S in the Inverse Seesaw, as we can see from the Lagrangian in eq.(3.44). In the previous chapter, we showed how to diagonalize the mass matrix by performing first a block-diagonalization and then diagonalize the light and heavy block separately. However, this is not the ideal way to proceed to get the matching contributions. Instead, we directly diagonalize the heavy block, without performing any operation on the light one. This leads to two heavy mass eigenstates χ_1 and χ_2 (each with its flavours) that are both coupled to the Higgs. In particular, we rotate the mass matrix in eq.(3.45) with the rotation matrix:

$$O = \begin{pmatrix} \mathbb{1} & 0 \\ 0 & W \end{pmatrix}, \tag{4.44}$$

where W is the matrix that diagonalizes the heavy block. In the case where we only have one flavour we write it as in eq.(3.57), while if we consider two flavours for the heavy states we write it as in eq.(3.64). Performing this rotation we get:

$$\mathcal{M}' = O^T \mathcal{M}\, O = \begin{pmatrix} 0 & Y_1^T \widetilde{H}^* & Y_2^T \widetilde{H}^* \\ Y_1 \widetilde{H}^\dagger & m_1 & 0 \\ Y_2 \widetilde{H}^\dagger & 0 & m_2 \end{pmatrix}. \tag{4.45}$$

Again, we must make the distinction between the one and two flavours case. When considering one flavour, m_1 and m_2 are the ones in eq.(3.58) and the new Yukawa couplings are defined by:

$$\begin{cases} Y_1 = i\, Y \cos\theta \\ Y_2 = Y \sin\theta \end{cases}. \tag{4.46}$$

Instead, if we are considering 2 flavours for the heavy eigenstates, m_1 and m_2 are 2×2 diagonal matrices with the eigenvalues shown in eq.(3.67). We recall that in this case the Yukawa matrix Y is defined as in eq.(3.63), so that we have:

$$\begin{aligned} Y_1 &= \begin{pmatrix} i\, Y_{11} \cos\phi_1 & i\, Y_{12} \cos\phi_1 & i\, Y_{13} \cos\phi_1 \\ Y_{11} \sin\phi_1 & Y_{12} \sin\phi_1 & Y_{13} \sin\phi_1 \end{pmatrix} \equiv \begin{pmatrix} Y_{1a} \\ Y_{1b} \end{pmatrix} \\ Y_2 &= \begin{pmatrix} i\, Y_{21} \cos\phi_2 & i\, Y_{22} \cos\phi_2 & i\, Y_{23} \cos\phi_2 \\ Y_{21} \sin\phi_2 & Y_{22} \sin\phi_2 & Y_{23} \sin\phi_2 \end{pmatrix} \equiv \begin{pmatrix} Y_{2a} \\ Y_{2b} \end{pmatrix}. \end{aligned} \tag{4.47}$$

The last thing to do before writing the Lagrangian is to perform the rotations:

$$\begin{cases} n = O\, n' \\ \bar{n^c} = \bar{n^c}'\, O^T \end{cases} \qquad with \quad n' = \begin{pmatrix} \ell_L \\ \chi_1^c \\ \chi_2^c \end{pmatrix}. \tag{4.48}$$

Now we can write the Lagrangian of the ISS as:

$$\mathcal{L} = -\frac{1}{2} \left(\bar{\chi_1}\, m_1\, \chi_1^c + \bar{\chi_2}\, m_2\, \chi_2^c \right) - \left(\bar{\chi_1} Y_1 \widetilde{H}^\dagger \ell_L + \bar{\chi_2} Y_2 \widetilde{H}^\dagger \ell_L \right) + h.c.. \tag{4.49}$$

We notice that the Lagrangian written in this notation is valid regardless of the number of flavours we are considering.

Now we can proceed to evaluate the matching contributions. In Fig.4.3 and Fig.4.4 are shown (some of) the diagrams that contribute to δm^2 and $\delta\lambda$ respectively. It is clear that the form of the diagrams is the same as the ones we had in the Type 1 Seesaw. In Fig.4.3 and Fig.4.4 we have kept the index structure of the previous case to highlight the similarities, but we adopt a different notation to write the results. In particular, we

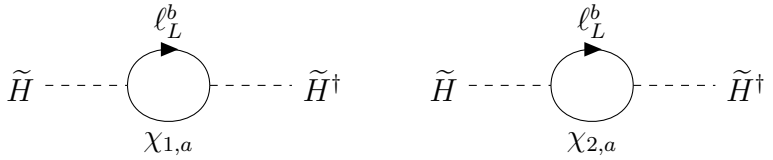

Figure 4.3: Loop diagrams contributing to δm^2.

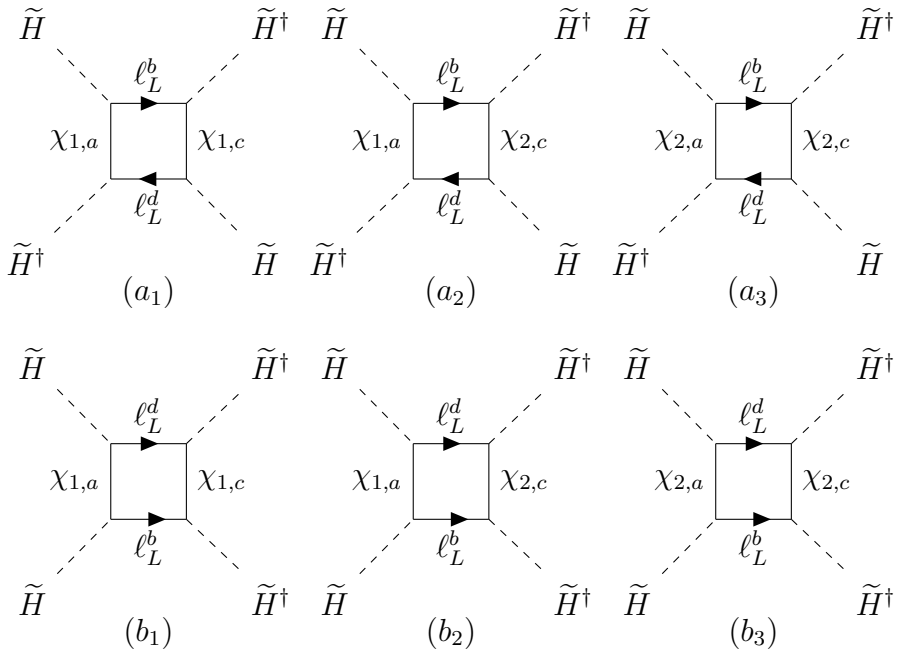

Figure 4.4: Some of the box-loop diagrams contributing to $\delta\lambda$.

rename the flavour indices of the heavy eigenstates as (α, β) and the flavour indices of the $SU(2)$ doublet as (k, l). For clarity, we write all the explicit sums:

$$\delta m^2 = -\frac{1}{4\pi^2} \sum_{\alpha} \left[\sum_{k=1}^{3} \left(Y_{\alpha,k} Y^*_{\alpha,k} \right) m_\alpha^2 \left(1 + \log \frac{\mu^2}{m_\alpha^2} \right) \right], \tag{4.50}$$

$$\delta\lambda = \frac{1}{16\pi^2} \sum_{\alpha,\beta} \left[\sum_{k=1}^{3} \left(Y_{\alpha,k} Y^*_{\beta,k} \right) \sum_{l=1}^{3} \left(Y_{\beta,l} Y^*_{\alpha,l} \right) \left(1 - \frac{m_\beta^2 \log \frac{\mu^2}{m_\beta^2} - m_\alpha^2 \log \frac{\mu^2}{m_\alpha^2}}{m_\alpha^2 - m_\beta^2} \right) \right] + \frac{1}{16\pi^2} \sum_{\alpha,\beta} \left[\left(\sum_{k=1}^{3} Y^*_{\alpha,k} Y_{\beta,k} \right)^2 \left(- m_\alpha m_\beta \frac{\log \frac{m_\alpha^2}{m_\beta^2}}{m_\alpha^2 - m_\beta^2} \right) \right]. \tag{4.51}$$

All the possible values of the indices (α, β) are:

$$\alpha, \beta = 1a, 1b, 2a, 2b, \tag{4.52}$$

and the corresponding values of the masses and the Yukawas are the ones in eq.(3.67) and eq.(4.47).

Now, as we did in the previous section, we show the results in the one flavour limit:

$$\delta m^2 = (-1)\frac{|Y_1|^2}{4\pi^2}\left[m_1^2\left(1+\log\frac{\mu_R^2}{m_1^2}\right)\right] + (-1)\frac{|Y_2|^2}{4\pi^2}\left[m_2^2\left(1+\log\frac{\mu_R^2}{m_2^2}\right)\right] \tag{4.53}$$

$$\begin{aligned}\delta\lambda = &\frac{|Y_1|^4}{16\pi^2}\left(\log\frac{\mu_R^2}{m_1^2}-1\right) + \frac{|Y_2|^4}{16\pi^2}\left(\log\frac{\mu_R^2}{m_2^2}-1\right) + \\ &\frac{|Y_1|^2|Y_2|^2}{8\pi^2}\left(1-\frac{m_2^2\log\frac{\mu_R^2}{m_2^2}-m_1^2\log\frac{\mu_R^2}{m_1^2}}{m_1^2-m_2^2}\right) + \\ &\frac{(Y_1^\dagger Y_2)^2+(Y_2^\dagger Y_1)^2}{16\pi^2}\left(-m_1\,m_2\,\frac{\log\frac{m_1^2}{m_2^2}}{m_1^2-m_2^2}\right).\end{aligned} \tag{4.54}$$

In this case masses and the Yukawas are the ones in eq.(3.58) and and eq.(4.46). We have relabelled the the energy scale μ that comes from dimensional regularization as $\mu \to \mu_R$, so that it is not confused with the parameter μ appearing in the mass matrix of the Inverse Seesaw model.

It can be shown that in the limit $\mu \to 0$ all the contributions that come from the lepton number violating diagrams cancel out. This is justified by the fact that μ is the only parameter in the model that violates lepton number.

As for the Seesaw 1 case, we can see that the decoupling limit is for $Y \to 0$.

Chapter 5

Phenomenology

In this chapter we carry out a phenomenological analysis using the results that we previously derived. In particular, we want to investigate whether it is possible to have a successful realization of the Neutrino Option also with the Inverse Seesaw.

After explaining the details of the Neutrino Option and presenting the methods that we use to reproduce the running of the parameters, we present the results of our analysis. For simplicity, we carried out a first broad analysis using the results in the limit of just one flavour generation for both the light and heavy neutrinos. This is done to get an estimate of the orders of magnitude that we are dealing with and to get some coarse constraints on the parameters. Then, to make contact with the fact that at least two of the light SM neutrinos are massive, we consider the case of three generations of light neutrinos and two generations for each of the heavy neutrinos, following the example of the original implementation of the Neutrino Option.

5.1 The Neutrino Option

The Neutrino Option [4, 5] is a minimal scenario that, adopting the EFT approach, radiatively generates the Higgs potential together with neutrino masses in the Type 1 Seesaw model starting from an almost conformal Lagrangian, where the only dimensional scale is the mass of the heavy neutrino. Integrating out the heavy particle it is possible to generate the light neutrino masses at dimension 5 through the Weinberg operator and the Higgs potential at 1-loop. By requesting that they are generated simultaneously, we can obtain a prediction for the heavy mass and the Yukawa coupling. In particular, the matching contributions fix the parameters of the Higgs potential and neutrino mass at a certain high energy scale Λ as functions of the Yukawa and the high scale itself. Λ is taken to be the heavy mass. Below this scale, all quantities evolve with the SMEFT RGEs down to the electroweak scale, where they can be compared with experimental measurements. We note that the running is actually relevant just for Higgs self-coupling. The goal is to

verify if there are any values of Y and Λ that make this construction compatible with the values of m, λ and m_ν measured at the EW scale. In order to perform the numerical analysis, we take the inverse approach and require that the Higgs and neutrino masses are compatible with the experimental measurements at the EW scale and solve for the parameters of the model, namely Y and Λ. Technically also λ should be included in the system, but due to its non-negligible running it is more convenient to verify afterwards at which scale the condition is satisfied.

The numerical analysis of this scenario is carried out in Ref. [5], and we use it for comparison with our implementation. As previously mentioned, this scenario is realised considering two generations of heavy Majorana neutrinos with masses $M_2 = xM_1$ with $1 < x < 10$. In addition to the matching contributions, a term $\lambda_0(H^\dagger H)^2$ is allowed in the scalar potential, so that the Neutrino Option is realised for values of (M_1, λ_0) that simultaneously satisfy:

$$m^2(M_1) = \delta m^2(M_1) \tag{5.1}$$

$$\lambda(M_1) = \lambda_0 + \delta\lambda(M_1). \tag{5.2}$$

The Yukawa couplings are required to reproduce the observed neutrino masses and

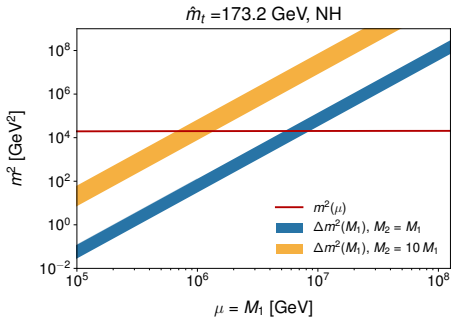

Figure 5.1: Numerical comparison between the values of the threshold correction $\delta m^2(M_1)$ compatible with neutrino physics constraints in the cases $x = 1, 10$ with the running Higgs mass $m^2(\mu)$ determined by the SM RGE and the measured SM parameters (red line). The figure is taken from Ref. [5].

mixings. The range of values for $\delta m^2(M_1)$, $\delta\lambda(M_1)$ compatible with this condition is determined scanning the low energy parameter space with a sample of 1000 points randomly selected within the 3σ allowed ranges for the neutrino masses and the U_{PMNS} parameters (including the Majorana phases). In Fig.5.1 and Fig.5.2 are shown the results.

The Neutrino Option predicts a heavy mass in the range 10^6 GeV $< M_1 < 10^7$ GeV for a value of the Yukawa coupling $Y \sim 10^{-4.5} - 10^{-6}$. In the following sections, we show how we can lower the prediction of the heavy mass exploiting the extra freedom in the parameter space of the Inverse Seesaw, reaching experimentally testable scales.

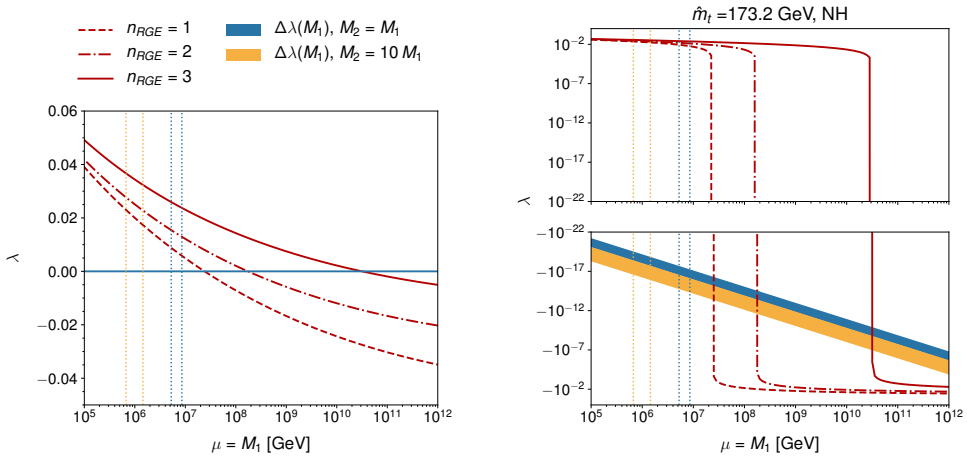

Figure 5.2: Numerical comparison between the values of the threshold correction $\delta\lambda(M_1)$ compatible with neutrino physics constraints in the cases $x = 1, 10$ with the running quartic coupling $\lambda(\mu)$ determined by the SM RGE and the measured SM parameters (red lines), shown in both linear and logarithmic scale. The right figure has been split in two symmetric panels for $\lambda > 0$ and $\lambda < 0$. The dotted vertical lines mark the mass regions where the matching for m^2 is fulfilled (cf. Fig. 5.1). The figures are taken from Ref. [5].

In Refs. [97–100] also conformal UV embeddings are explored. They consist in the addition of a set of scalar fields that generate the Majorana scale spontaneously by satisfying a Gildener-Weinberg condition [101]. As pointed out in [4], these scalars also turn out to be good Dark Matter candidates. A possible conformal embedding for the ISS is presented in Ref. [102], but we do not investigate these matters any further in this work.

5.2 Numerical Implementation of SM RGEs

In this section we present the methods that we used to perform the running of the SM parameters. The SM RGEs are taken from the files of the Mathematica package

DsixTools [103, 104], while the boundary conditions are taken from Ref. [105][1]:

$$\begin{aligned}
\lambda(M_t) &= 0.12604 + 0.00206\left(\frac{M_h}{\text{GeV}} - 125.15\right) - 0.00004\left(\frac{M_t}{\text{GeV}} - 173.34\right) \pm 0.00030_{\text{th}} \\
\frac{m(M_t)}{\text{GeV}} &= 131.55 + 0.94\left(\frac{M_h}{\text{GeV}} - 125.15\right) + 0.17\left(\frac{M_t}{\text{GeV}} - 173.34\right) \pm 0.15_{\text{th}} \\
y_t(M_t) &= 0.93690 + 0.00556\left(\frac{M_t}{\text{GeV}} - 173.34\right) + \frac{-0.00042\,\alpha_3(M_Z) - 0.1184}{0.0007} \pm 0.00050_{\text{th}} \\
g_2(M_t) &= 0.64779 + 0.00004\left(\frac{M_t}{\text{GeV}} - 173.34\right) + 0.00011\frac{M_W - 80.384\,\text{GeV}}{0.014\,\text{GeV}}, \\
g_Y(M_t) &= 0.35830 + 0.00011\left(\frac{M_t}{\text{GeV}} - 173.34\right) - 0.00020\frac{M_W - 80.384\,\text{GeV}}{0.014\,\text{GeV}} \\
g_3(M_t) &= 1.1666 + 0.00314\frac{\alpha_3(M_Z) - 0.1184}{0.0007} - 0.00046\left(\frac{M_t}{\text{GeV}} - 173.34\right).
\end{aligned} \tag{5.3}$$

The boundary conditions for the remaining Yukawa couplings are set to zero since they do not make any significant contribution to the running of the quantities we are interested in.

5.3 Results with 1 Flavour Generation

In this section we show the numerical analysis done using the results in the one flavour limit. We use the Higgs and light neutrino masses given by the ISS as physical constraints to get a solution for μ and Y, both as a function of Λ, and then substitute the results in the expression for $\delta\lambda$.

Let us start by considering the expressions of the matching contributions in the one flavour limit in eq.(4.53) and eq.(4.54). The first thing we need to do is to fix the renormalization scale μ_R. For simplicity, we consider the limit $\mu \ll \Lambda$, so that the two heavy masses $m_{1,2}$ in eq.(3.58) are almost degenerate and both equal to Λ at leading order. This way, since the energy scales m_1 and m_2 are close to one another, we can neglect the running between them without risking to miss any important physical effects. In this approximation, we fix the renormalization scale as $\mu_R = m_i\, e^{-3/4}$, where m_i is either mass m_1 or m_2 appearing in the logarithms of eq.(4.53) and eq.(4.54). The reason for the presence of the exponential in the substitution is related to the choice of renormalization scheme, as explained in [106]. After performing these substitutions, we

[1]The convention used for the Higgs potential in Refs. [103, 104] is different from the one in Ref. [105]. This has been taken into account in order to properly implement the RGEs.

are left with the expressions:

$$\delta m^2 = \frac{Y^2 \Lambda^2}{8\pi^2}, \tag{5.4}$$

$$m_\nu = \frac{v^2 Y^2 \mu}{\Lambda^2}, \tag{5.5}$$

$$\delta\lambda = -\frac{Y^4}{32\pi^2} f(\mu, \Lambda), , \tag{5.6}$$

where $f(\mu, \Lambda)$ is a more complicated function of μ and Λ. Solving eq.(5.4) and eq.(5.5) for Y and μ gives us:

$$Y = \frac{2\sqrt{2}\,\pi\,\delta m}{\Lambda} \quad \text{and} \quad \mu = \frac{m_\nu\,\Lambda^4}{4\pi^2\,v^2\,\delta m^2}. \tag{5.7}$$

As we previously mentioned, we now impose the physical constraints:

$$\delta m^2 = (125.1 \pm 0.2)^2\,\text{GeV}^2 \quad \text{and} \quad \begin{cases} m_\nu = 1\,\text{eV} \\ m_\nu = 10^{-3}\,\text{eV} \end{cases} . \tag{5.8}$$

Imposing these constraints we are momentarily neglecting the running of the Higgs and neutrino masses, but this can be justified by the fact that their running is almost negligible anyway. We wrote two values for m_ν in eq.(5.8) in order to account for the lack of a precise knowledge of the neutrino masses; however, as we show, only one quantity is affected by the value of m_ν.

In Fig.5.3 we show the order-of-magnitude predictions of the values of the Yukawa coupling and of μ/Λ that we got by substituting the values in eq.(5.8) in eq.(5.7). From plot (a) of Fig.5.3 we see that the Yukawa coupling takes perturbative values at almost all energy scales. Let us now look at plot (b) in Fig.5.3, that shows the ratio μ/Λ. First of all, we point out that this is the only quantity affected by different values of the neutrino mass in eq.(5.8). An important information that we get from this plot, is that we can identify two different physical regimes:

- $\mu/\Lambda \ll 1 \rightarrow$ in this region our initial approximation of $\mu \ll \Lambda$ is self consistent. Also, this regime is theoretically protected by the technical naturalness of μ, which justifies its smallness.

- $\mu/\Lambda \gg 1 \rightarrow$ in this region the energy separation between m_1 and m_2 can be potentially very high and neglecting the running between them (as we did in our calculations) would be incorrect, because we could miss effects that may be relevant. Evaluating each log in eq.(4.53) and eq.(4.54) at its corresponding scale would also be incorrect, because in this case the two different matching scales m_1, m_2 cannot both be approximated to Λ. Moreover, we would need a way to justify a big value for μ, which we do not have.

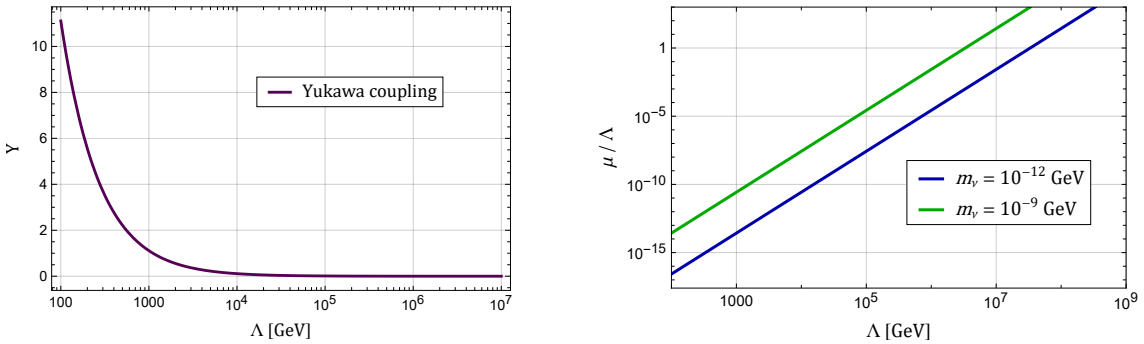

(a) Yukawa coupling **(b)** Ratio μ/Λ

Figure 5.3: Here we present the plots of the (a) - Yukawa coupling and (b) - ratio μ/Λ, compatible with realistic values of the Higgs and neutrino masses in eq.(5.8) for the 1-flavour toy example. The green line corresponds to $m_\nu = 1\,\text{eV}$ and the blue line to $m_\nu = 10^{-3}\,\text{eV}$. The x-axis of every plot is the energy scale Λ.

By looking at the plots in Fig.5.3 we can say that the most viable region for the realization of this version of the Neutrino Option is 500 GeV $\lesssim \Lambda \lesssim 10^6$ GeV. Below this range the Yukawa is not perturbative any more and the EFT approach breaks down due to the fact that we are matching onto the SMEFT, so we are required to stay above the EW scale. On the other hand, above this range we enter the region where $\mu/\Lambda \gg 1$, which we exclude for the reasons mentioned above. So we can conclude that this is the ideal energy range for the realisation of our scenario. As we showed, we can safely solve the constraints in eq.(5.8) and get a prediction for Λ which is lower than the one from the original implementation of the Neutrino Option, which was our goal.

Let us now consider the self-coupling. Substituting the solutions for μ and Y in the expression of $\delta\lambda$ in eq.(5.6), we get the expression of the matching contribution as a function of the energy scale Λ. Ideally, we would like for it to intersect the plot of the running of λ in the SM at some point. From there, we would get the matching condition at the scale where the intersection happens and then going to lower scales, λ would follow the SM running down to its measured value at the Electroweak scale. However, since $\delta\lambda$ is a correction given by a fermionic loop, it is negative by construction. This issue is actually unavoidable, because we are simultaneously generating both the Higgs mass and the self-coupling, that must have opposite sign in order to have Electroweak symmetry breaking. There are two possible approaches to resolve the problem. One possibility is to introduce scalar fields to the theory, so that their contribution could lead to a positive value of $\delta\lambda$. However, we take the approach proposed in Refs. [4, 102], which is to introduce a $\lambda_0 \geq 0$ so that:

$$\lambda = \delta\lambda + \lambda_0\,. \tag{5.9}$$

Since the self-coupling is not protected by any symmetry, there is no way of forbidding the presence of a term like $\lambda_0(H^\dagger H)^2$ in the scalar potential. However, this cannot be said for the Higgs mass, that can be set to zero in the UV by imposing a conformal symmetry. In particular, what we do is introducing λ_0 at tree-level so that at the EW scale λ has the corresponding measured value. Introducing this new parameter may bring some fine tuning issues, that can be quantified by the quantity:

$$\frac{\delta\lambda + \lambda_0}{\lambda_0} = \frac{\lambda}{\lambda - \delta\lambda}. \tag{5.10}$$

In Fig.5.4 we show $|\delta\lambda|$, the running of λ in the SM (with its error bars), λ_0 and the tuning. It is important to notice that these plots make sense only in the limit where $\mu_R \sim \Lambda$ (i.e. in region where $\mu/\Lambda < 1$), because $\delta\lambda$ is a function of Λ and the SM running is a function of μ_R. From Fig.5.4 we see that $\delta\lambda$ (red line) is always be negligible with

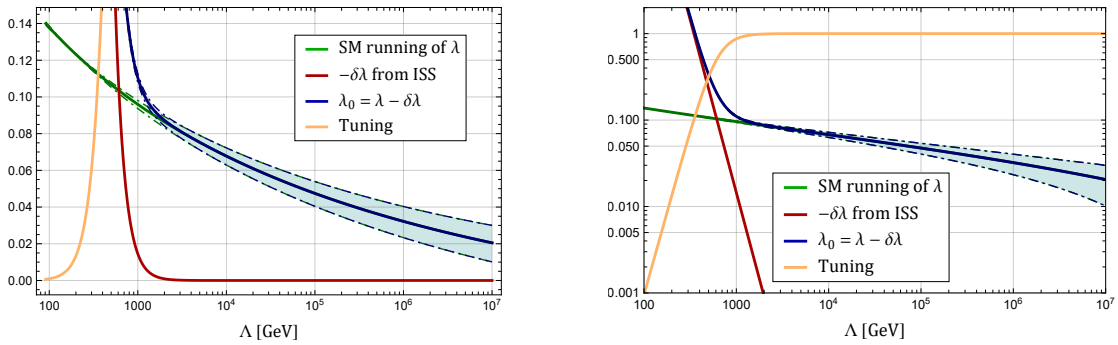

Figure 5.4: Here we present the plots of $|\delta\lambda|$ (red line), the running of λ in the SM (green line), λ_0 (blue line) and the tuning (yellow line). The only difference between the two plots is the scale on the y-axis, which is linear (left) or logarithmic (right). The error bars on the SM running correspond to $m_t = 171.1 - 175.6$ GeV, as in [105]. The error on $|\delta\lambda|$ given by varying the Higgs mass within the 3σ range and varying the neutrino mass is negligible, so the error on λ_0 is dominated by the one on the SM running. σ is given in eq.(5.8).

respect to λ_0 (blue line), since $\delta\lambda$ goes to zero very rapidly. The only region where this is not true is at low energies, where λ is given by a cancellation between λ_0 and $\delta\lambda$. That is also the only region where we have a non negligible fine tuning (yellow line). However, we mentioned above that we are interested in the region $\Lambda \gtrsim 500$ GeV, in which the tuning is always below 10%, which is an acceptable value.

We can now make some considerations based on the results that we got so far. In particular, we recognize 3 different physical regions:

- $\Lambda \lesssim 10^3$ GeV $\rightarrow$ in this region it is possible to have direct searches for the heavy neutrinos, which should have almost degenerate masses since we have $\mu/\Lambda \ll 1$.

- 10^3 GeV $\lesssim \Lambda \lesssim 10^6$ GeV $\rightarrow$ this is the most viable region, since the tuning needed is almost negligible and the approximation $\mu \ll \Lambda$ is still consistent.
- $\Lambda \gtrsim 10^6$ GeV $\rightarrow$ above this scale we enter the region where $\mu/\Lambda \gg 1$, which we already excluded for the above mentioned reasons.

5.3.1 Bounds from Direct Searches

As we previously said, in the region $\Lambda \lesssim 10^3$ GeV we can have direct searches for the heavy neutrinos. For example, colliders can look for same-sign dilepton signatures and trilepton signatures through the s-channel Drell–Yan process, shown in Fig.5.5. We

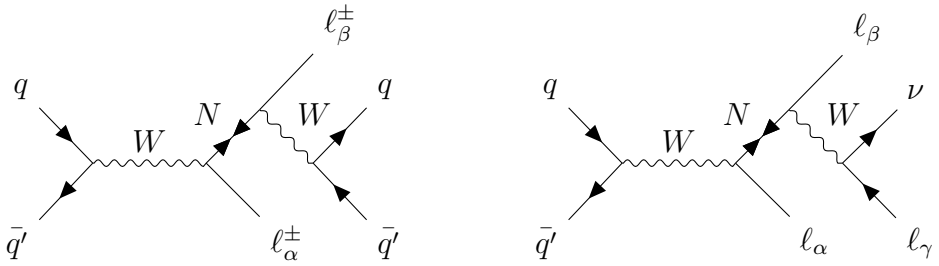

Figure 5.5: s-channel Drell–Yan process that generates same-sign dilepton signatures (left) and trilepton signature (right).

notice that the observation of a same-sign dilepton signature would constitute direct evidence of lepton number violation. Ref. [107] presents a search by the CMS collaboration that infers some of the most stringent upper bounds on the values of the elements of the mixing matrix V in eq.(3.53) as a function of the mass of the heavy neutrinos. The bounds are shown in the left plot of Fig.5.6. They come from the trilepton channel and are represented in a plane mixing vs mass. Since in this section we are working with the results in the one flavour limit, we can consider just the electron channel. Ref. [107] presents bounds for the muon channel as well, that are numerically similar.

In our case, the expressions of the masses are the ones in eq.(3.58) and the mixings are the ones in eq.(3.62). They are both functions of μ and Λ, however the mixings depend also on the Yukawa. We can get the function $Y(\mu, \Lambda)$ by inverting eq.(5.5) and fixing m_ν. Doing this leads to an expression of masses and mixings that are functions of just μ and Λ, so we can project the CMS bound in a μ/Λ vs Λ plane. In particular, we can see what the forbidden regions are, given that a point in this parameter space is forbidden if it lies above the CMS upper bound. Since the bound is valid only for the plotted range of m_i, we are not able to exclude anything outside of this region. In Fig.5.6 we show both the CMS bound (left) and the corresponding forbidden region in our case (right), from which we see we can exclude the region $10^{1.5} \lesssim \Lambda[\text{GeV}] \lesssim 10^{2.8}$.

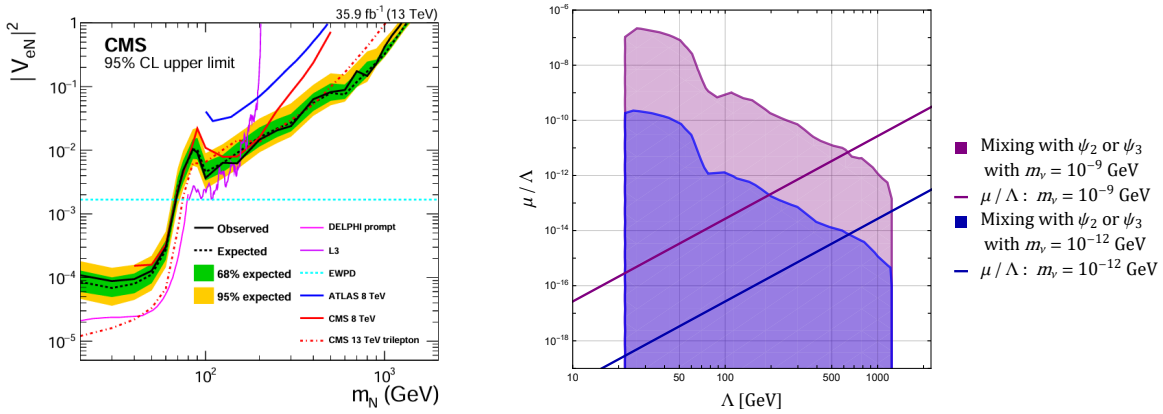

Figure 5.6: On the left we show the CMS bound from Ref. [107]. The constraints shown in this plot come from EWPD [108], DELPHI [109], L3 [110, 111], ATLAS [112] and CMS [113, 114]. On the right we show the corresponding forbidden regions in our case for the two different values of m_ν in eq.(5.8): purple for $m_\nu = 10^{-9}$ GeV and blue for $m_\nu = 10^{-12}$ GeV. Once m_ν is fixed, both mixings $V_{e\psi_2}$ and $V_{e\psi_3}$ lead to the same forbidden regions, which are the ones where the purple (blue) line enters the purple (blue) area. In both cases this happens for $10^{1.5} \lesssim \Lambda[\text{GeV}] \lesssim 10^{2.8}$.

We notice that we plot the forbidden regions for both $V_{e\psi_2}$ and $V_{e\psi_3}$ in the same plane because we recall that at these energy scales we have $m_{1,2} \sim \Lambda$.

5.4 Results with 2 Massive Light Neutrinos

In this section we present the results of the same analysis described above, but considering 3 flavours of light neutrinos and 2 flavours for each of the 2 heavy neutrinos, as in Ref. [5].

The analysis is performed with the same logic of the previous one, so we start by fixing the renormalization scale in eq.(4.51) in the same way we previously described. This leads to expressions of δm^2 and $\delta\lambda$ that depend on $\mu_{1,2}$, $\Lambda_{1,2}$, the masses $m_i(\mu_{1,2}, \Lambda_{1,2})$ defined in eq.(3.67) and the elements of the Yukawa matrix defined in eq.(3.63). Again, we want to use use the Higgs and neutrino masses as physical constraints, but we do it in a slightly different way. First of all, we invert the expression of the mass matrix of light neutrinos to write the Yukawa using the Casas-Ibarra parametrization as in eq.(3.77). At this point, the Yukawa depends on $\mu_{1,2}$, $\Lambda_{1,2}$, the free parameter r and the parameters of the U_{PMNS} matrix, namely the neutrino masses and mixings (including the 2 Majorana

phases). We recall that U_{PMNS} has the form:

$$U_{PMNS} = \begin{pmatrix} c_{12}c_{13} & s_{12}c_{13} & s_{13}e^{-i\delta} \\ -s_{12}c_{23} - c_{12}s_{23}s_{13}e^{i\delta} & c_{12}c_{23} - s_{12}s_{23}s_{13}e^{i\delta} & s_{23}c_{13} \\ s_{12}s_{23} - c_{12}c_{23}s_{13}e^{i\delta} & -c_{12}s_{23} - s_{12}c_{23}s_{13}e^{i\delta} & c_{23}c_{13} \end{pmatrix} \begin{pmatrix} 1 & 0 & 0 \\ 0 & e^{i\alpha_1} & 0 \\ 0 & 0 & e^{i\alpha_2} \end{pmatrix}. \tag{5.11}$$

We fix the parameters appearing in the Yukawa matrix in the following way:

- We fix the U_{PMNS} parameters as the central values in the first column of Tab.3.2, while for the Majorana phases we chose the values:

$$\alpha_1 = 180^\circ \quad \text{and} \quad \alpha_2 = 0^\circ. \tag{5.12}$$

- To fix $\mu_{1,2}$ and $\Lambda_{1,2}$ we define $\mu_1 \equiv \mu$ and $\Lambda_1 \equiv \Lambda$. Then we consider the following range for the remaining parameters:

$$0.1 \leq \frac{\mu_2}{\mu} \leq 10 \quad \text{and} \quad 0.1 \leq \frac{\Lambda_2}{\Lambda} \leq 10. \tag{5.13}$$

  As before, we work in the limit $\mu \ll \Lambda$. This way we ensure that the four heavy masses are almost degenerate, so that again all the matching scales are close to one another and are equal to Λ at leading order. We also recall that this limit is protected by the technical naturalness of μ_i.

- Fixing r is a more delicate business. Since it is a free parameter, we could in principle assign it any value. However, for big values of r the elements of the Yukawa matrix behave like $|Y_{1i}| = |Y_{2i}|$. This is actually a fine tuning due to the fact that no matter the value of r, the matrix R of the Casas-Ibarra parametrization is ensured to be orthogonal. For this reason, we choose a small value for r:

$$r = 0.5. \tag{5.14}$$

Performing these substitutions, the elements of the Yukawa matrix are functions of only μ and Λ, so we use them to solve the constraint on the Higgs mass and get a solution for $\mu(\Lambda)$, which we then substitute in the expression of $\delta\lambda$. All the plots are similar to the ones obtained in the one flavour case, so the same conclusions are valid.

Considering the results that are sensitive to flavours makes it possible to investigate several experimental constraints. In this work we consider bounds from direct searches for heavy neutral leptons (as for the previous case), the invisible width of the Z boson and lepton flavour violating processes.

5.4.1 Bounds from Direct Searches

Now that we are working with multiple flavour generations we can consider both bounds for the electron and muon channel presented in Ref. [107]. In Fig.5.7 we present the resulting forbidden regions for a value of the ratios in eq.(5.13) equal to 10. Additional plots for different values of the ratios are shown in Appendix D.

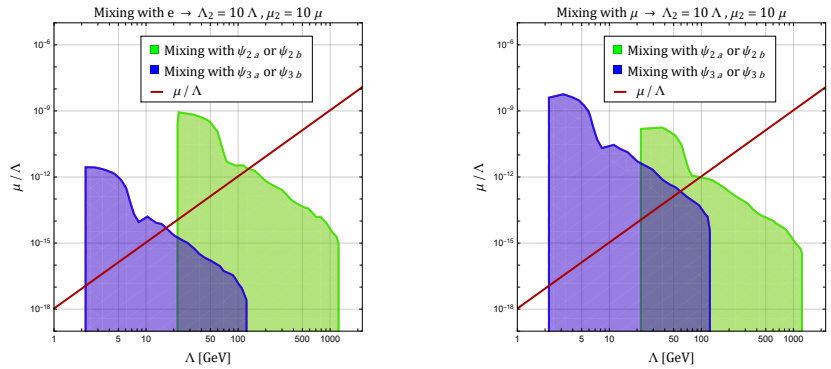

Figure 5.7: Here we present the forbidden regions coming from the upper bounds on the electron channel (left) and the muon channel (right) for a value of the ratios in eq.(5.13) equal to 10. The green (blue) areas correspond to the mixing with the heavy eigenstates ψ_{2a} or ψ_{2b} (ψ_{3a} or ψ_{3b}). The exclusion regions for the "a" and "b" eigenstates completely overlap. The red line corresponds to μ/Λ evaluated with the corresponding ratio.

5.4.2 Bounds from the Invisible Width of Z

As we mentioned after performing the tree-level matching of the dim-6 operator, we can impose some physical constraints on the neutral current interaction with neutrinos. In particular, we consider the bound on the invisible width of the Z boson. Taking into account also the SMEFT contribution, the invisible width is written as:

$$\Gamma_{inv.} = \sum_{i,j} \Gamma_{Z\to\nu_i\nu_j} \quad \text{with} \quad \Gamma_{Z\to\nu_i\nu_j} = \frac{G_F\, m_Z^3}{3\pi\sqrt{2}} \left[\frac{\delta_{ij}}{2} - \frac{v^2}{2}(C^{(1)}_{H\ell ij} - C^{(3)}_{H\ell ij})\right]^2 , \tag{5.15}$$

where G_F is the Fermi constant and m_Z is the mass of the Z boson. From eq.(4.14) we have the expression of the Wilson coefficient of the dim-6 operator resulting from the matching procedure. In Warsaw basis the dim-6 operator is written as in eq.(4.15) and $C^{(1)}_{H\ell ij}$, $C^{(3)}_{H\ell ij}$ are their corresponding Wilson coefficients. In our case we have that $C^{(3)}_{H\ell ij} = -C^{(1)}_{H\ell ij} = C_6/4$, so we get:

$$\Gamma_{Z\to\nu_i\nu_j} = \frac{G_F\, m_Z^3}{3\pi\sqrt{2}} \left(\frac{\delta_{ij}}{2} - v^2 C^{(1)}_{H\ell ij}\right)^2 \simeq \frac{G_F\, m_Z^3}{3\pi\sqrt{2}} \left(\frac{\delta_{ij}}{4} - v^2\, \delta_{ij}\, C^{(1)}_{H\ell ij}\right), \tag{5.16}$$

where we have kept only the terms up to linear order in $C^{(1)}_{H\ell\,ij}$. From this expression we see that only the diagonal elements of $C^{(1)}_{H\ell}$ contribute, so we can write the Z invisible width as:

$$\Gamma_{inv.} = \sum_{i,j} \Gamma_{Z\to\nu_i\nu_j} = \frac{G_F\, m_Z^3}{3\pi\sqrt{2}} \left(\frac{3}{4} - v^2\, \mathrm{Tr}[C^{(1)}_{H\ell}]\right). \tag{5.17}$$

The expression of $C^{(1)}_{H\ell}$, keeping only the leading term in eq.(4.14), is:

$$C^{(1)}_{H\ell} = \frac{C_6}{4} \simeq \frac{1}{4}\, Y^\dagger \Lambda^{T^{-1}} \Lambda^T Y, \tag{5.18}$$

where Λ is defined in eq.(3.63) and Y is the Yukawa matrix given by the Casas-Ibarra parametrization.

According to the PDG [115] the experimental value of the total invisible width is:

$$\Gamma_{inv.} = 499.3 \pm 1.5 \text{ MeV}, \tag{5.19}$$

and according to ATLAS [116] and CMS [117] the most precise measurement of the invisible width of Z in the Standard Model is:

$$\Gamma^{SM}_{inv.,exp} = 501.445 \pm 0.047 \text{ MeV}. \tag{5.20}$$

In our case we have:

$$\Gamma^{SM}_{inv.} = \frac{G_F\, m_Z^3}{3\pi\sqrt{2}} \frac{3}{4} = 497.493 \text{ MeV}. \tag{5.21}$$

The measurement of $\Gamma^{SM}_{inv.,exp}$ is highly precise and takes into account also radiative corrections, so the value that comes from eq.(5.21) is out of the permitted range in eq.(5.20). To resolve this issue and compare our prediction to the experimental values, we introduce a scale factor k such that:

$$\Gamma_{inv.} = \sum_{i,j} k\, \Gamma_{Z\to\nu_i\nu_j} \quad \text{with} \quad k = \frac{501.445}{497.493}. \tag{5.22}$$

From Ref. [115] we have that at 95% CL the bound we need to enforce is:

$$\chi^2(c) - \chi^2_{min}(c) \leq 3.84, \tag{5.23}$$

where $c = \mathrm{Tr}[C^{(1)}_{H\ell}]$ and $\chi^2(c)$ is the function:

$$\chi^2(c) = \frac{(\Gamma_{th}(c) - \Gamma_{exp})^2}{\sigma^2_{th} + \sigma^2_{exp}}, \tag{5.24}$$

with:

$$\begin{aligned} &\Gamma_{th}(c) = \Gamma_{inv.} && \sigma_{th} = 0.047 \text{ MeV} \\ &\Gamma_{exp} = 499.3 \text{ MeV} && \sigma_{exp} = 1.5 \text{ MeV}. \end{aligned} \tag{5.25}$$

As for the previous case, we can project the bound obtained by enforcing eq.(4.14) in a plane μ/Λ vs Λ. In Fig.5.8 we present the result for different values of the ratios in eq.(5.13).

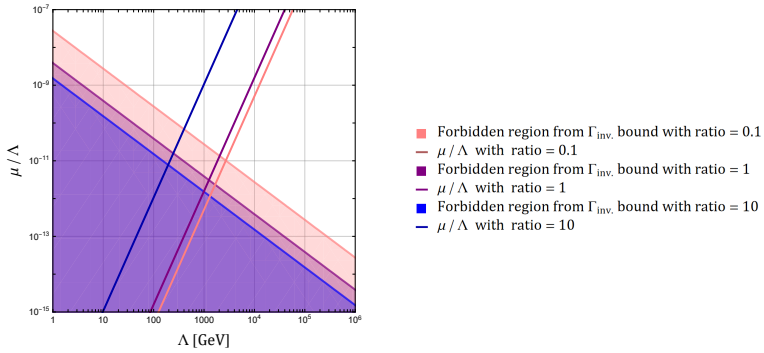

Figure 5.8: Here we present the forbidden regions resulting from enforcing the bound in eq.(4.14) for the following values of the ratios in eq.(5.13): 0.1 (red), 1 (purple) and 10 (blue). Following the same colour pattern, the lines represent the corresponding plots of μ/Λ compatible with a successful realization of the Neutrino Option.

5.4.3 Bounds from Lepton Flavour Violating Processes

As in Ref. [102], we also consider bounds coming from lepton violating processes. In particular, we take into account the branching ratio of lepton flavour violating (LFV) processes, which are mediated by heavy neutrinos at 1-loop. The contribution from these type of diagrams is:

$$\mathrm{BR}(\ell_\alpha \to \ell_\beta \gamma) = \frac{\alpha^3 \sin^2\theta_W}{256\pi^2}\left(\frac{m_{\ell_\alpha}}{m_W}\right)^4 \frac{m_{\ell_\alpha}}{\Gamma_{\ell_\alpha}} |G_{\alpha\beta}|^2, \tag{5.26}$$

where α is the fine-structure constant, θ_W is the Weinberg angle, m_{ℓ_α} is the mass of the decaying lepton, m_W in the mass of the W boson, Γ_{ℓ_α} is the total decay width of the decaying lepton, and:

$$G_{\alpha\beta} \equiv \sum_j V^*_{\alpha j} V_{\beta j} G_\gamma\left(\frac{m^2_{N_j}}{m^2_W}\right), \tag{5.27}$$

where V is the mixing matrix and its elements are given by eq.(3.69) and m_{N_j} are the heavy masses in eq.(3.67). $G_\gamma(x)$ is a photonic composite form factor obtained from expanding the loop integrals up to the first non-vanishing order [118], and is given by:

$$G_\gamma(x) = -\frac{2x^3+5x^2-x}{4(1-x)^3} - \frac{3x^3}{2(1-x)^4}\ln x. \tag{5.28}$$

The total widths of τ and μ are:

$$\Gamma_\mu = \frac{G_F^2 m_\mu^5}{192\pi^3}\left(1-8\frac{m_e^2}{m_\mu^2}\right)\left[1+\frac{\alpha}{2\pi}\left(\frac{25}{4}-\pi^2\right)\right] \quad [119]$$

$$\Gamma_\tau = (2.267 \pm 0.004)\cdot 10^{-2}\,\mathrm{GeV} \quad [120]. \tag{5.29}$$

From experiments we have the upper bounds on the following branching ratios:

$$\begin{aligned} &\mathrm{BR}(\mu \to e\gamma) < 4.2 \cdot 10^{-13} \quad [121] \\ &\mathrm{BR}(\tau \to e\gamma) < 1.5 \cdot 10^{-10} \quad [122] \\ &\mathrm{BR}(\tau \to \mu\gamma) < 1.5 \cdot 10^{-10} \quad [122]. \end{aligned} \tag{5.30}$$

In Fig.5.9 we show the forbidden regions resulting from enforcing the bounds in eq.(5.30) for a value of the ratios in eq.(5.13) equal to 10. Additional plots for different values of the ratios are shown in Appendix D. All the numerical values have been taken by the PDG summary tables [115].

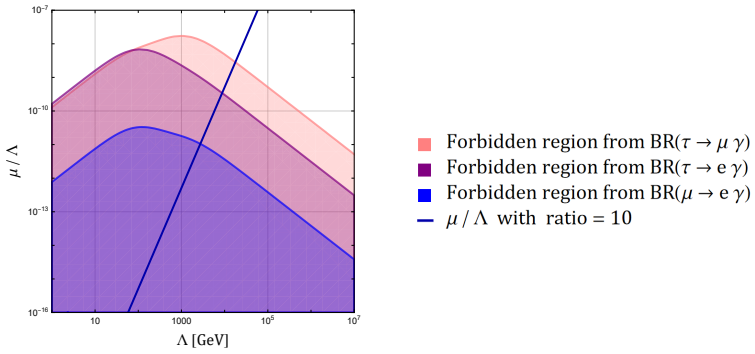

Figure 5.9: Here we present the forbidden regions resulting from enforcing the bound in eq.(5.30) for a value of the ratios in eq.(5.13) equal to 10. The blue line represents the corresponding plots of μ/Λ compatible with a successful realization of the Neutrino Option.

5.4.4 Summary

Here we present the summary plots of the forbidden regions resulting from enforcing the bounds coming from direct searches of heavy neutral leptons, the invisible width of Z and lepton flavour violating processes. Each plot in Fig.5.10 contains all the forbidden regions for a chosen value of the ratio in eq.(5.13). Each coloured area in the plots corresponds to the total forbidden region coming from the respective physical constraint. For example, the purple region in the bottom plot of Fig.5.10 is the union of the green and blue areas of both plots in Fig.5.7, the orange one corresponds to the blue one in Fig.5.8 and the yellow one corresponds to the union of the three regions in Fig.5.9. The plots for different values of the ratios are obtained in the same way.

From the summary plots in Fig.5.10 we can conclude that the experimental bounds allow us to exclude the region $\Lambda \lesssim 10^{3-4}$ GeV.

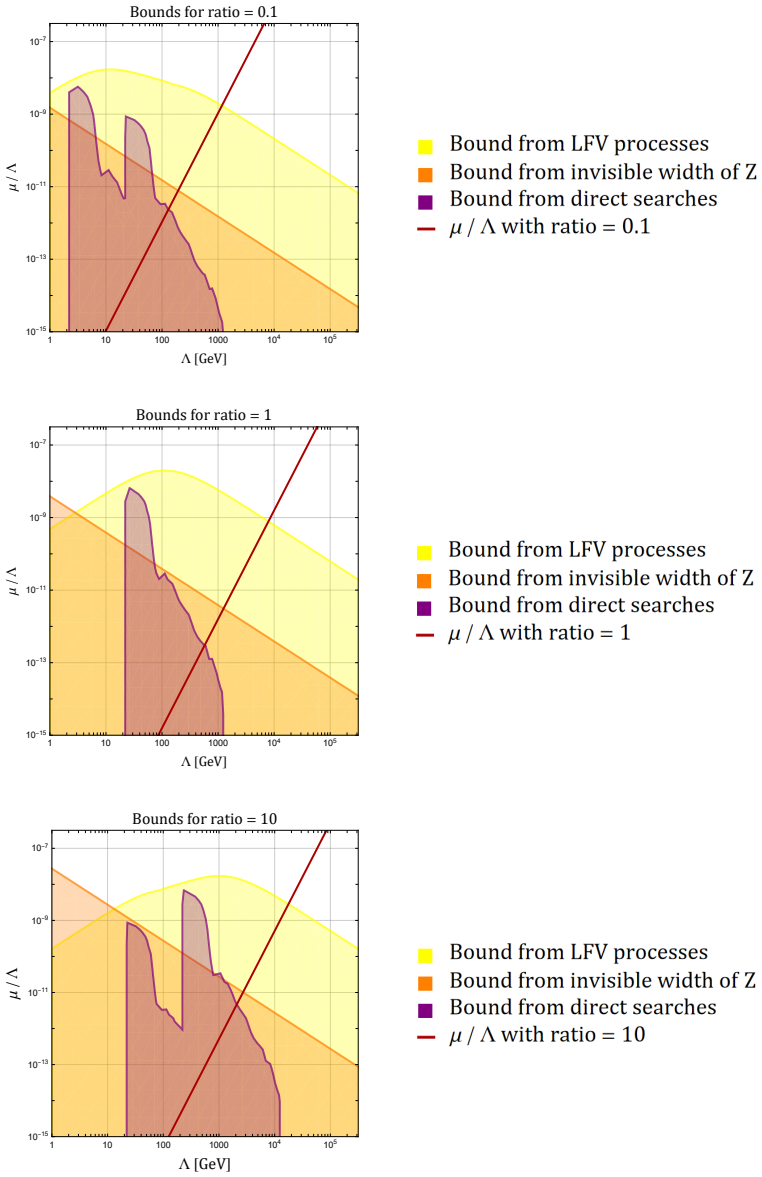

Figure 5.10: Here we present the summary plots of the forbidden regions resulting from all the experimental constraints we considered. The purple region corresponds to the bounds from direct searches of heavy neutral leptons. The orange regions corresponds to the bounds on the invisible width of Z. The yellow region corresponds to the bounds on the branching ratios of LFV processes. The red line corresponds to μ/Λ for the chosen values of the ratios in eq.(5.13), namely 0.1 (top), 1 (middle) and 10 (bottom).

5.5 Comparison between Type 1 and Inverse Seesaw

Now that we have concluded the analysis of our implementation of the Neutrino Option, we can compare our results to the ones in Ref. [5]. The crucial difference between these two scenarios, is that the Inverse Seesaw gives us more freedom by introducing an additional parameter with respect to the Type 1 Seesaw. This is particularly clear from the predictions of the light neutrino masses from the two Seesaw models:

$$\text{Type 1 Seesaw} \quad \rightarrow \quad m_\nu \sim \frac{Y^2}{\Lambda} \tag{5.31}$$

$$\text{Inverse Seesaw} \quad \rightarrow \quad m_\nu \sim \frac{Y^2 \mu}{\Lambda^2}. \tag{5.32}$$

The Type 1 Seesaw presents a greater interplay between all the quantities involved. Specifically, m_ν controls both the Yukawa and the matching contribution of the Higgs mass, as shown in Fig.5.1. The Inverse Seesaw instead presents a different scenario, where m_ν controls the ratio μ/Λ, while the Yukawa depends only on δm^2, as we can see from eq.(5.7). A remarkable consequence of the difference between the two models is the resulting prediction of the heavy mass:

$$\text{Type 1 Seesaw} \quad \rightarrow \quad 10^6\,\text{GeV} \lesssim \Lambda \lesssim 10^7\,\text{GeV} \tag{5.33}$$

$$\text{Inverse Seesaw} \quad \rightarrow \quad 10^{3-4}\,\text{GeV} \lesssim \Lambda \lesssim 10^6\,\text{GeV}. \tag{5.34}$$

As we can see, the Inverse Seesaw predicts a much lower mass for the heavy neutrino, reaching experimentally testable energy scales. Moreover, we notice that the bounds coming from the invisible width of Z and LFV processes are almost irrelevant for the Type 1 Seesaw, since they do not reach the energy scales at which this implementation of the Neutrino Option is viable.

Chapter 6

Conclusions

In this work we have presented an alternative implementation of the Neutrino Option, a scenario that simultaneously addresses two of the open problems of the Standard Model: neutrino masses and the hierarchy problem. In particular, using the EFT approach it simultaneously generates the light neutrino masses at tree-level at dimension 5 and the Higgs potential through 1-loop diagrams. Different from existing studies in the literature, we have adopted an Inverse Seesaw model instead of a Type 1 Seesaw for the realization of the Neutrino Option, and we have performed an original phenomenological study exploring the viability of this scenario from an EFT perspective, without committing to any specific UV completion. Specifically, our goal was to investigate the possibility of getting a lower prediction for the mass of the heavy neutrinos exploiting the extra freedom given by the parameter space of the ISS.

In Chapter 2 we have presented the technical tools of the EFT approach, emphasising the importance and advantages of using Effective Field Theories. In particular we showed how to perform the matching of an EFT onto a UV theory, how to use the Renormalization Group Equations and we introduced the Standard Model Effective Field Theory.

In Chapter 3 we extensively discussed the problem of neutrino masses in the SM and we presented different scenarios that could potentially solve it. We focused on the Seesaw models, with particular attention to the Type 1 and Inverse Seesaw. For both models, we derived the prediction of the light neutrino masses and we showed the Casas-Ibarra parametrization of the Yukawa matrix. Finally, we presented the state of the art of neutrino physics showing the latest results from several experiments.

In Chapter 4 we performed the tree-level and 1-loop matching of the Seesaw models onto the SMEFT, going up to dimension 6 at tree-level and dimension 4 at 1-loop. We started by reproducing the results for the Type 1 Seesaw and later we generalized them

to obtain the matching contributions given by the Inverse Seesaw. The 1-loop matching of the ISS constitutes the first original part of this work.

In Chapter 5 we showed the original results of the alternative implementation of the Neutrino Option. Our goal was to find an energy scale at which the ISS predictions are compatible with constraints coming from neutrino physics, the measured value of the Higgs mass and some experimental constraints. In the first place, we performed the numerical analysis using the results of the matching contributions in the limit of just one flavour generation for both light and heavy neutrinos in order to get some order-of-magnitude predictions. Afterwards, in order to get more realistic results, we extended the analysis by considering three generations of light neutrinos and two generations for each of the two heavy neutrinos. In this limit we were able to enforce some experimental bounds from direct searches for heavy neutral leptons, the invisible width of Z and some lepton number violating processes. Since our goal was not to perform an accurate study of the flavour structure, we made some simplifications by considering both the matrices μ and Λ to be diagonal and neglecting the running of the light neutrino masses. However, we point out that the results in the one flavour limit remain valid also in the more general case.

From our analysis, we conclude that the prediction for the masses of the heavy neutrinos that is compatible with this realization of the Neutrino Option is:

$$10^{3-4}\,\mathrm{GeV} \lesssim \Lambda \lesssim 10^{6}\,\mathrm{GeV}.$$

This is exactly the result we were hoping for, since it lowers the prediction of the Type 1 Seesaw, reaching experimentally testable energy scales.

There are several directions that can be explored in order to expand the study that we proposed in this work:

- Starting from a conformal UV embedding we can have a fully scale invariant UV theory.
- We can refine the flavour structure by removing the simplifications that we previously mentioned. This would also lead to additional free parameters.
- We can introduce additional sources of lepton number violations, such as a second Yukawa in the ISS Lagrangian that couples S_R to the SM $SU(2)$ doublet, as well as a Majorana mass term for N.
- We can explore additional physical constraints in addition to the ones we considered in this work, such as existing bounds the meson decay $B \to K\nu\bar{\nu}$.

Appendix A

EFT Amplitude Scaling

An amplitude obtained from the insertion of V dimension > 4 scales as:

$$\mathcal{A} \sim p^{N_p+F/2} \left(\frac{1}{\Lambda}\right)^{\sum N_{\Lambda_i}}, \tag{A.1}$$

where the factor $F/2$ at the exponent of the momentum comes from the polarizations of external fermions scaling as: $u, v \sim \sqrt{p}$. An operator of dimension > 4 can in general be written as:

$$\mathcal{O}_i^{(D)} \sim \phi^{b_i}\, \psi^{f_i}\, \partial^{q_i}, \tag{A.2}$$

where ϕ are boson fields, ψ are fermion fields and ∂ are derivatives. Using this expression we can write:

$$\sum N_{\Lambda_i} = \sum \left(b_i + \frac{3}{2} f_i + q_i - 4\right), \tag{A.3}$$

where $b_i + (3/2)f_i + q_i = D_i$ is the mass dimension of the Lagrangian term. We recall that we are considering only $\mathcal{O}_i^{(D>4)}$ operators, for which $D_i \geq 5$. Let us now consider the following relations:

$$\sum b_i = B + 2I_B \tag{A.4}$$

$$\sum f_i = F + 2I_F \tag{A.5}$$

$$N_p = 4L - 2I_B - I_F + \sum q_i, \tag{A.6}$$

where B and F are the number of external bosons and fermions respectively, $I_{B/F}$ is the number of internal lines and L the number of loops. Substituting these expressions in eq.(A.3) we get:

$$\sum N_{\Lambda_i} = B + \frac{3}{2} F + N_p + 4I_B + 4I_F - 4L - 4V, \tag{A.7}$$

where V is the number of vertices. Finally, using the relation:

$$L = I - V + 1, \tag{A.8}$$

we get:

$$\sum N_{\Lambda_i} = B + \frac{3}{2}F + N_p - 4. \tag{A.9}$$

Inverting this expression we get:

$$N_p + \frac{F}{2} = \sum N_{\Lambda_i} + 4 - B - F = \sum N_{\Lambda_i} + 4 - N, \tag{A.10}$$

where N is the number of external legs. Putting everything together we get that the amplitude scales as:

$$\mathcal{A} \sim p^{4-N} \left(\frac{p}{\Lambda}\right)^n \quad \text{with} \quad n = \sum (D_i - 4). \tag{A.11}$$

Appendix B

Algebra of Gamma Matrices

The gamma matrices γ^μ are 4×4 complex matrices, that in the Dirac notation are defined as:

$$\gamma^0 = \begin{pmatrix} \mathbb{1} & 0 \\ 0 & -\mathbb{1} \end{pmatrix}, \quad \gamma^i = \begin{pmatrix} 0 & \sigma^i \\ -\sigma^i & 0 \end{pmatrix}, \tag{B.1}$$

where σ^i are the Pauli matrices:

$$\sigma_1 = \begin{pmatrix} 0 & 1 \\ 1 & 0 \end{pmatrix}, \quad \sigma_2 = \begin{pmatrix} 0 & -i \\ i & 0 \end{pmatrix}, \quad \sigma_3 = \begin{pmatrix} 1 & 0 \\ 0 & -1 \end{pmatrix}. \tag{B.2}$$

The algebra of gamma matrices is defined by the anti-commutation relation:

$$\{\gamma^\mu, \gamma^\nu\} = 2\eta^{\mu\nu}\mathbb{1}, \tag{B.3}$$

where $\eta^{\mu\nu} = \text{diag}(+, -, -, -)$ is the Minkowski metric. The gamma matrices satisfy the relations:

$$\gamma^\mu\gamma_\mu = 4\mathbb{1}, \quad (\gamma^\mu)^\dagger = \gamma^0\gamma^\mu\gamma^0. \tag{B.4}$$

Starting from the gamma matrices we can define the γ^5 matrix as:

$$\gamma^5 = i\gamma^0\gamma^1\gamma^2\gamma^3 = \begin{pmatrix} 0 & \mathbb{1} \\ \mathbb{1} & 0 \end{pmatrix}, \tag{B.5}$$

which satisfies the properties:

$$(\gamma^5)^2 = \mathbb{1}, \quad \text{Tr}\big[\gamma^5\big] = 0, \quad \{\gamma^5, \gamma^\mu\} = 0. \tag{B.6}$$

There are several properties of the gamma matrices that are particularly useful when performing calculations that involve fermions:

$$\text{Tr}[\gamma^\mu] = 0, \tag{B.7}$$

$$\text{Tr}[\gamma^\mu\gamma^\nu] = 4\eta^{\mu\nu}, \tag{B.8}$$

$$\text{Tr}[\gamma^{\mu_1}...\gamma^{\mu_N}] = 0 \quad \text{for } N \text{ odd}, \tag{B.9}$$

$$\text{Tr}\big[\gamma^\mu\gamma^\nu\gamma^5\big] = 0, \tag{B.10}$$

$$\text{Tr}\big[\gamma^{\mu_1}...\gamma^{\mu_N}\gamma^5\big] = 0 \quad \text{for } N \text{ odd}. \tag{B.11}$$

Other important quantities that are defined using the gamma matrices are the projection operators and the charge conjugation matrix. The projector operators are defined as:

$$P_L = \frac{1}{2}(1-\gamma_5), \quad P_R = \frac{1}{2}(1+\gamma_5), \tag{B.12}$$

and they satisfy the following properties:

$$P_{L,R}^2 = P_{L,R} \tag{B.13}$$
$$P_{L,R}^\dagger = P_{L,R}^\dagger \tag{B.14}$$
$$P_L P_R = P_R P_L = 0 \tag{B.15}$$
$$P_L + P_L = \mathbb{1}. \tag{B.16}$$

The notation independent definition of the charge conjugation matrix is:

$$C\gamma^\mu C^{-1} = -(\gamma^\mu)^T, \tag{B.17}$$

which in Dirac notation corresponds to $C = i\gamma^2\gamma^0$, and satisfies the relations:

$$C^\dagger = C^{-1}, \quad C^T = -C, \quad C\Gamma_i^T C^{-1} = \eta_i \Gamma_i, \tag{B.18}$$

with:

$$\eta_i = \begin{cases} +1 & \text{for} \quad \Gamma_i = 1, i\gamma_5, \gamma_\mu\gamma_5 \\ -1 & \text{for} \quad \Gamma_i = \gamma_\mu, \sigma_{\mu\nu} \end{cases} . \tag{B.19}$$

Using all the properties that we presented above, we can demonstrate the relations we used to perform some of the calculations in this work:

(a) A useful relation that is often used is:

$$\bar{\psi_L} = \psi_L^\dagger\gamma^0 = (P_L\psi)^\dagger\gamma^0 = \psi_L^\dagger P_L\gamma^0 = \psi_L^\dagger\gamma^0 P_R = \bar{\psi_L}P_R. \tag{B.20}$$

(b) The charged conjugate of a LH spinor behaves as a RH spinor and vice versa. The charge conjugate is defined as:

$$\psi^c = C(\bar{\psi})^T. \tag{B.21}$$

Using this definition we have:

$$(\psi_L)^c = C\bar{\psi_L}^T = C(\bar{\psi_L}P_R)^T = CP_R\bar{\psi_L}^T = P_R C\bar{\psi_L}^T = P_R(\psi_L)^c. \tag{B.22}$$

(c) The bar of a charge conjugate spinor is:

$$\bar{\psi^c} = (C\bar{\psi_L}^T)^\dagger\gamma^0 = (\psi^\dagger\gamma^0)^* C^\dagger\gamma^0 = \psi^T\gamma^0 C^\dagger\gamma^0 = -\psi^T C^{-1}. \tag{B.23}$$

(d) The mass Lagrangian of a Dirac spinor in Weyl components is:

$$\begin{aligned}\mathcal{L}_{mass} &= m\bar{\psi}\psi = m\bar{\psi}(\psi_L + \psi_R) = m\psi^\dagger\gamma^0 P_L^2\psi + m\psi^\dagger\gamma^0 P_R^2\psi \\ &= m\psi^\dagger P_R\gamma^0 P_L\psi + m\psi^\dagger P_L\gamma^0 P_R\psi \\ &= m(\bar{\psi}_R\psi_L + \bar{\psi}_L\psi_R).\end{aligned} \tag{B.24}$$

Following the same steps we can get the mass Lagrangian of a Majorana spinor.

(e) The mass matrix in a Majorana mass term is symmetric:

$$\begin{aligned}\bar{\psi}_L^c M\psi_L &= -\psi_L^T M^T(\bar{\psi}_L^c)^T = \bar{\psi}_L^c C M^T(-\psi_L^T C^{-1})^T \\ &= \bar{\psi}_L^c C M^T(-C^{-1})^T\psi_L = \bar{\psi}_L^c M^T(-C^{-1}C)^T\psi_L \\ &= \bar{\psi}_L^c M^T\psi_L,\end{aligned} \tag{B.25}$$

where we have used the relation $\bar{\psi}M\chi = -\chi^T M^T\bar{\psi}^T$.

(f) The type 1 Seesaw mass Lagrangian is:

$$\mathcal{L}_{mass} = -\frac{1}{2}\left(\bar{N}Y\widetilde{H}^\dagger\ell_L + \bar{\ell}_L^c\widetilde{H}^* Y^T N^c + \bar{\ell}_L\widetilde{H}Y^\dagger N + \bar{N}Y^*\widetilde{H}^T\ell_L^c\right). \tag{B.26}$$

We can show that the first and the second terms are equivalent:

$$\bar{\ell}_L^c\widetilde{H}^* Y^T N^c = -\ell_L^T C^{-1}\widetilde{H}^* Y^T C\bar{N}^T = -\ell_L^T\widetilde{H}^* Y^T\bar{N}^T = \bar{N}Y\widetilde{H}^\dagger\ell_L. \tag{B.27}$$

This is true also for the third and fourth terms.

(g) Writing N or N_R in the mass Lagrangian is the same, since only the RH component of N contributes:

$$\bar{N}\ell_L = (\bar{N}_R P_L + \bar{N}_R^c P_L)P_L\ell_L = \bar{N}_R\ell_L. \tag{B.28}$$

(h) The Inverse Seesaw mass Lagrangian is:

$$\begin{aligned}\mathcal{L}_{mass} = &-\frac{1}{2}\left(\bar{\ell}_L Y^\dagger\widetilde{H}N_R + \bar{N}_R^c Y^*\widetilde{H}^T\ell_L^c\right) + h.c. \\ &-\frac{1}{2}\left(\bar{N}_R^c\Lambda S_R + \bar{S}_R^c\Lambda^T N_R + \bar{S}_R^c\mu S_R\right) + h.c.\end{aligned} \tag{B.29}$$

Similarly to the previous case, the two terms in the first line are equivalent:

$$\bar{N}_R^c Y^*\widetilde{H}^T\ell_L^c = -N_R^T\, C^{-1}\, Y^*\,\widetilde{H}^T\, C\bar{\ell_L}^T = -N_R^T\, Y^*\,\widetilde{H}^T\,\bar{\ell_L}^T = \bar{\ell_L}\,\widetilde{H}\,Y^\dagger\,N_R. \tag{B.30}$$

(i) Performing the matching of the Type 1 Seesaw to the dim-6 operator, after inserting the solutions of the EOMs in the kinetic term of the Lagrangian we get:

$$\mathcal{L} = \frac{1}{2}\left[\bar{\ell_L}\widetilde{H}\,(Y^\dagger M^{-2} Y)\, i\not{\partial}(\widetilde{H}^\dagger \ell_L) + \bar{\ell_L^c}\widetilde{H}^*\,(Y^T M^{-2} Y^*)\, i\not{\partial}(\widetilde{H}^T \ell_L^c)\right]. \tag{B.31}$$

When writing the equivalent of the second term, we must put a minus as eq.(B.19) tells us, In this way we have:

$$\mathcal{L} = \frac{1}{2}\left[\bar{\ell_L}\widetilde{H}\,(Y^\dagger M^{-2} Y)\, i\not{\partial}(\widetilde{H}^\dagger \ell_L) - \widetilde{H}^\dagger \ell_L\,(Y^\dagger M^{-2} Y)\, i\not{\partial}(\bar{\ell_L}\widetilde{H})\right]. \tag{B.32}$$

Now the second term is actually equivalent to the first by IBP, so we have:

$$\mathcal{L} = \bar{\ell_L}\widetilde{H}\,(Y^\dagger M^{-2} Y)\, i\not{\partial}(\widetilde{H}^\dagger \ell_L). \tag{B.33}$$

Appendix C

Overall factors in box-loop diagrams

The overall factors of loop diagrams can be tricky to evaluate since they keep track of many things, such as symmetry factors (that require some careful considerations) and in our case also constants that come from the matching between the EFT and the UV theory.
We now consider one of the box diagrams that give a contribution to the correction of λ given by the type 1 See-Saw Model and derive explicitly its overall factor, then the same procedure can be applied to the other diagrams. Let us start by considering the loops (A_1) in Fig.4.2. From the Feynman rule we have the factors:

$$\begin{aligned} &\times 2 \quad \rightarrow \quad \text{from the trace} \\ &\times 2 \quad \rightarrow \quad \text{from the Feynman parametrization} \\ &\times \frac{1}{32} \quad \rightarrow \quad \text{from the Tadpole integral}\,. \end{aligned}$$

Now we can start to consider the symmetry factors. At first sight we might think that diagrams (A_1) and (A_2) in Fig.4.2 are a multiplicity of the same digram, as the case of a 1-loop correction to a propagator where the internal lines are identical. The factor $1/2$ that appears in this kind of diagrams is due to an exchange of *internal* lines that gives rise to a diagram with the same topology. However, diagrams (A_1) and (A_2) differ from an exchange of *external* lines, so they are not multiplicities of the same diagram, but rather two independent diagrams. In this particular case though, they have the same Feynman rule, so we have an additional:

$$\times 2 \quad \rightarrow \quad \text{from having 2 independent diagrams with the same Feynman rule}\,.$$

Even after this considerations, we still have to evaluate the symmetry factor of the diagram and to do it we use the rules in Appendix D of [96]. Let us proceed by steps:

- We have four external lines in the diagram and each of them can be chosen in 2 different ways, so we have a factor 2×2. Once the external lines are chosen, there is a unique way to connect the internal lines for each topology.

- The number of permutations of points having identical vertices is: 2!2!.

Putting these things together we get the symmetry factor of the diagram:

$$S = \frac{2 \times 2}{2! \times 2!} = 1\,.$$

The last thing we need to do is consider the matching with the SMEFT. The loop we are evaluating is a $1PI$ diagram (evaluated in the UV theory) and we must impose that it is equal to the tree-level diagram of the interaction term appearing in the SMEFT[1]:

$$\mathcal{L}_H \supset \lambda\,(H^\dagger H)^2 \quad \rightarrow \quad i\mathcal{M}_{tree-lev} = i\,4\,\lambda\,.$$

Since λ is what we are interested in, we must divide the result of the loop by 4, giving us the additional factor:

$$\times\,\frac{1}{4} \quad \rightarrow \quad \text{from the matching with the SMEFT}\,.$$

Now, putting together everything we have said so far, we get the overall factor of the 1-loop correction to λ given by the type 1 See-Saw Model:

$$O = \frac{2 \times 2 \times 2 \times S}{32 \times 4} = \frac{1}{16}\,.$$

[1]The 4 in the tree-level amplitude comes from having two pairs of identical particles.

Appendix D

Additional Plots

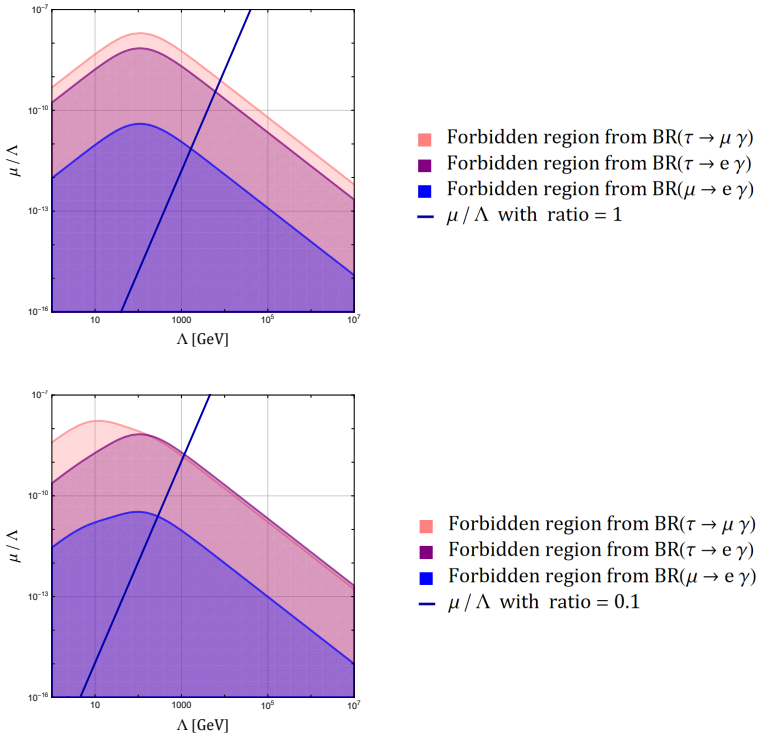

Figure D.1: Here we present the forbidden regions coming from the upper bounds on the branching ratios of lepton number violating processes. The first (second) plot is derived with a value of the ratio in eq.(5.13) equal to 1 (0.1). The blue line corresponds to μ/Λ evaluated with the corresponding ratio.

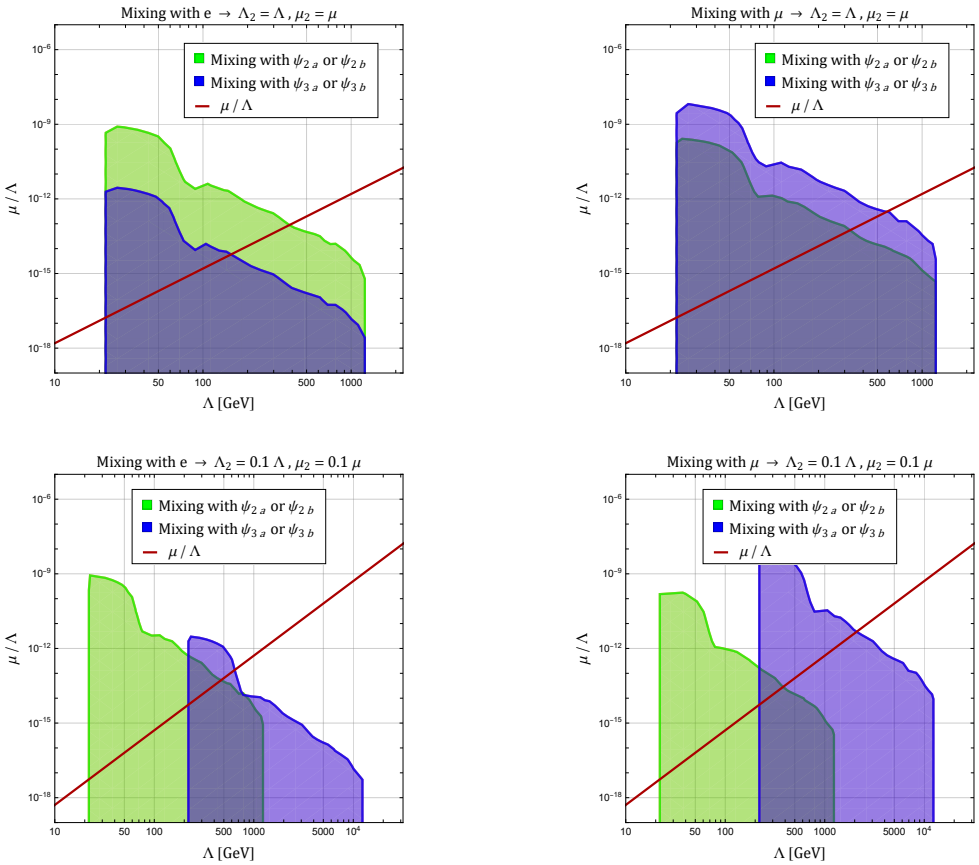

Figure D.2: Here we present the forbidden regions coming from the upper bounds on the electron channel (left) and the muon channel (right). The plots in the first (second) row are derived with a value of the ratio in eq.(5.13) equal to 1 (0.1). The green (blue) areas correspond to the mixing with the heavy eigenstates ψ_{2a} and ψ_{2b} (ψ_{3a} and ψ_{3b}). The red line corresponds to μ/Λ evaluated with the corresponding ratio.

Bibliography

[1] S. L. Glashow. Partial symmetries of weak interactions. *Nucl. Phys.*, 22:579–588, 1961.

[2] Steven Weinberg. A model of leptons. *Phys. Rev. Lett.*, 19:1264–1266, 1967.

[3] A. Salam. Proc. of the 8th nobel symposium on "elementary particle theory, relativistic groups and analyticity". Stockholm, Sweden, 1968.

[4] Ilaria Brivio and Michael Trott. Radiatively generating the higgs potential and electroweak scale via the seesaw mechanism. *Physical Review Letters*, 119(14), October 2017.

[5] Ilaria Brivio and Michael Trott. Examining the neutrino option. *Journal of High Energy Physics*, 2019(2), February 2019.

[6] Thomas Appelquist and J. Carazzone. Infrared singularities and massive fields. *Phys. Rev. D*, 11:2856–2861, May 1975.

[7] Wolfgang Pauli. Letter to a physicist's gathering at tübingen, december 4, 1930. In R. Kronig and V. Weisskopf, editors, *Collected Scientific Papers*, volume 2, page 1313. Interscience, New York, 1964. Originally written in 1930.

[8] C. L. Cowan, F. Reines, F. B. Harrison, H. W. Kruse, and A. D. McGuire. Detection of the free neutrino: a confirmation. *Science*, 124(3212):103–104, 1956.

[9] C. S. Wu, E. Ambler, R. W. Hayward, D. D. Hoppes, and R. P. Hudson. Experimental test of parity conservation in β decay. *Phys. Rev.*, 105:1413–1414, 1957.

[10] M. Goldhaber, L. Grodzins, and A. W. Sunyar. Helicity of neutrinos. *Phys. Rev.*, 109:1015–1017, 1958.

[11] L. D. Landau. On the conservation laws for weak interactions. *Nucl. Phys.*, 3:127–131, 1957.

[12] T. D. Lee and Chen-Ning Yang. Parity nonconservation and a two component theory of the neutrino. *Phys. Rev.*, 105:1671–1675, 1957.

[13] Abdus Salam. On parity conservation and neutrino mass. *Nuovo Cim.*, 5:299–301, 1957.

[14] B. Pontecorvo. Mesonium and Antimesonium. *Sov. Phys. JETP*, 6:429–431, 1958.

[15] B. Pontecorvo. Inverse Beta Processes and Nonconservation of Lepton Charge. *Sov. Phys. JETP*, 7:172–173, 1958.

[16] Ziro Maki, Masami Nakagawa, and Shoichi Sakata. Remarks on the unified model of elementary particles. *Progress of Theoretical Physics*, 28(5):870–880, 11 1962.

[17] B. Pontecorvo. Neutrino Experiments and the Problem of Conservation of Leptonic Charge. *Zh. Eksp. Teor. Fiz.*, 53:1717–1725, 1967.

[18] V. N. Gribov and B. Pontecorvo. Neutrino astronomy and lepton charge. *Phys. Lett. B*, 28:493, 1969.

[19] Shalom Eliezer and Arthur R. Swift. Experimental consequences of $\nu e - \nu \mu$ mixing in neutrino beams. *Nuclear Physics B*, 105(1):45–51, 1976.

[20] H. Fritsch and P. Minkowski. Vectorlike weak currents, massive neutrinos, and neutrino beam oscillations. *Physics Letters B*, 62(1):72–76, 1976.

[21] S.M. Bilenky and B. Pontecorvo. Majorana and dirac masses, neutrino oscillations and the number of charged leptons. *Physics Letters B*, 95(2):233–236, 1980.

[22] Samoil M. Bilenky and B. Pontecorvo. Again on Neutrino Oscillations. *Lett. Nuovo Cim.*, 17:569, 1976.

[23] Y. et all Fukuda. Solar neutrino data covering solar cycle 22. *Phys. Rev. Lett.*, 77:1683–1686, Aug 1996.

[24] Combined analysis of all three phases of solar neutrino data from the sudbury neutrino observatory. *Phys. Rev. C*, 88:025501, Aug 2013.

[25] Gerard 't Hooft. Naturalness, chiral symmetry, and spontaneous chiral symmetry breaking. *NATO Sci. Ser. B*, 59:135–157, 1980.

[26] Matthew McCullough. Lectures on Physics Beyond the Standard Model. In *6th Tri-Institute Summer School on Elementary Particles*, 2018.

[27] Howard Baer and Xerxes Tata. *Weak Scale Supersymmetry: From Superfields to Scattering Events*. Cambridge University Press, 2006.

[28] STEPHEN P. MARTIN. *A SUPERSYMMETRY PRIMER*, page 1–98. WORLD SCIENTIFIC, July 1998.

[29] Roberto Contino. Tasi 2009 lectures: The higgs as a composite nambu-goldstone boson, 2010.

[30] Giuliano Panico and Andrea Wulzer. *The Composite Nambu-Goldstone Higgs*. Springer International Publishing, 2016.

[31] Aneesh V. Manohar. Introduction to effective field theories, 2018.

[32] Kenneth G. Wilson. Quantum field - theory models in less than 4 dimensions. *Phys. Rev. D*, 7:2911–2926, May 1973.

[33] John C. Collins. *Renormalization : An Introduction to Renormalization, the Renormalization Group and the Operator-Product Expansion*, volume 26 of *Cambridge Monographs on Mathematical Physics*. Cambridge University Press, Cambridge, 1984.

[34] Michael E. Peskin and Daniel V. Schroeder. *An Introduction to quantum field theory*. Addison-Wesley, Reading, USA, 1995.

[35] José Santiago. Granada lectures on effective field theories, July 2024. VERY PRELIMINARY version.

[36] H. Georgi. Effective field theory. *Ann. Rev. Nucl. Part. Sci.*, 43:209–252, 1993.

[37] Joseph Polchinski. Renormalization and Effective Lagrangians. *Nucl. Phys. B*, 231:269–295, 1984.

[38] Timothy Cohen. As scales become separated: Lectures on effective field theory, 2020.

[39] Curtis G. Callan. Broken scale invariance in scalar field theory. *Phys. Rev. D*, 2:1541–1547, Oct 1970.

[40] K. Symanzik. Small distance behavior in field theory and power counting. *Commun. Math. Phys.*, 18:227–246, 1970.

[41] K. Symanzik. Small distance behavior analysis and Wilson expansion. *Commun. Math. Phys.*, 23:49–86, 1971.

[42] Thomas Appelquist and J. Carazzone. Infrared singularities and massive fields. *Phys. Rev. D*, 11:2856–2861, May 1975.

[43] Ilaria Brivio and Michael Trott. The standard model as an effective field theory. *Physics Reports*, 793:1–98, February 2019.

[44] Gino Isidori, Felix Wilsch, and Daniel Wyler. The standard model effective field theory at work. *Reviews of Modern Physics*, 96(1), March 2024.

[45] Hein Lehmann, Kurt Symanzik, and Wolf Zimmermann. Zur formulierung quantisierter feldtheorien. *Il Nuovo Cimento (1955-1965)*, 1:205–225, 1955.

[46] C. Arzt. Reduced effective lagrangians. *Physics Letters B*, 342(1–4):189–195, January 1995.

[47] Howard Georgi. On-shell effective field theory. *Nuclear Physics B*, 361(2):339–350, 1991.

[48] H. David Politzer. Power corrections at short distances. *Nuclear Physics B*, 172:349–382, 1980.

[49] Markus Fierz. Zur Fermischen Theorie des β-Zerfalls. *Z. Phys.*, 104(7-8):553–565, 1937.

[50] C. C. Nishi. Simple derivation of general fierz-type identities. *American Journal of Physics*, 73(12):1160–1163, December 2005.

[51] Andrew Kobach. Baryon number, lepton number, and operator dimension in the standard model. *Phys. Lett. B*, 758:455–457, 2016.

[52] W. Buchmuller and D. Wyler. Effective Lagrangian Analysis of New Interactions and Flavor Conservation. *Nucl. Phys. B*, 268:621–653, 1986.

[53] B. Grzadkowski, M. Iskrzyński, M. Misiak, and J. Rosiek. Dimension-six terms in the standard model lagrangian. *Journal of High Energy Physics*, 2010(10), October 2010.

[54] Steven Weinberg. Baryon- and lepton-nonconserving processes. *Phys. Rev. Lett.*, 43:1566–1570, Nov 1979.

[55] Frank Wilczek and A. Zee. Operator analysis of nucleon decay. *Phys. Rev. Lett.*, 43:1571–1573, Nov 1979.

[56] L. F. Abbott and Mark B. Wise. Effective hamiltonian for nucleon decay. *Phys. Rev. D*, 22:2208–2212, Nov 1980.

[57] Landon Lehman. Extending the standard model effective field theory with the complete set of dimension-7 operators. *Physical Review D*, 90(12), December 2014.

[58] Landon Lehman and Adam Martin. Low-derivative operators of the standard model effective field theory via hilbert series methods. *Journal of High Energy Physics*, 2016(2), February 2016.

[59] Brian Henning, Xiaochuan Lu, Tom Melia, and Hitoshi Murayama. 2, 84, 30, 993, 560, 15456, 11962, 261485, ...: Higher dimension operators in the sm eft, 2019.

[60] Yi Liao and Xiao-Dong Ma. An explicit construction of the dimension-9 operator basis in the standard model effective field theory. *Journal of High Energy Physics*, 2020(11), November 2020.

[61] R. V. Harlander, T. Kempkens, and M. C. Schaaf. Standard model effective field theory up to mass dimension 12. *Phys. Rev. D*, 108(5):055020, 2023.

[62] Silvia Pascoli. Neutrino physics. *CERN Yellow Rep. School Proc.*, 6:213–259, 2019.

[63] Carlo Giunti and Chung W. Kim. *Fundamentals of Neutrino Physics and Astrophysics*. 2007.

[64] J. de Blas, J. C. Criado, M. Pérez-Victoria, and J. Santiago. Effective description of general extensions of the standard model: the complete tree-level dictionary. *Journal of High Energy Physics*, 2018(3), March 2018.

[65] Peter Minkowski. $\mu \to e\gamma$ at a rate of one out of 109 muon decays? *Physics Letters B*, 67(4):421–428, 1977.

[66] Murray Gell-Mann, Pierre Ramond, and Richard Slansky. Complex spinors and unified theories, 2013.

[67] Osamu Sawada and Akio Sugamoto, editors. *Proceedings: Workshop on the Unified Theories and the Baryon Number in the Universe: Tsukuba, Japan, February 13-14, 1979*, Tsukuba, Japan, 1979. Natl.Lab.High Energy Phys.

[68] Rabindra N. Mohapatra and Goran Senjanović. Neutrino mass and spontaneous parity nonconservation. *Phys. Rev. Lett.*, 44:912–915, Apr 1980.

[69] M Magg and C Wetterich. Neutrino mass problem and gauge hierarchy. *Phys. Lett. B*, 94:61–64, 1980.

[70] J. Bijnens and C. Wetterich. Quark, lepton and neutrino masses in grand unified theories with local generation group. *Nuclear Physics B*, 292:443–460, 1987.

[71] G. Lazarides, Q. Shafi, and C. Wetterich. Proton lifetime and fermion masses in an SO(10) model. *Nuclear Physics B*, 181(2):287–300, 1981.

[72] Rabindra N. Mohapatra and Goran Senjanović. Neutrino masses and mixings in gauge models with spontaneous parity violation. *Phys. Rev. D*, 23:165–180, Jan 1981.

[73] Robert Foot, H. Lew, X. G. He, and Girish C. Joshi. Seesaw Neutrino Masses Induced by a Triplet of Leptons. *Z. Phys. C*, 44:441, 1989.

[74] Ernest Ma. Pathways to naturally small neutrino masses. *Phys. Rev. Lett.*, 81:1171–1174, Aug 1998.

[75] GORAN SENJANOVIĆ. See-saw and grand unification. In *SEESAW 25*, page 45–64. WORLD SCIENTIFIC, April 2005.

[76] Manimala Mitra, Goran Senjanović, and Francesco Vissani. Neutrinoless double beta decay and heavy sterile neutrinos. *Nuclear Physics B*, 856(1):26–73, March 2012.

[77] Walter Grimus and Luís Lavoura. The seesaw mechanism at arbitrary order: disentangling the small scale from the large scale. *Journal of High Energy Physics*, 2000(11):042–042, November 2000.

[78] D. Wyler and L. Wolfenstein. Massless neutrinos in left-right symmetric models. *Nucl. Phys. B*, 218:205–214, 1983.

[79] R. N. Mohapatra and J. W. F. Valle. Neutrino mass and baryon number nonconservation in superstring models. *Phys. Rev. D*, 34:1642, 1986.

[80] D. Cogollo, F.F. Freitas, C.A. de S. Pires, Yohan M. Oviedo-Torres, and P. Vasconcelos. Deep learning analysis of the inverse seesaw in a 3-3-1 model at the lhc. *Physics Letters B*, 811:135931, December 2020.

[81] Céline Degrande, Olivier Mattelaer, Richard Ruiz, and Jessica Turner. Fully automated precision predictions for heavy neutrino production mechanisms at hadron colliders. *Physical Review D*, 94(5), September 2016.

[82] J. A. Casas and A. Ibarra. Oscillating neutrinos and $\mu \to e, \gamma$. *Nucl. Phys. B*, 618:171–204, 2001.

[83] Fernando Arias-Aragón, Enrique Fernández Martínez, Manuel González-López, and Luca Merlo. Dynamical minimal flavour violating inverse seesaw. *Journal of High Energy Physics*, 2022(9), September 2022.

[84] Vincenzo Cirigliano, Gino Isidori, and Valentina Porretti. Cp violation and leptogenesis in models with minimal lepton flavour violation. *Nuclear Physics B*, 763(1–2):228–246, February 2007.

[85] Ananya Mukherjee and Nimmala Narendra. Retrieving inverse seesaw parameter space for dirac phase leptogenesis, 2022.

[86] Matthew J. Dolan, Tomasz P. Dutka, and Raymond R. Volkas. Dirac-phase thermal leptogenesis in the extended type-i seesaw model. *Journal of Cosmology and Astroparticle Physics*, 2018(06):012–012, June 2018.

[87] Ivan Esteban, M. C. Gonzalez-Garcia, Michele Maltoni, Ivan Martinez-Soler, João Paulo Pinheiro, and Thomas Schwetz. NuFit-6.0: updated global analysis of three-flavor neutrino oscillations. *Journal of High Energy Physics*, 2024(12), December 2024.

[88] NuFIT Website.

[89] Alexander Barabash. Double beta decay experiments: Recent achievements and future prospects. *Universe*, 9(6), 2023.

[90] KATRIN group. Direct neutrino-mass measurement based on 259 days of katrin data, 2024.

[91] Helen Shao, Jahmour J. Givans, Jo Dunkley, Mathew Madhavacheril, Frank Qu, Gerrit Farren, and Blake Sherwin. Cosmological limits on the neutrino mass sum for beyond-λcdm models, 2024.

[92] Patrick Stöcker, Csaba Balázs, Sanjay Bloor, Torsten Bringmann, Tomás E. Gonzalo, Will Handley, Selim Hotinli, Cullan Howlett, Felix Kahlhoefer, Janina J. Renk, Pat Scott, Aaron C. Vincent, and Martin White. Strengthening the bound on the mass of the lightest neutrino with terrestrial and cosmological experiments. *Physical Review D*, 103(12), June 2021.

[93] Juan José Gómez-Cadenas, Justo Martín-Albo, Javier Menéndez, Mauro Mezzetto, Francesc Monrabal, and Michel Sorel. The search for neutrinoless double-beta decay. *Riv. Nuovo Cim.*, 46(10):619–692, 2023.

[94] Di Zhang and Shun Zhou. Complete one-loop matching of the type-i seesaw model onto the standard model effective field theory. *Journal of High Energy Physics*, 2021(9), September 2021.

[95] Ansgar Denner, H. Eck, O. Hahn, and J. Kublbeck. Feynman rules for fermion number violating interactions. *Nucl. Phys. B*, 387:467–481, 1992.

[96] Martinus Veltman. *Diagrammatica: The Path to Feynman Diagrams*. Cambridge Lecture Notes in Physics. Cambridge University Press, 1994.

[97] Vedran Brdar, Yannick Emonds, Alexander J. Helmboldt, and Manfred Lindner. Conformal realization of the neutrino option. *Physical Review D*, 99(5), March 2019.

[98] Jisuke Kubo, Jeffrey Kuntz, Manfred Lindner, Jonas Rezacek, Philipp Saake, and Andreas Trautner. Unified emergence of energy scales and cosmic inflation. *JHEP*, 08:016, 2021.

[99] Vedran Brdar, Alexander J. Helmboldt, Sho Iwamoto, and Kai Schmitz. Type-I Seesaw as the Common Origin of Neutrino Mass, Baryon Asymmetry, and the Electroweak Scale. *Phys. Rev. D*, 100:075029, 2019.

[100] Mayumi Aoki, Vedran Brdar, and Jisuke Kubo. Heavy dark matter, neutrino masses, and Higgs naturalness from a strongly interacting hidden sector. *Phys. Rev. D*, 102(3):035026, 2020.

[101] Eldad Gildener and Steven Weinberg. Symmetry breaking and scalar bosons. *Phys. Rev. D*, 13:3333–3341, Jun 1976.

[102] Aqeel Ahmed, Juan P. Garcés, and Manfred Lindner. Radiative symmetry breaking with a scale invariant seesaw, 2025.

[103] Javier Fuentes-Martín, Pedro Ruiz-Femenía, Avelino Vicente, and Javier Virto. Dsixtools 2.0: the effective field theory toolkit. *The European Physical Journal C*, 81(2), February 2021.

[104] Alejandro Celis, Javier Fuentes-Martín, Avelino Vicente, and Javier Virto. Dsixtools: the standard model effective field theory toolkit. *The European Physical Journal C*, 77(6), June 2017.

[105] Dario Buttazzo, Giuseppe Degrassi, Pier Paolo Giardino, Gian F. Giudice, Filippo Sala, Alberto Salvio, and Alessandro Strumia. Investigating the near-criticality of the higgs boson. *Journal of High Energy Physics*, 2013(12), December 2013.

[106] J.A. Casas, V. Di Clemente, and M. Quirós. The effective potential in the presence of several mass scales. *Nuclear Physics B*, 553(1–2):511–530, July 1999.

[107] CMS Collaboration. Search for heavy majorana neutrinos in same-sign dilepton channels in proton-proton collisions at $\sqrt{s} = 13$ TeV. *Journal of High Energy Physics*, 2019(1), January 2019.

[108] Jorge de Blas. Electroweak limits on physics beyond the standard mode. *EPJ Web of Conferences*, 60:19008, 2013.

[109] P. Abreu et al. Search for neutral heavy leptons produced in Z decays. *Z. Phys. C*, 74:57–71, 1997. [Erratum: Z.Phys.C 75, 580 (1997)].

[110] O. Adriani et al. Search for isosinglet neutral heavy leptons in Z^0 decays. *Phys. Lett. B*, 295:371–382, 1992.

[111] L3 Collaboration. Search for heavy isosinglet neutrino in e^+e^- annihilation at lep. *Physics Letters B*, 517(1–2):67–74, September 2001.

[112] ATLAS Collaboration. Search for heavy majorana neutrinos with the atlas detector in pp collisions at $\sqrt{s} = 8$ TeV. *Journal of High Energy Physics*, 2015(7), July 2015.

[113] CMS Collaboration. Search for heavy majorana neutrinos in ee + jets and eμ + jets events in proton-proton collisions at $\sqrt{s} = 8$ TeV. *Journal of High Energy Physics*, 2016(4), April 2016.

[114] CMS Collaboration. Search for heavy neutral leptons in events with three charged leptons in proton-proton collisions at $\sqrt{s} = 13$ TeV. *Physical Review Letters*, 120(22), May 2018.

[115] S. Navas et al. Review of particle physics. *Phys. Rev. D*, 110(3):030001, 2024.

[116] ATLAS collaboration. Measurement of the Z boson invisible width at $\sqrt{s} = 13$ TeV with the ATLAS detector. *Physics Letters B*, 854:138705, July 2024.

[117] CMS Collaboration. Precision measurement of the Z boson invisible width in pp collisions at $\sqrt{s} = 13$ TeV. *Physics Letters B*, 842:137563, July 2023.

[118] Takeo Inami and C. S. Lim. Effects of superheavy quarks and leptons in low-energy weak processes KL$\rightarrow \mu\mu$, K+ $\rightarrow \pi + \nu\nu$ and $K0 \leftrightarrow K0$. *Progress of Theoretical Physics*, 65(1):297–314, 1981.

[119] A. Ilakovac and A. Pilaftsis. Flavour-violating charged lepton decays in seesaw-type models. *Nuclear Physics B*, 437(3):491–519, March 1995.

[120] Particle Data Group. Review of particle physics. *Progress of Theoretical and Experimental Physics*, 2020(8):083C01, 08 2020.

[121] The MEG Collaboration. Search for the lepton flavour violating decay $\mu^+ \rightarrow e^+\gamma$ with the full dataset of the MEG experiment, 2016.

[122] B. et all Aubert. Searches for lepton flavor violation in the decays $\tau \rightarrow e\gamma$ and $\tau \rightarrow \mu\gamma$. *Physical Review Letters*, 104(2), January 2010.